



**CHALMERS**  
UNIVERSITY OF TECHNOLOGY

---



# **Assessment of simulation codes for offshore wind turbine foundations**

*Master's Thesis in the Master's Programme Structural Engineering and Building Technology*

**ÖMER FARUK HALICI**  
**HILLARY MUTUNGI**

---

Department of Civil and Environmental Engineering  
Division of Structural Engineering  
Concrete Structures Research Group  
CHALMERS UNIVERSITY OF TECHNOLOGY  
Gothenburg, Sweden 2016  
Master's Thesis BOMX02-16-138



MASTER'S THESIS BOMX02-16-138

# Assessment of simulation codes for offshore wind turbine foundations

*Master's Thesis in the Master's Programme Structural Engineering and Building Technology*

ÖMER FARUK HALICI

HILLARY MUTUNGI

Department of Civil and Environmental Engineering

*Division of Structural Engineering*

*Concrete Structures Research Group*

CHALMERS UNIVERSITY OF TECHNOLOGY

Gothenburg, Sweden 2016



Assessment of simulation codes for offshore wind turbine foundations  
*Master's Thesis in the Master's Programme Structural Engineering and Building  
Technology*

ÖMER FARUK HALICI

HILLARY MUTUNGI

© ÖMER FARUK HALICI, HILLARY MUTUNGI 2016

Examensarbete BOMX02-16-138/ Institutionen för bygg- och miljöteknik,  
Chalmers tekniska högskola 2016

Department of Civil and Environmental Engineering  
Division of *Structural Engineering*  
*Concrete Structures Research Group*  
Chalmers University of Technology  
SE-412 96 Göteborg  
Sweden  
Telephone: + 46 (0)31-772 1000

Cover:

Figure shows the wind turbines located at Middelgrunden, 2 km off shore east of  
Copenhagen, Denmark (Bertrand, 2002)

Department of Civil and Environmental Engineering, Gothenburg, Sweden, 2016



Assessment of simulation codes for offshore wind turbine foundations

*Master's thesis in the Master's Programme* Structural Engineering and Building Technology

ÖMER FARUK HALICI

HILLARY MUTUNGI

Department of Civil and Environmental Engineering

Division of *Structural Engineering*

*Concrete Structures Research Group*

Chalmers University of Technology

## ABSTRACT

Offshore wind energy has the potential to become a leading renewable energy source. However, the cost of offshore wind turbine foundations is a major obstacle to the breakthrough of offshore wind energy development. There are a number of simulation codes that describe aerodynamic, hydrodynamic and serviceability response of offshore wind turbines. Nonetheless, each of these codes has its own limitations and capabilities in terms of; foundation type, environmental loading conditions as well as general modelling assumptions. Most simulation codes currently used in practice are limited to simple towers with monopile or gravity base foundations. However, they are being extended to model more developed foundation types, including tripods, jackets etc. Therefore, it is important to assess and judge the applicability of these codes to model such developed structures, which forms the purpose for this thesis.

To assess the capabilities and limitations of the studied simulation codes, principles and theories used were established. A classification of the codes was then made according to the observed principles. After that, three simulation codes (FASTv8, FOCUS6 and ASHES) were selected and examined through case studies with different types of foundations and loading conditions in order to study the codes practically. As expected, the results showed a variety of differences and similarities. In addition, some codes were more functional than others. For instance, in terms of the ability to describe loads with more advanced models, ability to create design load combinations etc.

In conclusion, it was confirmed that prior to choosing the appropriate simulation code for a given design, one has to consider the ability to describe the environmental conditions that the structure will face during its service life and the appropriate background required for the code to model the foundation.

Key words: Offshore wind energy, Simulation codes, Wind turbine, Foundations





# Contents

ABSTRACT	I
CONTENTS	III
PREFACE	VII
NOTATIONS	VIII
1 INTRODUCTION	1
1.1 Background and project description	1
1.2 Purpose and objectives	1
1.3 Scope	1
1.4 Method	2
2 DESCRIPTION OF OFFSHORE WIND TURBINE	4
2.1 Offshore wind turbine foundation	4
2.2 Offshore wind turbine tower	4
2.3 Loads acting on OWT	5
2.3.1 Wind	5
2.3.2 Waves	5
2.3.3 Currents	6
2.3.4 Seismic loads	6
2.3.5 Ice loads	6
2.3.6 Dead loads	7
2.3.7 Accidental loads	7
2.3.8 Further design consideration	7
2.4 Dynamic nature of an OWT	8
3 OFFSHORE WIND TURBINE FOUNDATIONS	10
3.1 Monopiles	10
3.2 Jacket structures	11
3.3 Gravity based structures	11
3.4 Tripod structures	12
3.5 Floating structures	13
4 PRINCIPLES USED IN OWT SIMULATION CODES	14
4.1 Soil interaction modelling	14
4.1.1 Coupled spring model	14
4.1.2 Distributed springs model	14
4.1.3 Effective /Apparent fixity model	15
4.2 Wind modelling and aerodynamic loads	15
4.2.1 Stochastic wind profiles	15

4.2.2	Aerodynamic loads	17
4.3	Wave modelling and hydrodynamic loads	19
4.3.1	Deterministic wave models	19
4.3.2	Stochastic wave models	21
4.3.3	Hydrodynamic loads	24
4.4	Currents	25
4.5	Analysis methods	26
4.6	Analysis techniques	27
4.6.1	Sequential approach technique	27
4.6.2	Semi-coupled approach technique	28
4.6.3	Fully coupled approach technique	28
5	SIMULATION CODES AND CLASSIFICATION	30
5.1	Current simulation codes in use	30
5.1.1	FAST (Fatigue, Aerodynamics, Structures and Turbulence)	30
5.1.2	Flex5	31
5.1.3	Bladed	32
5.1.4	ADCoS	33
5.1.5	ADAMS/WT & AeroDyn	35
5.1.6	HAWC2	36
5.1.7	ASHES	37
5.1.8	TURBU Offshore	38
5.1.9	FOCUS6	39
5.1.10	OneWind	41
5.1.11	USFOS-vpOne	42
5.1.12	SESAM	43
5.2	Comparison of codes	45
6	OWT DESIGN PROCESS	47
6.1	Design Environment loads	47
6.1.1	Wind loads	47
6.1.2	Wave loads	47
6.1.3	Wind generated waves	48
6.1.4	Wind generated current	48
6.2	Design input data for the codes	49
6.2.1	Geometry and material properties.	49
6.2.2	Aerodynamic data	49
6.2.3	Hydrodynamic data	49
6.2.4	Initial and boundary conditions	50
6.2.5	Soil interaction data	50
6.2.6	Computational specifications	50
6.2.7	Summary	50
7	CASE STUDY AND CODE COMPARISON	52
7.1	Pre-study	52

7.1.1	Pre-Study with OC4 Load Case 2.1	52
7.1.2	Pre-Study with OC4 Load Case 2.3a	53
7.1.3	Special case of OC4 Load Case 2.3a	54
7.2	RNA and tower definitions used in the studies	56
7.2.1	NREL 5MW Wind turbine model	56
7.2.2	Tower	57
7.3	Definition of load cases	57
7.3.1	Environmental effects measured from the site.	59
7.4	Comparison study for tripod structure	60
7.4.1	Description of the structure	60
7.4.2	Modelling the support structure	62
7.4.3	Foundation model	62
7.4.4	Results	62
7.5	Comparison study for the gravity base structure	71
7.5.1	Description of the structure	71
7.5.2	Modelling the support structure	73
7.5.3	Foundation model	73
7.5.4	Results	73
8	DISCUSSION	82
8.1	Comparison of the simulation codes	82
8.2	Discussion of the results from a design vantage point	84
9	CONCLUSION AND FUTURE RECOMMENDATIONS	86
9.1	Conclusion	86
9.2	Future recommendations	87
10	REFERENCES	88
11	APPENDICES	92
11.1	Appendix 1 – Matlab code for gravity base model	92
11.2	Appendix 2 – Fast input data for tripod structure model for load case 6	97



## Preface

In this project, classification and assessment of offshore wind turbine simulation codes have been made based on literature and case studies. In the classification study, several simulation codes were studied and adopted theories and principles were outlined. The case studies though, included only three of these simulation codes namely, FASTv8 (NREL), FOCUS6 (WMC) and ASHES (SIMIS). Moreover, a jacket, a tripod and a gravity base foundation models were created in these codes and studied in detail with specific load cases. The results were then used to assess and establish the limitations and capabilities of these simulation codes in relation to modelling such structures. This thesis is part of an ongoing research project named ISEAWIND financed by Swedish Energy Agency and NCC. The project was carried out at the Department of Structural Engineering, Concrete Structures Research Group.

The project has been carried out with Alexandre Mathern as the supervisor and Dr. Rasmus Rempling as the main supervisor and examiner. We would like to thank them for their devoted assistance and guidance throughout this project. In addition, we would like to thank Dr. Jason Jonkman of NREL, Dr. Paul E. Thomassen of SIMIS and the support team of WMC for their valuable contributions and technical advice.

Gothenburg, June 2016

Ömer Faruk Halici & Hillary Mutungi

# Notations

## Roman upper case letters

$C_D$	Variable notation for the drag coefficient
$C_L$	Variable notation for the lift coefficient
$C_M$	Variable notation for the inertia coefficient
$D$	Variable notation for the diameter of the structure
$F$	Variable notation for the fetch
$K_L$	Notation for spring lateral stiffness
$K_R$	Notation for spring rocking stiffness
$K_V$	Notation for spring vertical stiffness
$K_{VL}$	Notation for spring cross-coupling stiffness
$L_U$	Variable notation for the length scale of the wind speed
$L_v$	Variable notation for the integral length scale
$S_u(f)$	Variable notation for spectral density function
$S(\omega)$	Variable for the wind wave function
$U(H)$	Variable for the 10-minute wind speed at a height H
$U(z)$	Variable for the 10-minute wind speed at a height z
$U_0$	Variable notation for the 1-hour mean wind speed at 10m height
$U_{1/3}$	Variable notation for the velocity of the wave at the significant wave height
$U_{10}$	Variable notation for the 10-minute mean wind speed
$z_0$	Notation for the ground roughness parameter
$V$	Variable notation for the absolute velocity
$V_w$	Variable notation for mean wind speed

## Roman lower case letters

$a$	Variable notation for the induction factor
-----	--

$f$	Variable notation for the frequency
$f_t$	Variable notation for the total wave load on a structure
$f_D$	Variable notation for the drag load on a structure due to waves
$f_M$	Variable notation for the inertia load on a structure due to waves
$g$	Notation for the gravitation acceleration
$r$	Variable notation for element radius
$u$	Variable Notation for the horizontal wave particle velocity
$u_c$	Variable Notation for the velocity of a current
$\dot{u}$	Variable Notation for the horizontal wave particle acceleration
$U_{wind0}$	Variable notation for the wind generated current velocity

### **Greek upper case letters**

$\Omega$	Variable notation for the blade rotational speed
----------	--

### **Greek lower case letters**

$\alpha$	Notation for the constant that relates the wind speed and fetch length
$\beta$	Variable notation for the flow angle to the blade
$\gamma$	Variable notation for the peak factor
$\lambda_r$	Variable notation for tip speed ratio
$\mu_c$	Variable notation for the direction of a current
$\rho$	Variable notation for air density
$\sigma$	Variable notation for local solidity
$\sigma'$	Variable notation for local solidity
$\sigma_U$	Variable notation for the standard deviation of the wind speed
$\omega_0$	Variable notation for modal angular frequency
$\omega$	Variable notation angular frequency
$\omega_p$	Variable notation for peak angular frequency





# 1 Introduction

## 1.1 Background and project description

An offshore wind turbine is a power production unit having a large vanned wheel rotated by the wind, situated at a considerable distance from the sea shore to capture stronger winds. In this context, an offshore wind turbine (OWT) refers to the entire assembly of the wind turbine including the rotor nacelle assembly (RNA) and its support structure (tower and foundation). Offshore wind energy has a large potential to become a serious part of renewable energy sources in the near future. However, the main obstacle to building an offshore wind turbine is being relatively low cost efficient which is mainly generated from the high expenditure of foundations. Apart from that, the improvement of OWT foundation design is not an easy task due to complicated loading cases that these structures are exposed to (wind loads, wave loads, ice and currents)

Today there exists a number of advanced simulation codes to model OWTs and their foundations, however, each code has its own limitations as being suitable for a specific type of foundations and/or loading conditions. Moreover, there exists various necessary input data for each code and different assumptions that the model is based on. It is important to note though, that the term “simulation code” as used in this thesis refers to a computer program. This should not be misunderstood for the term “design code”, which refers to a documented standard of practice.

Most of the simulation codes currently used in practice were until recently limited to simple towers with monopile or gravity base foundations. However, they are extended to meet the requirements of modelling more developed support structures like tripods, jackets and to some extent, floating structures. It is therefore important to judge the accuracy, suitability and capability of these codes based on a detailed study of their application.

This master’s thesis is part of a research project named ISEAWIND that is financed by the Swedish Energy Agency and NCC.

## 1.2 Purpose and objectives

The main purpose of this thesis project was to study and assess the codes currently used in practical OWT simulation and design, particularly foundations.

The objectives of the thesis were as follows;

- Literature study of the currently used OWT simulation codes.
- Classification of the OWT simulation codes.
- Assessing suitable codes by using them on case studies of different foundation forms for OWT.
- Describing the limitations and capabilities of these simulation codes.

## 1.3 Scope

Although an OWT refers to the entire wind turbine structure, the scope of this thesis was limited to aspects relevant to the foundation and its design. In addition, the case

studies were based only on the NREL offshore 5-MW baseline OWT as discussed in Section 7.2.1.

The case study in this thesis investigated three types of OWT support structures namely; jacket structure, symmetric tripod structure and gravity base structure. The jacket structure was used in the pre-study of the simulation codes (see Section 7.1). The tripod and the gravity base structures were studied according to real environmental conditions measured at Blekinge offshore site. The foundation type used was the fixed type whereby the flexible aspects of the soil were disregarded.

Models of these support structures were studied and tested using only three simulation codes i.e. FAST v8 developed by the National Renewable Energy Laboratory (USA), ASHES 2.3.1 developed by SIMIS (Norway) and FOCUS6 developed by WMC (Netherlands). The reasons for limiting the study to only these three codes were mainly due to the timeline of the project, the availability of the code licence as well as technical support from the code developers. All information about the rest of the codes discussed in Section 5.1 is based solely on written documentation about the codes.

Although API (2007) and DNV-OS-J101 (2014) specify more loads against which an OWT should be designed, this project was limited to only such environmental loads as waves, wind and currents. In just a few instances, the gravity load was considered but solely for model verification purposes.

## **1.4 Method**

The first task of this thesis was to investigate the state-of-the-art simulation codes existing for OWT foundations. This involved studying a vast amount of literature and searching for the codes and software that are currently used to design. The logic behind the codes was investigated to understand the necessary input data and different assumptions on which OWT models are based.

Following the literature study, the second task was to make a classification of the simulation codes. It was then possible to understand which kind of design the code applies to, for instance, the type of structure and underlying design principles on which the code is based.

The third task was to assess the codes by applying them on case studies with certain types of turbine foundations in order to make comprehensive code-to-code and code-to-real data comparisons. This provided a deeper understanding of simulation codes and made it possible to analyse the accuracy of the results and capabilities of codes. It was not possible to access actual turbine data and instead, previous project results were used. One such project was the OC4 project (Vorpahl et al., 2011) and indeed this provided the basis for the code pre-study task. In the pre-study, the codes were used to model the exact support structure and load cases studied in the OC4 project to ensure that similar results were obtained. The sole reason for this exercise was to ensure familiarity with these codes before taking on other support structures.

Following the pre-study, a symmetric tripod and a gravity base foundation was modelled in FASTv8 (NREL), FOCUS6 (WMC) and ASHES (SIMIS) with a variety of load cases to inspect the limitations and capabilities of the simulation codes.

Supervisory meetings as well as discussions with the technical support teams from the code developers were used as a means to ensure that the modelling procedure was done correctly. In addition, the analysis results were constantly reviewed to validate that the output was consistent. While the pre-study was done on dummy environmental load conditions adopted from the OC4 project, the case study featured actual environmental load conditions from Blekinge offshore site in South-Eastern Sweden. This provided grounds to simulate how such OWT support structures would behave if they were actually constructed.

Finally, with sufficient information, the limitations and capabilities of each code were established based on such criteria as: type of foundation that the code can be applied, the methodologies and design principles of codes as well as the ability to define and handle different types of loads.

## 2 Description of offshore wind turbine

In this chapter, primary components of offshore wind turbines and the fundamental design principles will be discussed. Passon and Kühn define the support structure of an OWT as consisting of the whole structure below the yaw system (2005). Moreover, it is convenient to separate the support structure into distinct parts or modules for the purpose of modelling and conceptual disposition (Ibid.). In the context of this study, the OWT support structure is divided into the tower and the foundation. A detailed discussion of these components, their dynamic nature, as well as the loads that affect them follows in Section 2.1 to 2.4.

### 2.1 Offshore wind turbine foundation

A foundation is the main component that supports the OWT structure against horizontal and vertical loads. As Kaiser and Snyder mentioned, there exists various types of foundations that can be applied to different environmental properties of an OWT structure such as, water depth, wind speed, wave heights and weight of the turbine (2012). In order to meet today's high energy demand and catch greater wind potential, OWTs need to be placed further away from the shore in deeper waters. However, it is apparent that hydrodynamic and aerodynamic loads increase as the water depth and distance from the shore increases.

Foundation selection plays an important role in the design of offshore wind farms, since there are large financial implications that accompany the choice of the foundation. Typically the foundation costs 25% to 34% of the overall cost of building an OWT (Bhattacharya 2014). In addition to the financial viability of the project, the nature of the loads acting on OWTs means that the foundation forms a critical component of the OWT structure, as will be seen later.

Foundations for OWTs can be classified into two main types; the fixed types and floating types. The fixed type foundations are only effective in relatively shallow waters (<60m), whereas the floating type foundations are developed for deeper waters (>60m). As Passon and Kühn (2005) pointed, OWT structures can be grouped into the first, second and third generation. The first generation includes fixed foundations such as mono-pile and gravity base foundations. These are effective in shallow waters less than 30m deep. The second generation covers a more sophisticated range of foundations such as tetrapod caisson, asymmetric-tripod caisson, jacketed caisson, tripod caisson and tripod pile foundations. These are effective even in deeper waters, but still limited to 60m (Bhattacharya 2014). The third generation is the floating type. It is by all means the most cost effective solution in deep waters and has no limit to which water depth it can be installed.

### 2.2 Offshore wind turbine tower

The tower is considered as part of the turbine support structure that resides above the foundation. According to Jonkman et al. (2009), the tower properties will depend on the type of foundation used to carry the RNA. The type of foundation will in turn depend on the site conditions. The properties of the site vary significantly in terms of water depth, soil type, and wind and wave severity.

A tower structure can be a mono-tower or a jacket. In addition, a variety of tower and foundation combinations can be made depending on the design requirements.

## **2.3 Loads acting on OWT**

The loads acting on an OWT structure can be grouped into static or dynamic loads. Static loads relate mainly to the self-weight of the components. A case of static loads due to the environment is ice on the structure. Dynamic loads relate mainly to the environment in the form of wind or water interaction, and thus classified as aerodynamic and hydrodynamic respectively.

As Bhattacharya (2014) states, the most challenging of these load classes are the dynamic loads. Moreover, Van Der Tempel et al. (2011) add that for OWTs, the assessment of environmental parameters is more extensive than for land turbines. On land, turbines can be designed following a class prescribing the wind regime and the required resilience of the turbine itself. However for OWTs, the winds are less turbulent but more formidable. In addition, the offshore environment features other actions due to the water waves and currents. This implies that an engineer designing an OWT faces a more daunting challenge and must fully understand the behaviour and magnitude of the dynamic loads before proceeding with the design. In this section, the loads will be discussed in detail.

Other loads that affect offshore structures in general include; earthquakes, accidental loads, fire and blast loading. (API RP 27, cited in Bai and Jin 2016).

### **2.3.1 Wind**

Field experiments have shown that the distributed wind velocity is variable in space, time and direction (Molenaar, cited in Van Der Tempel et al. 2011). It is rather complicated though to consider the effect of variation of wind velocity in more than one direction. For simplicity, wind is only considered in the horizontal (frontal) direction. This assumption reduces the complexity of the wind model such that it only varies with height and time (see Figure 2.1).

Wind is a significant design factor. The wind conditions used in design should be determined from appropriate and detailed wind data statistics for a specific site. In addition, this data should be consistent with other associated environmental parameters (Bai and Jin 2016).

### **2.3.2 Waves**

Sea waves result from wind blowing across the surface of the water and they form one of the major components of environmental forces affecting OWTs. These often start as minute ripples and can grow considerably with time. As the waves crush against the OWT foundation, they cause considerable action whose magnitude depends on the wave height and wave period. Waves are random, varying in height and length and as Bai and Jin state; they can approach an OWT from more than one direction simultaneously (2016). Due to this random nature, the sea state is usually described in terms of statistical wave parameters such as significant wave length, spectral peak period, spectral shape, and directionality.

Van Der Tempel et al. (2011) reasonably simplify the description of the wave climate at a specific location by considering it to be stationary within periods of three hours. This implies that the stochastic aspects of a given wave climate can be assumed to be constant over the three-hour period. The wave aspects in this duration can be described statistically by a form of wave spectrum known as the variance density spectrum. This is obtained by performing a Fast Fourier Transform (FFT) on the time series of the wave characteristics. The most common examples of standard wave spectra that have been developed to describe a wave climate are the Pierson-Moskowitz wave spectrum and the JONSWAP wave spectrum. The former is developed for fully developed seas while the latter is for fetch-limited wind-generated seas. Details on these spectra will follow in Section 4.3.

### **2.3.3 Currents**

The mechanism of currents is similar to that of wind, in such a way that both their velocities vary in time and space. However, Van Der Tempel et al. (2011) point out that the length and timescales of the variations are considerably more pronounced in currents. They are also large in comparison to the horizontal dimensions of the substructure and the range of periods used to determine the substructure's dynamic behaviour. This prompts the consideration of currents as a horizontal uniform flow field of constant velocity, a function of only the vertical coordinate.

According to Bai and Jin (2016), currents are commonly categorised into; tidal currents (associated with astronomical tides), loop and eddy currents, circulation currents (associated with oceanic-scale circulation patterns) and storm generated currents where the total effect of these currents is the vector sum. The variation of current speed and direction with elevation is represented by a current profile whose total profile associated with an extreme storm sea should be specified. A detailed description of how currents are treated follows in Section 4.4.

### **2.3.4 Seismic loads**

Seismic activity is another site specific design aspect. Although some regions have little or no earthquake risk, some regions are extremely prone to considerable seismic activity. In fact, in such areas, earthquake loading may be one of the governing factors. Therefore, it is important that a designer should have a specific seismic study about the area of interest as one of the primary design requirements.

The effect of seismic activity on an OWT varies in magnitude depending on the type of substructure. El-Reedy (2012) discusses that fixed offshore structures are usually long-term structures that are likely to spend 1 to 5 seconds subjected to lateral, flexural and torsion stress. The ductility requirements are intended to ensure that the structure retains sufficient reserve capacity to prevent a collapse during intense seismic motion, although some structural damage may occur. In regions with low seismic activity, the design resistance against environmental actions will be sufficient against earthquake motion.

### **2.3.5 Ice loads**

Consideration of ice loads has more to do with the proposed location of a wind farm. Some of the seas freeze during a certain period while others will stay unfrozen even in

sub-zero temperatures. A typical example of a sea which does not often freeze is the North Sea, while the Baltic Sea often freezes during winter. The freezing of the water obviously creates a challenge for all possible exploration efforts. To imagine the effect of ice on an OWT substructure, it is important to understand the drifting of ice in a sea. El-Reedy (2012) reports that, drifting ice travels at a speed of 1-7% of the speed of the wind, of course depending on the mass of ice lump. The bigger the ice mass, the more momentum it will have. Consequently, the more impact it will have on an OWT structure.

El-Reedy (2012) adds that the effect of ice load depends on the spacing of individual members, and generally the following rules will apply;

- 1- Spacing  $\geq 6$  times the substructure element diameter; Ice is idealised to crush against the tubular members and pass through and around the platform. For groups of tubular members of different sizes, the average tubular diameter can be used to determine the spacing.
- 2- Spacing  $\leq 4$  times the substructure element diameter; with decreased spacing between substructure legs, ice blocks can wedge inside the structure and the contact area becomes the out to out dimension across the closely spaced members in the direction of the ice movement.
- 3-  $4 \leq \text{Spacing} \leq 6$  times the substructure diameter; linear interpolation takes effect.

It is worth noting that the frost and ice which may build up as gravity load on the turbine blades is often not considered since it is accounted for in the blade design.

### **2.3.6 Dead loads**

As briefly explained earlier, the dead load is the total weight of each individual component that makes up the entire OWT. The certainty of this category of loads makes them relatively simple to deal with in design since the density of the materials used to set up the structure is known as well as the weight of the elements of the RNA.

### **2.3.7 Accidental loads**

Due to the situation of an OWT, the occurrence of accidental loads is something of low probability. However, it is worth noting that ship collisions must be taken into consideration in the design.

### **2.3.8 Further design consideration**

In addition to the loads discussed, it is important to consider the effect of marine growth as well as scour. Marine growth increases the diameter of a jacket or pile member and thereby enhances the drag force from currents and waves. Consideration of marine growth is as much a site specific aspect as scour prediction. For further reading, the reader is referred to API 1.5 cited in El-Reedy (2012).

## 2.4 Dynamic nature of an OWT

OWTs are dynamically sensitive structures because of their shape and form. The eigenfrequencies of these slender structures are very close to the excitation frequencies imposed by the environment and mechanical loads. Therefore, in order to avoid resonance, it requires a fundamental knowledge of structural response and precise calculations.

According to Bhattacharya (2014) dynamic loads acting on OWTs can be measured from 4 sources; wind load, wave crushing, aerodynamic asymmetry of the rotor and blade shadowing effect. Dynamic effect of wind load and wave crushing shows variation depending on the wind and wave climate of the turbine location and can be obtained from field measurements. The dynamic load created by the rotor asymmetry is equal to the frequency of the rotor circulation which is compatible with the frequency band at which the OWT operates (1P). In addition, blade shadowing effect is developed when a blade passes in front of the tower which blocks the wind and initiates a temporary reduction in wind load acting on the tower. This dynamic effect is also dependent on the range of rotational frequencies of the rotor. In fact, with three bladed wind turbines, the frequency is three times greater than the rotational frequency of the rotor (3P), whereas with two bladed wind turbines the frequency is two times greater (2P). In Figure 2.1, the external loads acting on OWTs are described with their waveforms.

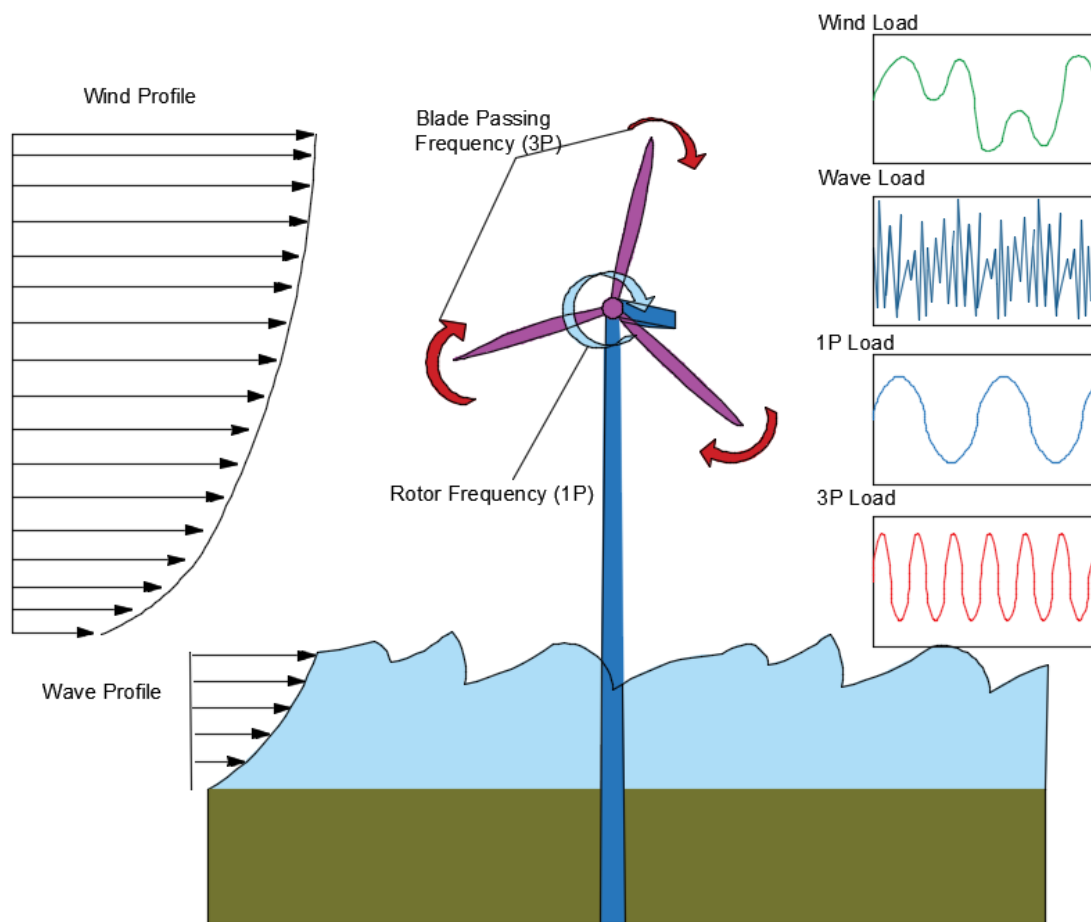


Figure 2.1 External loads acting on an offshore wind turbine, along with their typical waveforms.



To prevent dynamic amplifications in the structure, the system frequencies of the OWT should not coincide especially with the frequencies of the cyclic dynamic excitation forces (aerodynamic imbalance of the rotor and blade shadow effect). Bhattacharya (2014) outlined the design alternatives for OWTs in three different methods: soft-soft design, soft-stiff design and stiff-stiff design as shown in Figure 2.2.

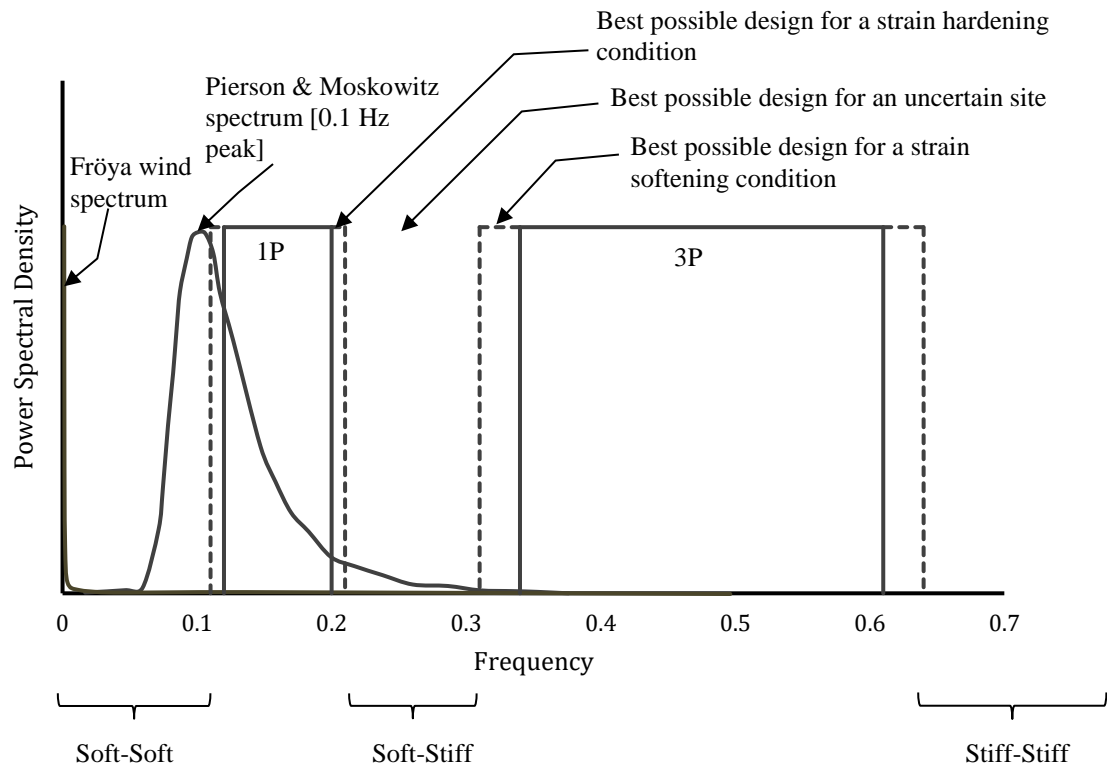


Figure 2.2 Frequency spectrum of the dynamic loads and design choices

The soft-soft design option requires a very flexible structure for which the first natural frequency is smaller than the rotor frequency range (1P) which is achievable only with floating systems (Bhattacharya 2014). Moreover, OWT structures can be designed with the stiff-stiff design principle with a greater natural frequency than the range of the blade shadowing effect frequency (3P/2P). To accomplish this, it is mandatory to have a massive foundation which as already seen, is associated with a higher costs. Therefore, the stiff-stiff design alternative is not feasible to construct. Apart from those two options, the soft-stiff is the most common design practice in OWT which limits the natural frequency of the structure between 1P and 3P/2P range. With this alternative, it is not necessary to build very flexible or too stiff foundations. But on the contrary, the structure must comply with calculations and the natural frequency range should remain between 1P and 3P/2P. Any changes in the behaviour caused by strain hardening or softening during service life will increase dynamic amplifications, internal stresses and fatigue damage, hence, the soft-stiff method requires a comprehensive design and detailed future expectations.

## 3 Offshore Wind Turbine Foundations

### 3.1 Monopiles

As mentioned in the introduction, monopiles are the most common foundation alternative for OWT structures. They consist of a pile and a transition piece (see Figure 3.1) which offers a relatively simple design and cheap support solution. A monopile is a thick walled steel pipe with a large diameter from 4 to 6 meters which can either be driven/hammered into the seabed or be grouted into drilled rock. The general practice is inserting the 40-50% of the pile into the seabed, depending on water depth, soil type, design load, etc. (Kaiser and Snyder 2012). It is also possible to use suction caissons for anchoring a monopile in tough soil conditions where driving/hammering is hard and expensive. In some cases, monopiles can be fastened/guyed using cables anchored to the seabed so as to increase the stiffness of the structure.

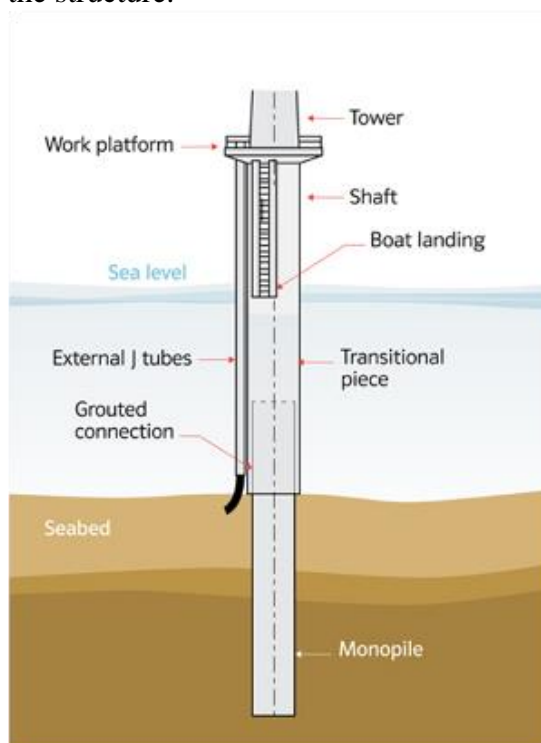


Figure 3.1 Monopile foundation (4C Offshore LTD 2016)

Monopile foundations are feasible up to 30 meters of water depth, but due to its simplicity, there is a big trend to build it in deeper waters. However, increasing diameter and length bring other challenges including buckling problems, limited information in design codes, installation issues and cost (Bhattacharya 2014). On the other hand, considering current developments in design and the fact that not all shallow waters with great wind potential have been utilized yet by wind power, one can say that monopile foundations will still be a good option in foundation design in near future.

### 3.2 Jacket structures

The foundation can be built with a truss system (jacket) of steel tubular elements that can be placed on caissons, piles and gravity based platforms to provide required stiffness to OWT structures. A jacket structure is a good alternative to monopile foundations in deeper waters. It can be built with a 3-leg or a 4-leg configuration depending on environmental conditions at the site. Kaiser and Snyder (2012) claim that since jacket structures are heavy and require expensive transportation equipment, they are preferred usually in deeper waters (>50m). Today's trend is building OWTs in shallow waters to reduce the cost, therefore, jacket structures are not selected often. Figure 3.2 (Crampsie 2014) captures a jacket structure that is already built.



Figure 3.2 Jacket structure (Crampsie 2014)

### 3.3 Gravity based structures

Gravity based foundations are basically concrete shell structures that transfer vertical loads to the ground and resist horizontal (wave, wind, etc.) loads by their own gravity. These structures are usually preferred in sites where driving a pile is tough and expensive. Although constructing a gravity based foundation is less expensive than building a monopile, this method requires ground improvement and capability of handling massive concrete blocks onshore and offshore. There is also a need for a shipyard near the wind farm from where the massive structures can be floated, dragged to the wind farm yard and sunk (Malhotra 2010). Figure 3.3 (Kaiser and Snyder 2012) shows gravity base foundations under construction.



Figure 3.3 Gravity base foundations (Kaiser and Snyder 2012)

### 3.4 Tripod structures

Tripod structure is an acceptable solution to restrict the horizontal movements of the wind turbine structure in extreme environments. Tripod is a combination of a steel pile which is connected to three cylindrical steel pipes in both horizontal, vertical and diagonal directions (Kaiser and Snyder 2012). They are more expensive structures in comparison to monopiles, but being stiffer makes them preferable in deep water. Tripod structures can be built as a straight tripod or asymmetric tripod depending on circumstances. The structure can be anchored into the seabed by driven piles or suction caissons.

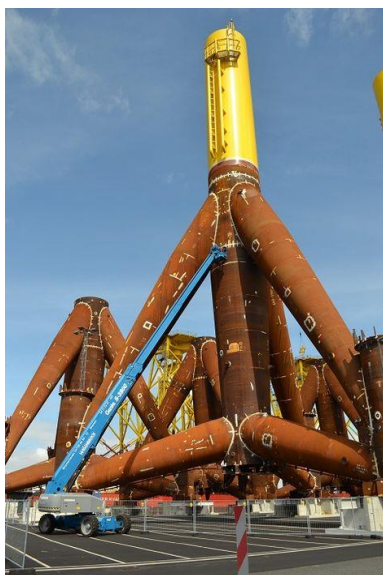


Figure 3.4 Tripod structure (Vertikal Press 2013)

### 3.5 Floating structures

Another foundation alternative for OWTs is the floating structure which is beneficial in deep waters where it is not possible or feasible to build a fixed (gravity base, jacket, tripod and monopile) support structure. Submerged floating platforms are pre-tensioned via anchorages on the seabed to increase the stiffness of the structure and absorb the movements against environmental loads. However, since this is a very fresh concept, there is a need for a comprehensive study of floating systems to investigate their response and dynamic behaviour. So far, a small number of floating foundation applications has been established. One of them is built by StatoilHydro (Hywind) in Norway for the purpose of investigating the behaviour. In Figure 3.5 (Statoil 2008) the concept of Hywind is represented.



*Figure 3.5 Hywind turbine and support structure (Statoil 2008)*

## 4 Principles Used in OWT Simulation Codes

This section presents the design principles and theories on which the simulation codes are based. It covers models that represent how the soil behaves under loading. The effect of wind, waves and currents on the OWT support structure is explained in detail. Simulation models of the wind, waves and currents are also presented.

### 4.1 Soil interaction modelling

#### 4.1.1 Coupled spring model

A foundation system can be idealised as a simple model in which the soil is replaced by a system of springs to represent the soil stiffness in the appropriate direction. For example, Bhattacharya(2014) discusses a model in which the foundation is replaced by four sets of springs; one representing stiffness in the lateral direction ( $K_L$ ) and another representing stiffness against rocking and rotation ( $K_R$ ). The third and fourth sets represent stiffness in the vertical direction ( $K_V$ ) and cross-coupling ( $K_{RL}$ ) respectively. This coupled springs model is illustrated in Figure 4.1 (a) (Bhattacharya 2014).

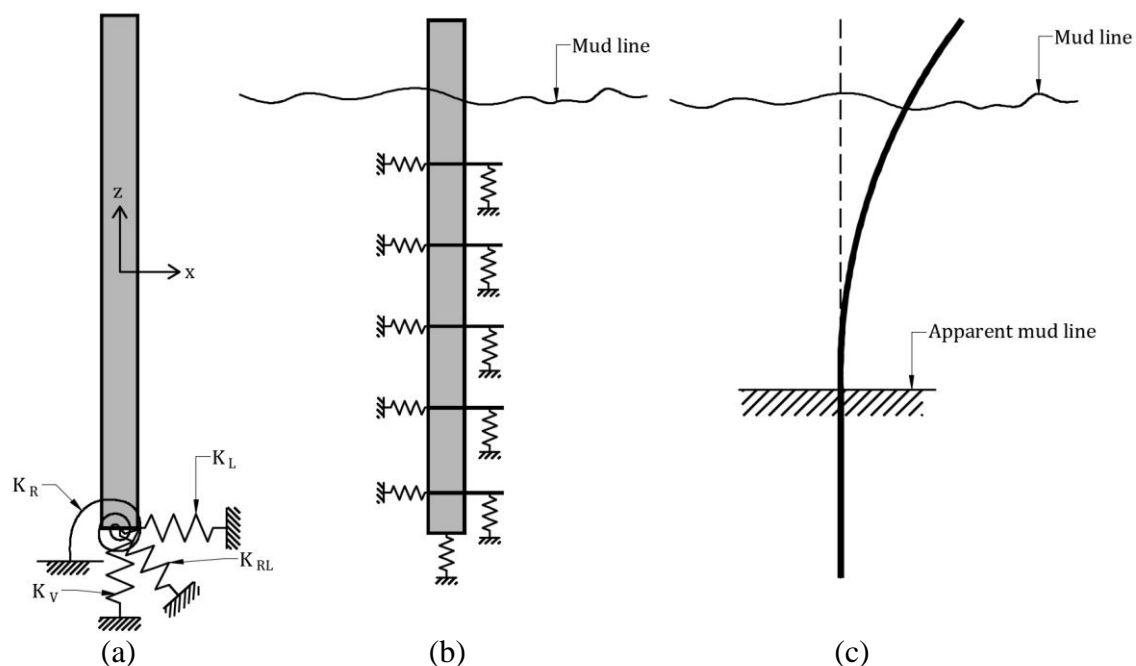


Figure 4.1 (a) coupled springs model, (b) distributed springs, (c) effective fixity length model.

#### 4.1.2 Distributed springs model

Another interesting foundation system is one discussed by Abhinav and Saha (2015) as well as Zaaier (2006). This model is the most comprehensive for monopile foundations and is modelled using lateral and axial nonlinear spring elements attached to the ground, along the length of the pile (See Figure 4.1 (b)). The properties of the spring elements can be derived from the  $p$ - $y$ ,  $t$ - $z$  and  $Q$ - $z$  curves recommended by API (2007). The  $p$ - $y$  curves account for the lateral interaction between the soil and the pile,

whereas the vertical interaction is accounted for using  $t$ - $z$  curves which represent pile skin friction. The  $Q$ - $z$  curves account for end bearing.

### **4.1.3 Effective /Apparent fixity model**

This model is discussed by Zaaier (2006) and it is well suited for monopile foundations. The soil-pile environment is represented by a clamped model of the pile at an effective length below the seabed (see Figure 4.1 (c)). In this model, the pile is not fixed at the original mud line but rather at a lower depth. This point is known as the point of effective fixity for the cantilever pile. Kühn, cited in Zaaier (2006) suggests that the effective length should be between 3.3 and 3.7 times the pile diameter.

To reduce the computational time and effort required to simulate the foundations, these models need to be as simple as possible. However, a reasonable degree of accuracy should also be maintained. Such requirements often complicate the process of OWT foundation design. Bhattacharya (2014) notes that OWTs have to resist moments that are disproportionately larger than the vertical loads and due to the dynamic nature of the loads, the fatigue risk is considerably high.

## **4.2 Wind modelling and aerodynamic loads**

Aerodynamic loads mainly result from wind turbulence and can either be direct or indirect. Their magnitude depends on the turbulent wind speed. In this section, definitions of wind fields and their interaction with the OWT structure (aerodynamic loads) will be presented.

According to Matha et al. (2010), aerodynamic loads can be further grouped into three categories;

- Steady aerodynamic loads due to mean wind speed
- Periodic aerodynamic loads due wind shear, rotor rotation, off-axis winds and tower shadowing
- Randomly fluctuating aerodynamic loads resulting from gusts, turbulence and dynamic effects.

Wind fields can be described in deterministic and stochastic approaches. The deterministic approach is based on real data measured from a specific site and specific conditions. It can be utilised to investigate the behaviour of the structure in extreme conditions (Passon and Kühn 2005). On the other hand, the stochastic approach is based on probabilistic methods to describe wind field. It is also the stochastic approach that is the most appropriate for calculating fatigue loads.

### **4.2.1 Stochastic wind profiles**

According to DNV (2010), in case the measured wind data is insufficient to establish site-specific spectral densities, the wind speed process can be represented by the following spectra.



- *Davenport spectrum*

This spectrum expresses spectral densities in terms of the 10 minute mean wind speed irrespective of the elevation. The Davenport spectrum is represented by the following spectral density function;

$$S_u(f) = \sigma_U^2 \frac{\frac{2}{3} \left( \frac{L_U}{U_{10}} \right)^2 f}{\left( 1 + \left( \frac{f \cdot L_U}{U_{10}} \right)^2 \right)^{4/3}} \quad (4.1)$$

where  $f$  is the frequency and  $L_U$  is the length scale of the wind speed. The DNV (2010) also specifies that this spectrum is developed for wind over land with  $L_U$  of 1200 m.  $\sigma_U$  is the standard deviation of the wind speed.

However, this spectrum is not appropriate for use in the low frequency range (less than 0.01 Hz). What is noted too is that it is difficult to consider the Davenport spectrum when analysing data in this range, due to the abrupt fall in the spectral density value of the Davenport spectrum in the vicinity of zero frequency.

- *Kaimal spectrum*

The Kaimal spectrum has the following expression;

$$S_u(f) = \sigma_U^2 \frac{6.868 \frac{L_U}{U_{10}}}{\left( 1 + 10.32 \frac{f \cdot L_U}{U_{10}} \right)^{5/3}} \quad (4.2)$$

Again here,  $f$  denotes the frequency but  $L_U$  is the integral length scale which can be computed as;

$$L_U = 300 \left( \frac{z}{300} \right)^{0.46 + 0.074 \ln z_0} \quad (4.3)$$

where  $z$  is the height above the ground or the sea and  $z_0$  is the terrain roughness.

IEC (2005) proposes an alternative integral length independent of the terrain roughness as;

$$L_U = \begin{cases} 3.33 z & \text{for } z < 60 \text{ m} \\ 200 \text{ m} & \text{for } z \geq 60 \text{ m} \end{cases}$$

- *The Harris spectrum*

Similar to the Davenport spectrum, the Harris spectrum defines the spectral density without considering the elevation as follows;

$$S_u(f) = \sigma_U^2 \frac{4 \frac{L_U}{U_{10}}}{\left( 1 + 70.8 \left( \frac{f L_U}{U_{10}} \right)^2 \right)^{5/6}} \quad (4.4)$$



where  $L_U$  is the integral length scale in the range 60-400 m with a mean value of 180m. If there is no data indicating otherwise,  $L_U$  can be calculated as for the Kaimal spectrum. The DNV reports that this spectrum is originally developed for turbines over land and is not suitable in the low frequency range ( $f < 0.01$  Hz).

- *Von Karman spectrum*

The Von Karman spectrum is another alternative for defining wind profiles and is one of the most commonly used methods in OWT simulation. DNV(2010) expresses the Von Karman spectrum as follows;

$$S_{Karman}(f) = \frac{\sigma_U^2 4L_v / V_w}{(1 + 70.8(fL_v / V_w)^2)^{5/6}} \quad (4.5)$$

where  $\sigma_u$  stands for the standard deviation of the wind speed (m/s) and  $V_w$  is the mean wind speed (m/s). Similar to the other spectra mentioned above,  $L_v$  represents integral length scale (m) and  $f$  means frequency (Hz).

- *Other spectra*

In addition to the spectra discussed, the DNV (2010) says that the empirical *Simiu and Leigh* spectrum as well as the empirical *Ochi and Shin* spectrum may be applied to the design of offshore structures. The *Simiu and Leigh* spectrum takes into account the wind energy over a seaway in the low frequency range. Similarly, the *Ochi and Shin* spectrum is developed from measured spectra over a seaway and it has more energy content in the low frequency range than the Kaimal, Harris and Davenport spectra.

## 4.2.2 Aerodynamic loads

There are some methods developed to calculate the wind load acting on OWTs by describing a relation between the wind profile and the blades of the structure. Simulation codes for OWTs generally utilise Blade Element Momentum (BEM) theory or Generalised Dynamic Wake (GDW) theory.

- *Blade element momentum theory*

Blade element momentum theory is the most common aerodynamic load calculation method in OWT design that calculates the velocity change imposed by wind flow. In fact, it is a combination of blade element theory and momentum theory. Moriarty and Hansen (2005) defined blade element theory as a method that divides the blade into small independent elements and lets the blade act as a two-dimensional aileron and then calculates the aerodynamic forces acting on each element from the local flow. For momentum theory, Moriarty and Hansen also added that the momentum theory assumes that the loss of pressure and momentum in the rotor plane is the result of the work performed by the airflow which migrates through the blades (2005). The velocity change of the blades in axial and tangential directions can be calculated based on the work done by airflow. Therefore, one can assert that blade element momentum theory is a method that utilises the blade element theory considering the changes in the airflow. These changes are calculated using the momentum theory.

Like all theories used in OWT design, BEM has some limitations too. One limitation is that since the momentum theory considers momentum equilibrium in the rotor plane, BEM theory fails to give proper results if the blades deflect out of the rotor

plane (Moriarty and Hansen 2005). Another limitation is that BEM does not consider wind flow definition along the span since it only assumes two-dimensional wind flow. Another limitation is that BEM theory is only capable of linear analysis and therefore, it does not consider time lag effects when the wind speed or direction changes. Apart from that, BEM theory needs some modifications to define tip losses and wake aerodynamics.

Blade element momentum theory consists of four equations, two of them generated from momentum theory. One equation defines the torque produced by the blades (equation 4.6), another equation expresses the thrust extracted in each cycle (equation 4.7).

$$dT = Q4a'(1-a)\rho V\Omega r^3\pi dr \quad (4.6)$$

$$dF_x = Q\rho V_1^2 4a(1-a)\pi r dr \quad (4.7)$$

In these equations  $Q$  stands for the tip loss correction factor,  $\rho$  represents air density,  $V$  is the absolute velocity,  $a$  represents induction factor,  $r$  stands for the radius of each element and  $\Omega$  is the blade rotational speed.

Moreover, there are two more equations derived from blade element theory that express torque (equation 4.8) and thrust (equation 4.9) considering lifting and dragging effect of the blades (Ingram 2011).

$$dT = \sigma' \pi \rho \frac{V^2 (1-a)^2}{\cos^2 \beta} (C_L \cos \beta - C_D \sin \beta) r^2 dr \quad (4.8)$$

$$dF_x = \sigma' \pi \rho \frac{V^2 (1-a)^2}{\cos^2 \beta} (C_L \sin \beta + C_D \cos \beta) r dr \quad (4.9)$$

In the equations shown above,  $\sigma'$  stands for local solidity,  $\beta$  is the flow angle to the blade,  $C_L$  represents lift coefficient, whereas  $C_D$  is drag coefficient.

For the scope of this thesis, it was not necessary to go deep into the derivations of those equations mentioned above. However, the reader is referred to (Ingram 2011) and (Moriarty and Hansen 2005) for more information.

Finally, the relationships obtained from the four equations written above follow;

$$\frac{a}{1-a} = \frac{\sigma' [C_L \sin \beta + C_D \cos \beta]}{4Q \cos^2 \beta} \quad (4.10)$$

$$\frac{a'}{1-a} = \frac{\sigma' [C_L \cos \beta - C_D \sin \beta]}{4Q \lambda_r \cos^2 \beta} \quad (4.11)$$

Where  $\lambda_r$  stands for local tip speed ratio.

- *Generalised dynamic wake*

Generalised dynamic wake (GDW) theory also known as potential acceleration method that provides more regular results of pressure distribution over the rotor plane compared to blade element momentum theory (BEM) (Moriarty and Hansen 2005). The most striking feature of GDW is the ability to express tip losses, wake aerodynamics and the time lag effect without requiring any modifications. However,

this method also has some limitations. GDW theory is not appropriate for heavily loaded rotors due to the assumption that if the propagated velocities are smaller than the mean flow, an instability occurs when the turbulent wake state is reached at lower wind speeds (Laino and Hansen, cited in Moriarty and Hansen 2005).

- *Dynamic stall effect*

Aerofoils under unsteady flow conditions with a periodically varying angle of attack exhibit aerodynamic characteristics that are different from those under steady flow conditions. This phenomenon is known as dynamic stall during which the aerofoil is oriented at an angle greater than the critical angle of wind attack. The resulting effect is characterised by airflow dispersion at the suction side of the aerofoil and causes an increase in the drag on the aerofoil. According to Vahdati et al. (2011), this phenomenon is more common in vertical axis wind turbines than in horizontal axis wind turbines. The blades are consequently subjected to recurring forces due the variation of incidence angle of the wind direction. Although the effect of dynamic stall at low tip speed ratios is an advantage in terms of power generation, the formation of vortexes causes extremely undesirable circumstances like vibrations, noise and a reduction in fatigue life of the blades due to unsteady forces.

### **4.3 Wave modelling and hydrodynamic loads**

Henderson et al. (2003) reckon that the calculation and determination of design wave loads on an OWT structure is a complex process that involves different wave models, load calculation methods and probability analyses. Still, it is important for a designer to go through this process in order to produce a cost effective and durable structural design. It is therefore important to understand the waves, their distribution and hydrodynamic properties.

The procedure of wave load calculation can be intended for peak loads or fatigue loads and is divided into three stages;

- Describing the wave and wave climate
- Selecting an appropriate wave load calculation procedure
- Computing the load effect.

According to Le Mehaute (1976), the choice of wave model depends on the wave type and the range of values of the parameters  $H/L$ ,  $H/d$  and  $L/d$  where  $H$ ,  $L$  and  $d$  are the wave height, wave length and water depth respectively. Three mathematical approaches are used to model wave characteristics, namely; linearization, power series and numerical methods. These are known as deterministic models. In addition, statistical (stochastic) methods can also be used to describe the complexity of sea states and waves generated by wind.

#### **4.3.1 Deterministic wave models**

- *Linear wave theory (Airy)*

Linear wave theories are the simplest case of water wave theories in which the convective inertia terms of the wave equation are completely ignored. A classic example of linear wave theories is the Airy wave model according to Airy (1845). Linear wave theories are only valid if the wave height is considerably small compared to wavelength and still water depth. The linear wave theory is relatively simple but

lacks accuracy and its primary weakness is that it truncates the wave peaks and troughs. However if integrated with other properties of the wave-load calculation for example stochastic waves, diffraction and some correction, its accuracy can be improved (Henderson et al. 2003).

- *Wheeler stretching*

This is generally a correction to the linear wave theory where the kinematics of the wave as calculated at the mean-water level are applied to the true surface with the distribution down to the seabed. This theory improves the prediction of wave kinematics which can be also applied to stochastic models (Henderson et al. 2003). In Chapter 5, the linear wave theory with such surface improvement (Wheeler stretching) is denoted as Airy<sup>+</sup>.

- *Power series (Stokes and Cnoidal waves)*

For cases where waves are too steep or water depths are too shallow, it is not practical to use the linear theory. Under such circumstances, the choice is to use higher order approximations in which the waves are modelled as a power series in terms of a characteristic parameter. This parameter is  $H/L$  in deep waters or  $H/d$  in shallow water. The former case is a characteristic of Stokes theory (2<sup>nd</sup>, 3<sup>rd</sup> and 5<sup>th</sup> order) and the first term of the power series is a solution of the linearised equations. The later parameter describes the Cnoidal theory in which the first term of the series constitutes the solution of nonlinear equations. These methods are not commonly used because of the complexity of dealing with terms of the series. Detailed discussions of these wave theories are given by Le Mehaute (1976) and (Fenton 1988).

- *Numerical wave models (Dean's stream function and Fenton's model)*

It is possible that no solution of the steady-state wave profile exists. For such a case, it is only possible to employ a numerical solution where the differentials are replaced by finite differences. According to Le Mehaute (1976), this is typical for very large values of  $H/L$  and  $H/d$  and consequently when the nonlinear terms are rather large compared to the local inertia. This happens commonly with long waves in very shallow water.

One of the most common numerical wave models is Dean's Stream Function, developed by Dean (1965) for the purpose of numerically examining fully non-linear water waves. The method computes a series of solutions to the fully nonlinear water wave problem involving the Laplace equation with two non-linear free surface boundary conditions (constant pressure and wave height).

Of course, a numerical approach such as the Stream Function can be used to solve linearised equations. In fact, the stream function is considered more accurate than the linear theory when it comes to simulating considerably large but linear waves. Various studies have brought out other advantages of the stream function; it has been shown that the stream function description of non-linear waves is the best when relatively shallow waters are considered (Eecen 2003).

The Fenton model is very similar to the stream function wave theory developed by Dean (1965). It is based on a system of rational approximations by Stokes theory and Cnoidal theory (Fenton 1988). The former makes the assumption that all variation in the horizontal direction can be represented by Fourier series, the coefficients being

expressed as perturbation expansions in terms of a parameter which increases with the wave height i.e.  $H/L$ .

### 4.3.2 Stochastic wave models

In reality, the sea is never in a regular state that has a constant wave height and length. Therefore, there is a need for more developed wave definitions to describe irregular sea waves in OWT design. Irregular sea states however can be defined with a combination of regular sea waves where the energy of the sea state must be the same as the sum of the energies of all subsidiary waves.

The energy distribution of a sea state can be described by a frequency spectrum, it is then also possible to observe the individual contribution of each subsidiary wave to the total energy. According to Lucas and Guedes Soares (2015), the wind force on the waves generates nonlinear interactions between waves which induce energy transfer across energy bands leading to spectra that are similar for a given level of sea state development. The most frequently used spectra to describe waves are; Pierson-Moskowitz spectrum and JONSWAP spectrum. However, there are many more that can be employed and these include; the Constrained NewWave spectrum, Bretschneider spectrum etc.

#### - Pierson-Moskowitz distribution

This was developed by Pierson and Moskowitz and has gained general acceptance for its adequacy to describe the spectra of fully developed sea states and therefore representing the balance between the forcing of the wind and wave conditions (Lucas and Guedes Soares 2015). According to Pierson and Moskowitz (1964), the wave function is of the form;

$$S(\omega) = \frac{\alpha \cdot g^2}{\omega^5} \exp \left[ -\beta \left( \frac{\omega_0}{\omega} \right)^4 \right] \quad (4.12)$$

$$\omega = 2\pi \cdot f \quad ; \quad \omega_0 = \frac{g}{U_{1/3}}$$

where  $f$  is the wave frequency,  $\alpha$  and  $\beta$  are constants, while  $U_{1/3}$  is the velocity of wave at the significant wave height. Figure 4.2 illustrates the wave form at different wind speeds.

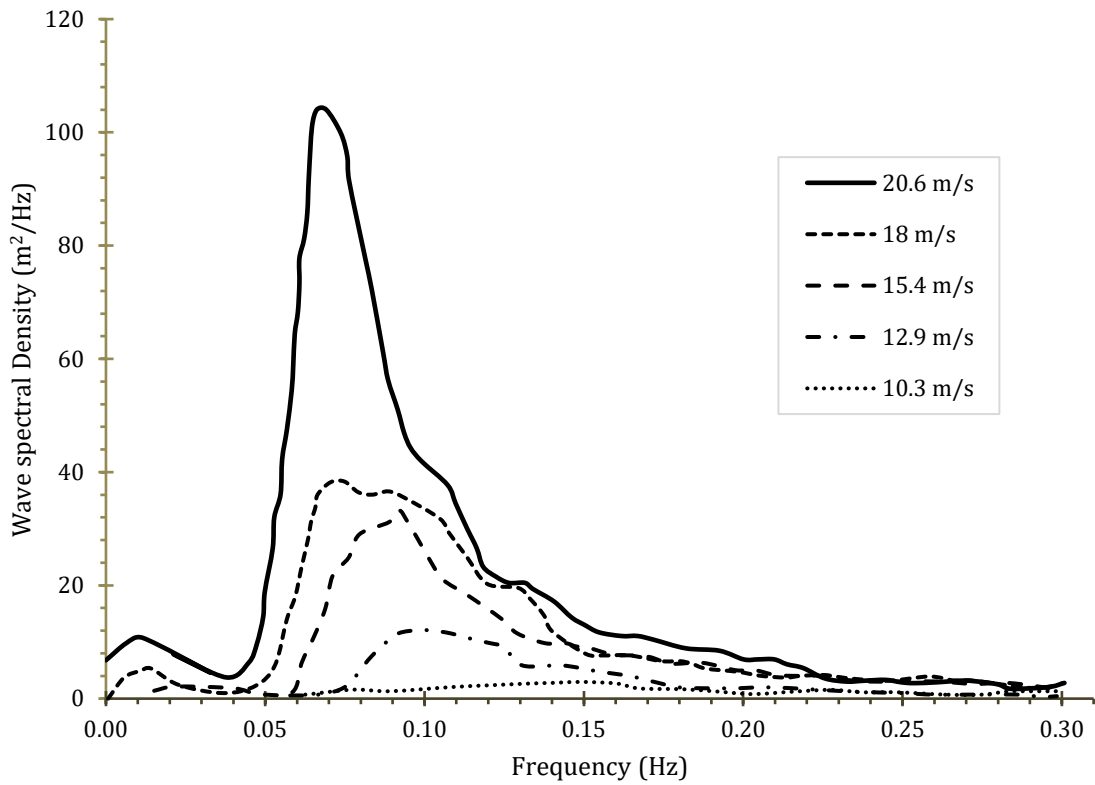


Figure 4.2 Wave spectra of a fully developed sea for different wind speeds.

A fully developed sea is assumed in which the waves are in equilibrium with the wind. This is based on an assumption that the wind blows steadily for a long time over a large area.

- *JONSWAP Spectrum*

This distribution was developed in a joint research project called the Joint North Sea Wave Project. During the project, Hasselmann et al. (1973) observed that a wave spectrum is never fully developed but rather it continues to develop through non-linear, wave-to-wave interactions even for longer periods and distances. This observation resulted into a spectrum of the form;

$$S(\omega) = \frac{\alpha \cdot g^2}{\omega^5} \exp\left[-\frac{5}{4} \left(\frac{\omega_p}{\omega}\right)^4\right] \gamma^r \quad (4.13)$$

$$r = \exp\left[-\frac{(\omega - \omega_p)^2}{2\sigma^2 \omega_p^2}\right] \quad (4.14)$$

$$\omega_p = 22 \left[ \frac{g^2}{U_{10} F} \right]^{1/3} \quad (4.15)$$

In the expressions above,  $F$  is the fetch (distance) over which the wind blows with constant velocity and  $\sigma$  is defined as;

$$\sigma = \begin{cases} 0.07 & \text{for } \omega \leq \omega_p \\ 0.09 & \text{for } \omega > \omega_p \end{cases}$$

Figure 4.3 shows a series of JONSWAP Spectra for different fetches.

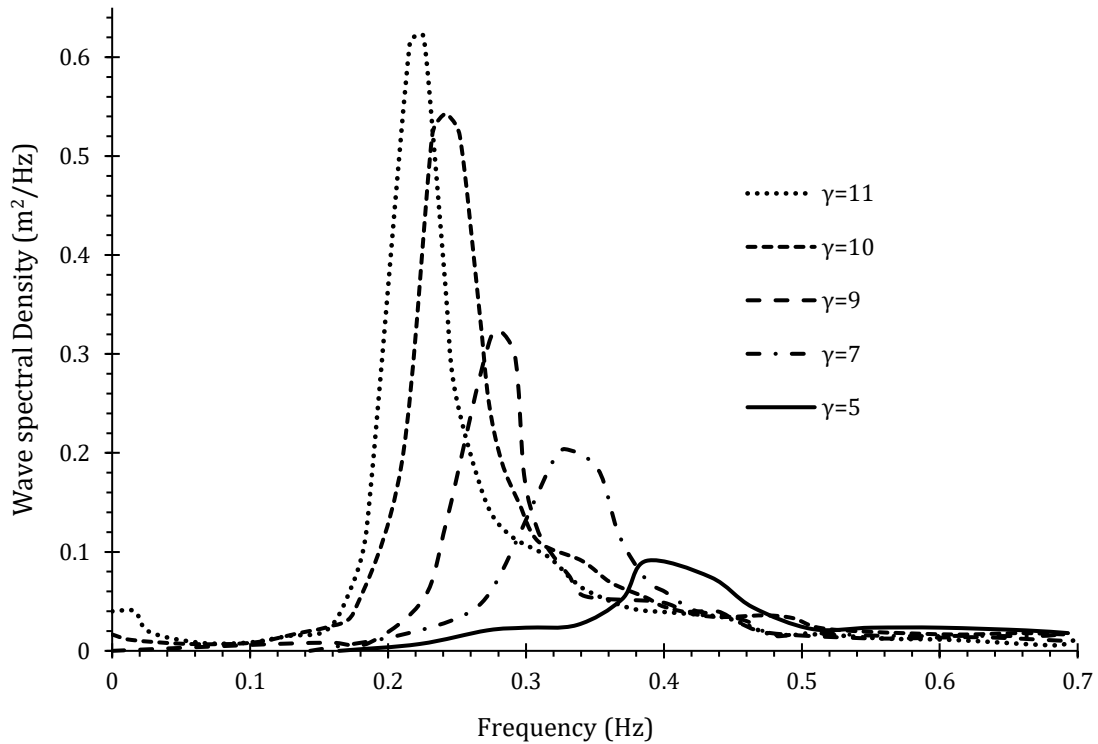


Figure 4.3 Wave spectra of a developing sea for different fetches.

It can be seen that this spectrum is actually a form of the Pierson-Moskowitz distribution enhanced by a peak factor,  $\gamma$ . During the development of the sea states, there is a higher concentration of energy around the dominant frequency and the spectrum appears more peaked than the Pierson-Moskowitz spectrum. This high concentration of energy is effected by a peak enhancement factor included in the expression.

- *New Wave model*

The New Wave theory as discussed by Tromans et al. (1991) involves modelling the sea surface using Gaussian statistics. It accounts for the spectral composition of the sea and can be used as an alternative to both regular waves and full random time domain simulations of lengthy time histories. Tromans et al. (1991) conclude that the theory provides a rational model for the extreme waves of a sea state.

According to Cassidy et al. (2001), the surface elevation around an extreme wave event (for instance a crest) can be modelled by the statistically most probable shape associated with its occurrence. Tromans et al. (1991) show that the surface elevation follows a normal distribution about the most probable shape. The surface elevation is represented by two terms, one deterministic and another random as follows;

$$\eta(\tau) = \alpha.r(\tau) + g(\tau) \tag{4.16}$$

In the expression, the first term represents the most probable value.  $\alpha$  is the crest elevation and  $r(\tau)$  is the autocorrelation function for the ocean surface elevation which is proportional to the inverse Fourier Transform of the surface energy spectrum.  $\tau$  is the relative time of the extreme event to the initial starting time. The second term in the expression is a non-stationary Gaussian process with a mean of zero and standard deviation that increases from zero at the crest to  $\sigma$  (the standard deviation of the underlying sea at a distance away from the crest). Cassidy et al. (2001) observe that as the crest elevation increases, the first term becomes dominant and can be used on its own in deriving the surface elevation and wave kinematics near the crest.

According to Cassidy et al. (2001), the autocorrelation function is defined as

$$r(\tau) = \int_0^{\infty} S_{\eta\eta}(\omega) e^{i\omega\tau} \quad (4.17)$$

From the discussion, it is evident that this wave model has both deterministic and stochastic properties.

### 4.3.3 Hydrodynamic loads

Hydrodynamic loads on an OWT can be computed using a number of methods including Morison equation, potential flow theory, diffraction theory and computation fluid dynamics.

#### 4.3.3.1 Morison equation

Morrison's equation is effective for wave loads on slender structures like monopiles and braced structures and it is defined as;

$$f_t = f_D + f_M = \frac{1}{2} C_D \rho D u |u| + \frac{\pi D^2}{4} C_M \rho \dot{u} \quad (4.18)$$

Where  $f_t$  is the force acting on the structure and  $f_D$  and  $f_M$  are drag and inertia forces respectively,  $C_D$  is the drag coefficient,  $C_M$  is the inertia coefficient and  $u$  is the horizontal water particle velocity while  $\dot{u}$  is the horizontal water particle acceleration.  $\rho$  is the density of water and  $D$  is the diameter of the structure in the water.

The validity of Morison equation is based on the assumption that the structure is small compared to the wave length of the water. Therefore, for massive structures in relatively shallow water, the accuracy of Morrison's equation is compromised since in such cases the structure has an influence on the wave field. It is then more appropriate to use the potential flow theory or modify the Morrison equation (MacCamy-Fuch, cited in Passon and Kühn 2005). In addition, the Morrison equation is limited by its inability to consider surface effects and the three dimensional effects of loads on the structure.

#### 4.3.3.2 Potential flow theory

Potential flow is also known as irrotational flow in which the fluid is considered inviscid (negligible viscous effects). Viscous effects are considered negligible for



flows at a high Reynold's number dominated by convective momentum transfer. Therefore, potential flow is useful for analysing external flows over solid surfaces at considerably high Reynold's number (rapid flow), given that the flows still remain laminar. The principle assumption is when the flow is over a surface is rapid, the viscous boundary layer region that forms next to the surface is very thin and therefore this boundary layer can be neglected. This implies that the potential flow can be assumed to follow the contours of the solid surface, as if the boundary layer was not present.

Potential flow theory is characterised by two concepts; the velocity potential function ( $V = \nabla\phi$ ) and the Stream function ( $V = \nabla\psi$ ). For more details about the mathematics of potential flow, the reader is referred to (White 2003).

#### **4.3.3.3 Diffraction theory**

The diffraction theory can also be used to study the wave forces on a body situated in water. The theory assumes that if the typical dimension of a body is considerably larger in relation to the wavelength and the wave height, then the effects of dispersion due to viscosity can be regarded as negligible and diffraction effects are assumed to be dominant. Another assumption is that the water flow is incompressible and non-rotational, and that the surface tension effects are negligible. A combination of these assumptions means that the flow can be described by a scalar velocity potential which in turn satisfies Laplace's equation within the fluid domain (Le Mehaute 1976).

#### **4.3.3.4 Computational fluid dynamics**

Computational fluid dynamics (CFD) is a branch of physics that deals with numerical modelling and simulation of fluid flow. It thus provides a qualitative prediction of fluid flow through numerical methods and mathematical models which can be implemented into computer solvers to further save time.

### **4.4 Currents**

According to DNV GL (2014a), current velocities can be treated with three different current models including; near surface currents, sub surface currents and near shore currents.

Near surface currents adopt a current profile following a power law that changes the shape of the current profile exponentially with depth. Moreover, sub surface currents employ a linear relationship down to a certain depth and remains stable. Near shore currents, however, assume a fixed current profile independently from the depth.

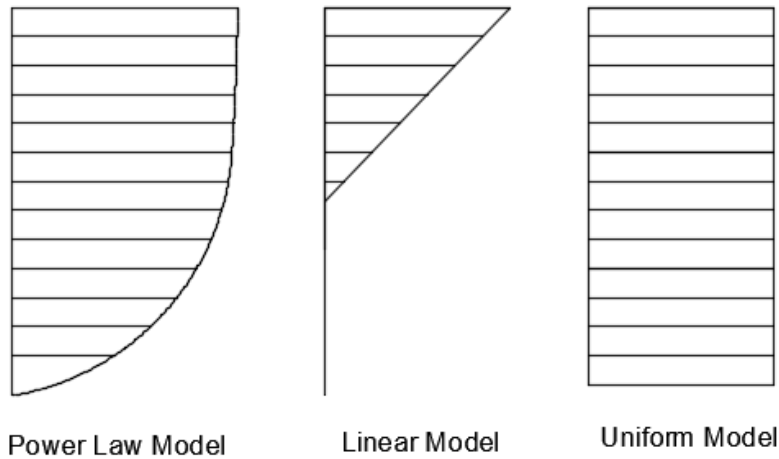


Figure 4.4 Current profiles used in simulation codes

Near surface currents are generated by wind or water waves whereas sub surface currents originate from tidal action. Near shore currents are induced by wind action from the shore. These three forms of currents are represented by velocities of the form;

$$u_{ci} = u_{ci}(z)(\cos \mu_{ci}, -\sin \mu_{ci}, (z=0)) \quad (4.19)$$

Where  $i$  represents the current type in description and  $z$  is the water depth from surface.  $\mu_{ci}$  is the direction from which the current component arrives at the OWT structure. As mentioned in Section 2.3.3, the components can then be combined linearly to obtain the total vector effect;

$$u_c = \sum_{i=1}^n u_{ci} \quad (4.20)$$

Some simulation codes are equipped to deal with all kinds of currents, while others only treat one or two kinds. As will be seen in Section 5.1, some of the codes have no ability to consider the effect of currents whatsoever.

## 4.5 Analysis methods

There are three different methods used in the simulation codes for analysing the dynamic behaviour of offshore wind turbines including, finite element method (FEM), multi-body system and modal analysis method.

Finite element method approach can be utilised by dividing the structure into finite elements and defining the mass and stiffness matrices. In order to obtain precise results, the mesh size should be selected fine enough. Therefore, this method usually results into a great number of degrees of freedom which require high computational time. As Passon and Kühn (2005) mentioned, modal approach has more limits for specific types of structures including jackets compared to FE method. Moreover, FE method enables non-linear material modelling which is necessary to define pile-soil interaction.

The modal analysis method in OWT design is the fastest option compared to the other methods. The structure is defined with a low number of eigenmodes by deselecting some degrees of freedom. Although the modal analysis method is computationally efficient due to having a low number of degrees of freedom, it has some limitations such as having the same type of degrees of freedom and only being capable of linear analysis (Passon and Kühn 2005).

As for the multi-body system, the structure is separated into finite elements in a way similar to the FE method. Apart from that, those elements usually consist of rigid bodies that are connected together with elastic joints. According to Passon and Kühn, the multi-body system associates the advantages of the modal approach and FE method by being capable of non-linear analysis while keeping the set of equations considerably small (2005).

The calculations for OWT structures can be done in both time domain and frequency domain in the context of different benefits. Time domain is the more frequently adopted calculation method in the industry in which the response of the structure (stress, strain, moment, deflection, etc.) is extracted for a certain time interval. However, since offshore environmental conditions (wind speed, wind direction, wave frequency and length, etc.) vary significantly over time, fatigue analysis for OWTs generates very time-consuming calculations. Therefore, calculations in the frequency domain become more efficient (van Engelen & Braam 2004). Moreover, frequency domain analysis is a good preliminary study to understand the response of the structure in a certain environment and define the frequency interval which the OWT structure must stay in. In order to perform a frequency domain analysis, sufficient data is needed to describe the behaviour of the environmental effects.

## **4.6 Analysis techniques**

Analysis approaches also play an important role in OWT design. The most common design approaches can be classified into three categories such as; sequential approach, semi-coupled loads approach and fully coupled loading approach.

### **4.6.1 Sequential approach technique**

In the sequential approach, the OWT structure is separated into its subsystems such as blades, rotor, tower and support structure. The core idea behind this approach is that each subsystem of the OWT requires different assumptions and approaches, therefore, it is more time efficient to treat them in isolated models.

*Such an approach introduces the necessity to exchange information regarding structural properties of all relevant subsystems as well as loads at one or more predefined interfaces, often the connection between the tower and foundation subsystem. (Passon and Branner 2013, p.435)*

Moreover, Zarafshan and Hall (2015) explain the application process as following;

- First, wave loads are applied to the substructure and foundation and then the internal forces at the interface are transferred to aero-elastic models.
- Secondly, wind loads are applied to the aero-elastic model and resultant force at the tower-substructure interface is recorded.

- Thirdly, the wave load is applied with the obtained load from second step (the load to the support structure and internal forces at each element can be checked).

In Figure 4.5, the whole process of the sequential approach is summarised.

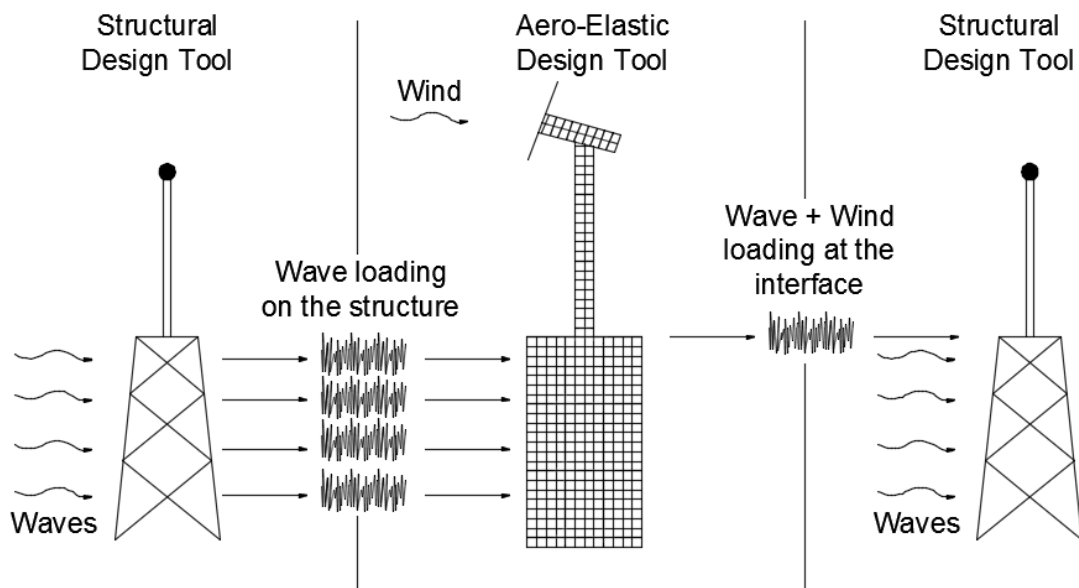


Figure 4.5 Sequential approach for design of support structure

#### 4.6.2 Semi-coupled approach technique

The main difference with this method compared to the sequential method is that the wind and the wave loads are applied together to the substructure model with proper soil boundary conditions to get the reaction force at the tower-substructure interface. In other words, the first and the second steps in sequential approach are merged together. Likewise, in sequential approach, the next step is applying the wave loads to obtain the forces in members.

#### 4.6.3 Fully coupled approach technique

This analysis approach models the OWT as a whole unit including the blades, rotor, tower, substructure and foundation. It takes all environmental effects such as wind, wave, current and soil properties into account simultaneously and investigates the response of the integrated system. Zarafshan and Hall asserted that although the fully coupled approach gives more developed results, it requires an advanced compatibility between aero-elastic design tools and offshore design tools (2015).

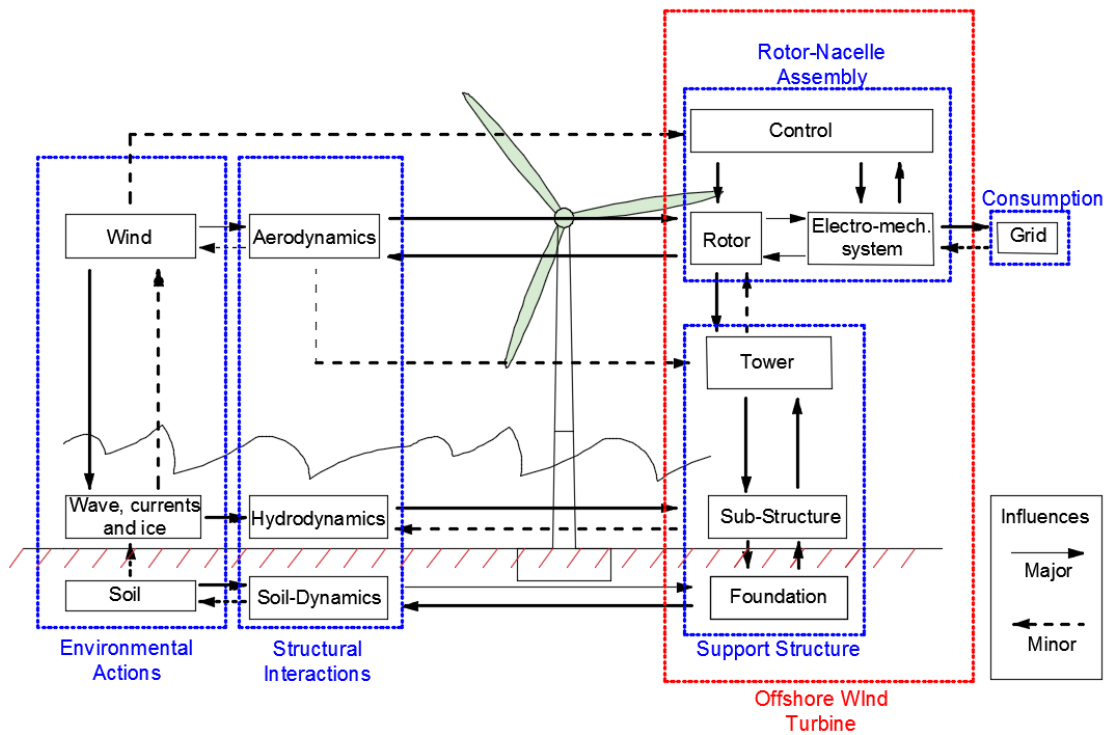


Figure 4.6 Integrated system with environmental effects

## 5 Simulation Codes and Classification

In this chapter the reader is introduced to some of the current simulation codes used in OWT design in connection with Chapter 4 that presents the principles used in each code, respectively. Moreover, the classification of codes that expresses the design principles and methodologies is shown.

### 5.1 Current simulation codes in use

#### 5.1.1 FAST (Fatigue, Aerodynamics, Structures and Turbulence)

Fast was created by the National Renewable Energy Laboratory (NREL) of USA and has evolved over two decades to increase its capabilities. The latest version FAST v8 incorporates several modules, such as: AeroDyn (ADAMS/WT) for aerodynamics; ServoDyn for electrical drive dynamics; SubDyn for structural dynamics; HydroDyn for hydrodynamics; MAP for mooring dynamics and IceFloe for ice loads, which is a big change in the architecture of the software compared to FAST v7. Main features of FAST are shown below:

- Prediction of fatigue loads for both two and three bladed systems.
- Aeroacoustic noise predictions.
- Ability of defining lateral offset, rotor furling and yaw control.
- Dynamic stationary simulations

The general specifications of the code are shown in Table 5.1.

Table 5.1 The main specifications of FAST.

	Specification	Adopted Principle	Reference
<b>Environmental Actions</b>	Deterministic Wave	Airy and possible modifications for surface effects (Airy <sup>+</sup> )	Jonkman et al. (n.d.)
	Stochastic Wave	Pierson-Moskowits, JONSWAP, user defined	
	Sea Current	Possible to define	
	Hydrodynamic Loads	Morison equation (Strip-Theory), Potential Flow Theory	
	Aerodynamic Loads	Blade Element Momentum Theory, Generalised Dynamic Wake and Dynamic Stall	J.M. Jonkman, G.J. Hayman, B.J. Jonkman (n.d.)
<b>Structural Modelling</b>	Analysis Method	Modal analysis and combined modal-multi body dynamic analysis	Passon and Kühn (2005)
	Analysis Technique	Fully coupled approach	Jonkman and Jonkman (2015)
	Time/Frequency Domain Calculations.	Time domain	
	Foundation Models	Apparent fixity length	Passon and Kühn (2005)
Tower	Mono-tower, space frame		
Foundation	Monopile, space frame, gravity based and floating		
<b>Support Structure Types</b>	Foundation Support	Monopile, general piles suction caisson	Jonkman and Jonkman (2015)
	Programming Language	Intel® Visual Fortran Composer	
	License and OS	Open source / MS Windows, Linux	

### 5.1.2 Flex5

Flex5 is an open-source, extensively used offshore wind turbine simulation code programmed in Turbo Pascal in early 1990s. The code mainly has the design capabilities for monopile, mono-tower OWT structures. In terms of environmental effects, similar to most of the other OWT simulation codes waves can be defined either as deterministic or stochastic waves. Since there is a lack of user's manual and the software requires a license key, specifications of Flex5 could not be collected. Therefore, previous studies were used to comprise the features of Flex5 in Table 5.2.

Table 5.2 The main principles of Flex5

	Specification	Adopted Principle	Reference
Environmental Actions	Deterministic Wave	Airy and possible modifications for surface effects (Airy <sup>+</sup> ), and Stream	Passon and Kühn (2005)
	Stochastic Wave	Pierson-Moskowitz, JONSWAP, user defined, Airy <sup>+</sup>	
	Sea Current	Sub-surface	
	Hydrodynamic Loads	Morison equation	
	Aerodynamic Loads	Blade Element Momentum Theory	Hillmer et al. (2007)
Structural Modelling	Analysis Method	Modal Analysis	Passon and Kühn (2005)
	Analysis Technique	Fully coupled	Ramachandran et al. (2013)
	Time/Frequency Domain Calculations.	Time domain	Hillmer et al. (2007)
	Foundation Models	Apparent Fixity Length	Passon and Kühn (2005)
Tower	Mono-tower		
Foundation	Monopile		
Support Structure Types	Foundation Support	Monopile	-
	Programming Language	Turbo Pascal	
	License and OS	Proprietary / MS Windows	

### 5.1.3 Bladed

This software was developed and is maintained by DNV-GL-Energy, an international company that certifies designs of OWTs. The latest version of the software is 4.6. This software is a full industrial standard package used for the design and certification of onshore and offshore turbines whose main applications include; preliminary wind turbine design, detailed design, component specification and certification of wind turbines. Bladed v4.6 has a sophisticated user interface and its main features are;

- Specification of all wind turbine parameters
- Specification of environmental inputs and load cases
- Rapid calculation of steady-state performance characteristics
- Dynamic simulations covering all turbine states
- Post-processing of results
- Presentation of graphs and reports

The specifications of Bladed are outlined in Table 5.3.



Table 5.3 The main principles of Bladed

	Specification	Adopted Principle	Reference
<b>Environmental Actions</b>	Deterministic Wave	Airy <sup>+</sup> , Stream function.	DNV GL (2014a), DNV GL (2014b), Passon and Kühn (2005)
	Stochastic Wave	Pierson-Moskowitz/JONSWAP and Airy <sup>+</sup> , user defined, Constrained New Wave	
	Sea Current	Subsurface, near surface, near shore each separately or in combination.	
	Hydrodynamic Loads	Morison Equation.	
	Aerodynamic Loads	Blade element momentum theory and generalised dynamic wake theory including dynamic stall effects.	DNV GL (2014a), DNV GL (2014b),
<b>Structural Modelling</b>	Analysis Method	Modal analysis combined with modal–multi body dynamic analysis.	DNV GL (2014a)
	Analysis Technique	Fully coupled	DNV GL (2014a)
	Time/Frequency Domain Calculations.	Time and frequency domain	DNV GL (2014a)
	Foundation Models	Apparent fixity length and distributed springs model (treated as equivalent point springs).	DNV GL (2014b), Passon and Kühn (2005)
Tower	Mono-tower, arbitrary space frame structure,		
<b>Support Structure Types</b>	Foundation	Monopile, gravity base, floating structures (with mooring lines),	DNV GL (2014b), Passon and Kühn (2005)
	Foundation Support	Monopile, suction caisson, general pile	
	Programming Language	VB6 with WPF interface, Fortran and C++ code engine	DNV GL (2014b)
License and OS	Commercial / MS Windows 7 or higher		

### 5.1.4 ADCoS

ADCoS stands for Aeroelastic and Dynamic Computation of Structures. This code was developed by AeroDynamik Consult GmbH, an engineering consultancy service provider related to wind energy. It has been in development since 1996 and its main features include;

- Fatigue calculations

- Simulation of non-linear foundations. Nonlinear soil behaviour can be calculated from commercial software like ALLPILE, L-PILE and added to ADCoS as a non-linear pile element.
- Being able to define “Super-Element” in the model to describe any type of structure by defining its mass and stiffness matrices.

The software uses ANSYS to define structural parameters and geometry; and use ASAS module to calculate the loads from sea states. This software computes the dynamic equation of motion using the finite element method. Each element is treated as a 2 node-beam with each node having 6 degrees of freedom. In Table 5.4 the main specifications of ADCoS are listed.

Table 5.4 The main principles of ADCoS

	<b>Specification</b>	<b>Adopted Principle</b>	<b>Reference</b>
<b>Environmental Actions</b>	Deterministic Wave	Airy and possible modifications for surface effects (Airy <sup>+</sup> ) and Stream	Robertson et al. (2014)
	Stochastic Wave	Pierson-Moskowitz user defined, JONSWAP and Airy <sup>+</sup>	Passon and Kühn (2005)
	Sea Current	Possible to define	Vorpahl et al. (2007)
	Hydrodynamic Loads	Morison equation	Robertson et al. (2014)
	Aerodynamic Loads	Blade element momentum theory, generalised dynamic wake and dynamic stall	Jonkman and Musial (2010)
<b>Structural Modelling</b>	Analysis Method	Finite element method	Vorpahl et al. (2007)
	Analysis Technique	Sequential approach	
	Time/Frequency Domain Calculations.	Time domain	
	Foundation Models	Apparent fixity length and discrete springs and user defined	
<b>Support Structure Types</b>	Tower	Mono-tower and space frame	Passon and Kühn (2005)
	Foundation	Monopile, space frame and gravity base	
	Foundation Support	Monopile, general pile	
	Programming Language	FORTRAN90	
	License and OS	Commercial / MS Windows, Linux	

### 5.1.5 ADAMS/WT & AeroDyn

ADAMS/WT (Wind Turbine) is an application-specific version of the well-known, general-purpose mechanical system simulation package ADAMS (Automated Dynamic Analysis of Mechanical Systems). According to Andrew and Todd (1996), it consists of two main components.

1. A set of ADAMS/view macros and panels which create a customised, high automated pre-processor for horizontal-axis wind turbine modelling
2. A set of ADAMS/Solver Fortran subroutine for computing the highly nonlinear unsteady air loads on the turbine blades

Specifications of ADAMS/WT & AeroDyn are shown in Table 5.5

Table 5.5 Specifications of ADAMS/WT & AeroDyn

	Specification	Adopted Principle	Reference
<b>Environmental Actions</b>	Deterministic Wave	Airy.	Andrew and Todd (1996)
	Stochastic Wave	Pierson-Moskowitz/JONSWAP and Airy, user defined	
	Sea Current	Not defined	Passon and Kühn (2005)
	Hydrodynamic Loads	Potential flow theory	
	Aerodynamic Loads	Blade element momentum theory and generalised dynamic wake theory including dynamic stall effects.	Hansen and Laino (2002)
<b>Structural Modelling</b>	Analysis Method	Multi body dynamic analysis.	Andrew and Todd (1996)
	Analysis Technique	Time domain	Jonkman and Buhl (2005)
	Time/Frequency Domain Calculations.	Sequential approach	
	Foundation Models	Apparent fixity length and distributed springs model.	Passon and Kühn (2005)
Tower	Mono-tower, arbitrary space frame structure,		
Foundation	Monopile, gravity base, floating structures, Arbitrary space frame structure.		
<b>Support Structure Types</b>	Foundation Support	Monopile, general pile	Hansen and Laino (2002)
	Programming Language	Fortran	
	License and OS	Commercial / MS Windows, Linux	

NREL no longer supports ADAMS/WT and does not produce any more updates of it. Instead, the functionality of ADAMS/WT has been replaced with an MSC.ADAMS pre-processor that is now built into the FAST code (see Section 5.1.11). The FAST-to-ADAMS pre-processor has all the functionalities of ADAMS/WT plus much more. It works with the updated ADAMS-to-AeroDyn (A2AD) interface routines that are part of the FAST modules.

### **5.1.6 HAWC2**

HAWC2 (Horizontal Axis Wind turbine simulation Code 2<sup>nd</sup> generation) is an aeroelastic code intended for analysing offshore wind turbine structures in time domain. According to Larsen and Hansen (2007), the core of the code was developed mainly within the years 2003-2006, by the Aeroelastic Design Research Program at DTU Wind Energy, DTU Risø Campus in Denmark. HAWC2 is developed and distributed by DTU Wind Energy and has been used in numerous research projects and industrial applications. HAWC2 has a large number of users and is used for design and verification purposes. Larsen and Hansen (2007) also asserted that the code is based on a multibody formulation where each body is an assembly of Timoshenko beam elements. The principles of HAWC2 can be seen in Table 5.6.

Table 5.6 The main principles of HAWC2

	Specification	Adopted Principle	Reference
<b>Environmental Actions</b>	Deterministic Wave	Airy <sup>+</sup> , Stream Function.	Larsen and Hansen (2007)
	Stochastic Wave	Pierson-Moskowitz/JONSWAP and Airy <sup>+</sup>	
	Sea Current	Constant, power law	
	Hydrodynamic Loads	Morison equation	
	Aerodynamic Loads	Blade element momentum theory and generalised dynamic wake theory including dynamic stall effects.	
<b>Structural Modelling</b>	Analysis Method	Multi body dynamic analysis	Passon and Kühn (2005)
	Analysis Technique	Fully coupled approach	Skaare et al. (2006)
	Time/Frequency Domain Calculations.	Time domain.	Larsen and Hansen (2007)
	Foundation Models	Apparent fixity length, Distributed springs model, User defined.	
<b>Support Structure Types</b>	Tower	Mono-tower, arbitrary space frame structure,	Passon and Kühn (2005)
	Foundation	Monopile, gravity base, floating structures, arbitrary space frame structure.	
	Foundation Support	Monopile, general pile, user defined.	
	Programming Language	Fortran	Larsen and Hansen (2007)
	License and OS	Commercial / MS-Windows, Linux, Mac	

### 5.1.7 ASHES

Ashes is a calculation tool for OWT design developed by Sismis AS (Norway). Ashes is able to do time domain analysis which comes with a very user friendly interface to show features of the model, such as loadings, deformations of the elements and blade geometry etc. (Thomassen et al. 2012). The software is still under development, there is no soil interaction definitions yet, but it is planned to include geotechnical properties in the future versions of the software. The main specifications of Ashes are outlined in Table 5.7.

Table 5.7 The main principles of ASHES

	Specification	Adopted Principle	Reference
Environmental Actions	Deterministic Wave	Airy <sup>+</sup> , Stream Function.	Robertson et al. (2014)
	Stochastic Wave	JONSWAP	-
	Sea Current	Not applicable	-
	Hydrodynamic Loads	Morison equation	Robertson et al. (2014)
	Aerodynamic Loads	Blade element momentum theory, dynamic stall	
Structural Modelling	Analysis Method	FEM	-
	Analysis Technique	Fully coupled approach	
	Time/Frequency Domain Calculations.	Time domain	Simis (2015)
	Foundation Models	No soil interaction	-
Support Structure Types	Tower	Mono-tower, space frame	
	Foundation	Monopile, space frame, floating structure	
	Foundation Support	Monopile, general pile	
	Programming Language	Visual studio, C++	
	License and OS	Commercial / MS-Windows	

### 5.1.8 TURBU Offshore

Turbu Offshore is developed by ECN (Energy research Centre of the Netherlands) for frequency domain analysis. The code is mainly capable of designing mono-tower and monopile structures. It is a package of software modules in the MATLAB programming language. The features of the code include;

- Ability to execute load calculations via power spectral density functions (frequency domain)
- Longitudinal turbulence
- Integrated linear model
- Rotational coupling rotor, tower (Coleman transformation)
- Multibody bending and torsion for tower and blades
- Lumped rotor shaft bending torsion
- Dynamic wake model
- Pitch and generator torque control loops

According to Savenije and Peeringa (2009), this code is a complementary tool developed for other time domain software and it has the following functionalities outlined in Table 5.8.

Table 5.8 Specifications of TURBU Offshore

	Specification	Adopted Principle	Reference
Environmental Actions	Deterministic Waves	Airy	Savenije and Peeringa (2009)
	Stochastic Waves	Pierson-Moskowitz/JONSWAP and Airy, User defined	
	Sea Current	Accounted for	
	Hydrodynamic Loads	Morison equation	
	Aerodynamic Loads	Blade element momentum theory.	
Structural Modelling	Analysis Method	Multi body dynamics	
	Analysis Technique	Fully coupled approach	
	Time/Frequency Domain Calculations.	Frequency domain	
	Foundation Models	Apparent fixity length, Distributed springs model	
Support Structure Types	Tower	Mono-tower	
	Foundation	Monopile	
	Foundation Support	Monopile	
	Programming Language	MATLAB	van Engelen and Braam (2004)
	License and OS	Proprietary / Windows	

### 5.1.9 FOCUS6

FOCUS6 is an integrated modular tool for designing wind turbines and wind turbine components developed by WMC and includes software modules of ECN. It has been in use for nearly two decades now and it is being used by wind turbine OEMs, engineering companies for blade design, certification bodies, research institutes and universities. FOCUS6 integrates onshore and offshore wind turbine design with blade and support structure design (Knowledge Centre WMC 2016).

FOCUS6 has the following features;

- Interactive3D blade modeller
- Ultimate and fatigue strength analysis
- Modal analysis
- Finite element export (to ANSYS, MSC Marc, MSC Nastran, Abaqus)
- Finite element solver
- GL/GH Bladed4 interface
- Integrated design approach in which the wind turbine and support structure are modelled and analysed as a whole.
- Offshore load generator

- Graphical post processing
- Aero elastic and hydro elastic structural design.
- 3D visualisation of results.

In operation, FOCUS6 integrates a number of module programs to analyse a given wind turbine structure. For instance, it uses the *PHATAS* program (Lindenburg 2005) to compute mechanical loads on wind turbines. Input for *PHATAS* comprises of environmental conditions such as wind, waves, currents, etc. To generate random linear waves to be used as input for the *PHATAS* program, Focus6 uses a program called *CurrentROWS* (Random Ocean Wave Simulation) developed by ECN (Peeringa 2013). In a similar fashion, the program *Streamfunction* is used to calculate the wave kinematics of deterministic nonlinear waves (Eecen 2003).

The program *SWIFT* (Simulation of Wind Fields in Time) is used to numerically simulate stochastic wind fields in the time domain whose resulting wind speed time series can be used as input for any horizontal axis wind turbine design tool (D.Winkelaar 1992). Similarly, the program *Blademode* is used to carryout aero elastic analysis of the turbine (Lindenburg & Holierhoek 2013).



Table 5.9 Specifications of FOCUS6

	Specification	Adopted Principle	Reference
<b>Environmental Actions</b>	Deterministic Waves	Airy <sup>+</sup> , Stream Function and Fenton's model	Peeringa (2005), Eecen (2003)
	Stochastic Waves	Pierson-Moskowitz/JONSWAP and Airy, User defined.	Eecen (2003)
	Sea Current	Uniform current	Peeringa (2013)
	Hydrodynamic Loads	Morison equation, Potential Flow Theory	Eecen (2003)
	Aerodynamic Loads	Blade element momentum theory, for tip loss with dynamic and oblique inflow correction. Dynamic stall effects included too.	Lindenburg & Holierhoek (2013)
<b>Structural Modelling</b>	Analysis Method	FEM	Remco Brood, <i>Email correspondence</i> , (April 25, 2016)
	Analysis Technique	Coupled(Integrated)	
	Time/Frequency Domain Calculations.	Time domain	D.Winkelaar (1992)
	Foundation Models	Coupled linear spring accounting for tilting and translation. Includes p-y modelling.	
<b>Support Structure Types</b>	Tower	Mono-tower, arbitrary space frame	Remco Brood, <i>Email correspondence</i> , (April 25, 2016)
	Foundation	Monopile, gravity base, arbitrary space frame, floating structures	
	Foundation Support	Monopile, general pile, user defined	
	Programming Language	Fortran, C#	
	License and OS	Commercial & Academic / Windows	

### 5.1.10 OneWind

OneWind is an integrated OWT simulation tool that uses a special modelling library to define and analyse structures. The language known as Modelica is an open source object-oriented language for physical modelling of large, complex and heterogeneous systems involving mechanical, electrical, hydraulic control and state machine subsystems (Modelica-Association 2012). According to OneWind (2016), the highlighted abilities of the software can be written as below;

- Being able to pre-process the functionality for preliminary design

- Considering the steady-state loading conditions
- Element based design
- Refactoring
- Optimized load simulation

The principles used in OneWind are outlined in Table 5.10

Table 5.10 The principles used in OneWind

	Specification	Adopted Principle	Reference
Environmental Actions	Deterministic Wave	Airy <sup>+</sup> , Stream Function	Vorpahl et al. (2011)
	Stochastic Wave	User defined	
	Sea Current	Accounted for (uniform in one direction)	Paul Robert Feja, <i>Email correspondence</i> , (March 22, 2016)
	Hydrodynamic Loads	Morison equation	Vorpahl et al. (2011)
	Aerodynamic Loads	Blade element momentum theory, generalised dynamic wake with dynamic stall	
Structural Modelling	Analysis Method	Multi body dynamics and FEM	Feja, <i>Email correspondence</i> , (March 22, 2016)
	Analysis Technique	Fully coupled approach	
	Time/Frequency Domain Calculations.	Time domain	
	Foundation Models	Apparent fixity length, distributed springs model	
Support Structure Types	Tower	Mono-tower, space frame	Feja, <i>Email correspondence</i> , (March 22, 2016)
	Foundation	Monopile, gravity base, space frame, floating structures	
	Foundation Support	Monopile, general pile	
	Programming Language	Modelica based C	
	License and OS	Commercial / Windows, Linux	

### 5.1.11 USFOS-vpOne

USFOS is a computer program developed by SINTEF marintek and the Norwegian University of Science and Technology (NTNU) through joint industry projects sponsored by oil companies and engineering consultants. It is mainly used for nonlinear static and dynamic analysis of space frame structures. It is used for integrity assessment, collapse analyses and accidental load analyses of offshore jacket structures, topsides, jackups and other framed structures, intact or damaged. The program accurately simulates the collapse process, from the initial yielding to the

formation of a complete collapse mechanism of the structure (SINTEF marintek & NTNU 2016). Since USFOS has no modules for hydrodynamic and aerodynamic loadings, there is a need of hydro-servo-aerodynamic simulation code to combine with. For OWT design, estimated wind and wave loads can be calculated with vpOne, which is a hydro-servo-aerodynamic tool developed by Virtual Prototyping, and applied to USFOS. The main principles of USFOS-vpOne are outlined in Table 5.11.

Table 5.11 Specifications of USFOS-vpOne

	<b>Specification</b>	<b>Adopted Principle</b>	<b>Reference</b>
<b>Environmental Actions</b>	Deterministic Wave	Airy <sup>+</sup> , Stream function, Stokes 5 <sup>th</sup> order theory.	Sintef Group (2010)
	Stochastic Wave	Pierson-Moskowitz/JONSWAP and Airy <sup>+</sup> , Grid wave (Computational fluid dynamics)	
	Sea Current	Accounted for, represented by a velocity vector.	
	Hydrodynamic Loads	Morison equation	
	Aerodynamic Loads	Blade element momentum theory and dynamic stall	Robertson et al. (2014)
<b>Structural Modelling</b>	Analysis Method	Finite Element Method	MARINTEK (1999)
	Analysis Technique	Sequential	
	Time/Frequency Domain Calculations.	Time domain	Sintef Group (2010)
	Foundation Models	Distributed springs model (springs in form of discs representing soil layers).	MARINTEK (2009)
Tower	Mono-tower, arbitrary space frame		
Foundation	Monopile, arbitrary space frame, floating structures.		
<b>Support Structure Types</b>	Foundation Support	Monopile, general pile	
	Programming Language	UNIX	MARINTEK (1999)
	License and OS	Commercial / MS Windows, Linux, Mac	(Usfos n.d.)

### 5.1.12 SESAM

This is another software package distributed by DNV GL. It is used for designing and analysing fixed and floating offshore and maritime structures. Modelling, analysis and results processing are performed in the same graphical user interface. According to DNV GL (2016), Some of the features of program include:

- Concept modelling and automated processes that support the need for fast design iterations.
- Static and dynamic structural analysis incorporating environmental load calculation (wind, waves, current).
- Analyses are run by the finite element methodology where beams and plates are all connected together.
- One graphical user interface for modelling, FE analysis and results evaluation.
- One common model used for all phases from initial to final design, as well as for modifications, repair and life extension.
- Wide range of analyses; code checking load-out, transportation, launching, installation, fatigue, earthquake, progressive collapse, accidents, explosions.
- It has the capability to import data from other FEA or CAD systems.

Table 5.12 Specifications of SESAM

	<b>Specification</b>	<b>Adopted Principle</b>	<b>Reference</b>
<b>Environmental Actions</b>	Deterministic Wave	Airy <sup>+</sup> , Stream function, Stokes theory, Cnoidal and NewWave theory.	Laurens Alblas, <i>Email correspondence,</i> (May 09, 2016)
	Stochastic Wave	Pierson-Moskowitz/JONSWAP and Airy, User defined	
	Sea Current	Applicable	
	Hydrodynamic Loads	Morison equation (for beam structures), Wave interaction and diffraction approach using panel models (for shell models)	
	Aerodynamic Loads	Wind turbine loads need to be calculated via a wind turbine load calculation tool (e.g. Bladed, BHawC, HawC2, Flex5 or other)	
<b>Structural Modelling</b>	Analysis Method	Multi body dynamics	
	Analysis Technique	Fully integrated (Coupled) analysis, Super-element analysis and Sequential analysis	
	Time/Frequency Domain Calculations.	Both frequency and time domain.	
	Foundation Models	Distributed linear or non-linear soil springs.	
<b>Support Structure Types</b>	Tower	Mono-tower, arbitrary space frame	
	Foundation	Monopile, arbitrary space frame, floating structures, gravity base	
	Foundation Support	Monopile, general pile,	
	Programming Language	Fortran, C#, C++ and .NET.	
	License and OS	Commercial or academic / Windows.	

## 5.2 Comparison of codes

In this section, readers are introduced to the comparison study of the simulation codes mentioned in Section 5.1. The comparison study of the simulation codes is outlined in Table 5.13 in terms of the principles adopted to define the environmental actions, the methods used in structural modelling and the types of support structure that can be modelled.

Specification	FAST	FLEX5	BLADED	ADCoS	ADAMS & AeroDyn	HAWC2	ASHES	TURBU OFFSHORE	FOCUS6	One Wind	USFOS	SESAM	
Deterministic Wave	Airy <sup>+</sup>	Airy <sup>+</sup> , ST	Airy <sup>+</sup> , ST	Airy <sup>+</sup> , ST	Airy <sup>+</sup>	Airy <sup>+</sup> , ST	Airy <sup>+</sup> , ST	Airy	Airy <sup>+</sup> , ST, FN	Airy <sup>+</sup> , ST	Airy <sup>+</sup> , ST, STK	Airy <sup>+</sup> , ST, CD, NW, STK	Environmental Actions
Stochastic Wave	PM, UD, JS, Airy <sup>+</sup>	PM, UD, JS, Airy <sup>+</sup>	PM, JS, UD, CN, Airy <sup>+</sup>	PM, UD, JS, Airy <sup>+</sup>	PM, UD, JS, Airy <sup>+</sup>	PM, JS, Airy <sup>+</sup>	JS	PM, UD, JS, Airy	PM	UD	PM, JS Airy <sup>+</sup> CFD	PM, JS Airy <sup>+</sup> UD	
Sea Current	Applicable	Sub Surface	Applicable	Applicable	Not Applicable	Applicable	Not Applicable	Applicable	Applicable	Applicable	Applicable	Applicable	
Hydrodynamic Loads	ME, PFT	ME	ME	ME	PFT	ME	ME	ME	ME, PFT	ME	ME	ME, WI	
Aerodynamic Loads	BEM, GDW+DS	BEM	BEM, GDW+DS	BEM, GDW+DS	BEM, GDW +DS	BEM, GDW +DS	BEM+ DS	BEM	BEM+ DS	BEM, GDW +DS	BEM+ DS	External Source	
Analysis Method	MA + MBS	MA	MA + MBS	FEM	MBS	MBS	FEM	MBS	FEM	MBS + FEM	FEM	MBS	
Analysis Technique	FC	FC	FC	SA	SA	FC	FC	FC	FC	FC	SA	FC, SA, SE	
Time/Freq. Domain Calculations	TD	TD	TD, FD	TD	TD	TD	TD	FD	TD	TD	TD	TD, FD	
Foundation Models	AF	AF	AF, DiS	AF, DiS, UD	AF, DiS	AF, DiS, UD	-	AF, DiS	CS	AF, DiS	DiS	CS, DiS	
Tower	MT, SF	MT	MT, SF	MT, SF	MT, SF	MT, SF	MT, SF	MT	MT, SF	MT, SF	MT, SF	MT, SF	Support Structure Types
Foundation	MP, SF, GB, FL	MP	MP, GB, FL, SF	MP, SF, GB	MP, SF, GB, FL	MP, SF, GB, FL	MP, SF, FL	MP	MP, SF, FL	MP, GB, SF, FL	MP, SF, FL	MP, GB, SF, FL	
Foundation Support	MP, GP, SC, GB	MP	MP, GP, SC	MP, GP	MP, GP	MP, GP, UD	MP, GP	MP	MP, GP, UD	MP, GP	MP, GP	MP, GP	
Programming Language	Fortran	Turbo Pascal	Fortran VB, C++	Fortran	Fortran	Fortran	Visual Studio, C++	Matlab	Fortran, C#	Modellica, C	UNIX	Fortran, C C++, .NET	
License and Operating S.	OS/ Win, Linux	PP/ Win	CM / Win	CM/Win, Linux	CM/ Win, Linux	CM/ Win, Linux, Mac	CM/ Win	PP/ Win	CM/ Win	CM/ Win, Linux	CM/ Win, Linux, Mac	CM / Win	
AIRY <sup>+</sup>	-Airy and possible modifications for surface effects	CN	- Constrained New Wave	FL	- Floating Structure	ME	- Morison Equations	SF	- Space Frame				
AF	- Apparent Fixity Length	CM	- Commercial	GDW	- Generalised Dynamic Wake	MP	- Monopile	ST	- Stream Function				
BEM	- Blade Element Momentum Theory	CS	- Coupled springs	GB	- Gravity Base Structure	MT	- Mono Tower	STK	- Stokes				
CD	- Cnoidal	DS	- Dynamic Stall	GP	- General Pile	NW	- NewWave	TD	- Time Domain				
CFD	- Computational Fluid Dynamics	DiS	- Distributed Springs	JS	- JONSWAP	OS	- Open Source	UD	- User Defined				
		FC	- Fully Coupled	MA	- Modal Analysis	PFT	- Potential Flow Theory	PM	- Pierson-Moskowitz				
		FN	- Fenton's Model	MBS	- Multi Body Dynamic Analysis	SA	- Sequential Analysis	PP	- Proprietary				
		FD	- Frequency Domain			SE	- Super Element Analysis	VB	- Visual Basic				
		FEM	- Finite Element Method			SC	- Suction Caisson	WI	- Wave Interaction				

Table 5.13 Comparison of OWT simulation codes

## 6 OWT Design Process

This chapter discusses the procedure of obtaining design loads from site data based on the guidelines provided by DNV(2010), IEC (2005) and (IEC 2009). The chapter also focuses on the main design loads considered in the context of the case study in Chapter 7. The load cases considered in the design are extracted from DNV (2014).

### 6.1 Design environment loads

#### 6.1.1 Wind loads

The wind climate of a given site is normally described using statistical distributions which are then used to compute the 10-minute mean wind speed at hub height. According to DNV (2010), the wind profile against an OWT structure can be obtained in terms of the 10 minute mean wind speed using the following equation;

$$U(z) = U(H) \left( 1 + \frac{\ln\left(\frac{z}{H}\right)}{\ln\left(\frac{H}{z_0}\right)} \right) \quad (6.1)$$

$U(H)$  is the 10-minute mean wind speed at a certain height  $H$  while  $U(z)$  is the sought mean wind speed at a height  $z$ .  $z_0$  is the terrain roughness parameter based on Table 2-1 of DNV(2010).

From the site wind climate statistics, extreme wind speed at certain heights are obtained for a set of expected return periods. Some load cases in DNV (2014) specify such extreme wind cases instead of the mean.

To include the effects of turbulence in power production and the response of the structure, the turbulence intensity factor is needed. This parameter is obtained from the site wind measurements for given heights and also depends on the direction of the incident wind.

#### 6.1.2 Wave loads

Wave loads are characterised by the wave period and significant wave height. According to DNV(2010), the significant wave height refers to the average height (trough to crest) of the highest one-third waves in a given time period.

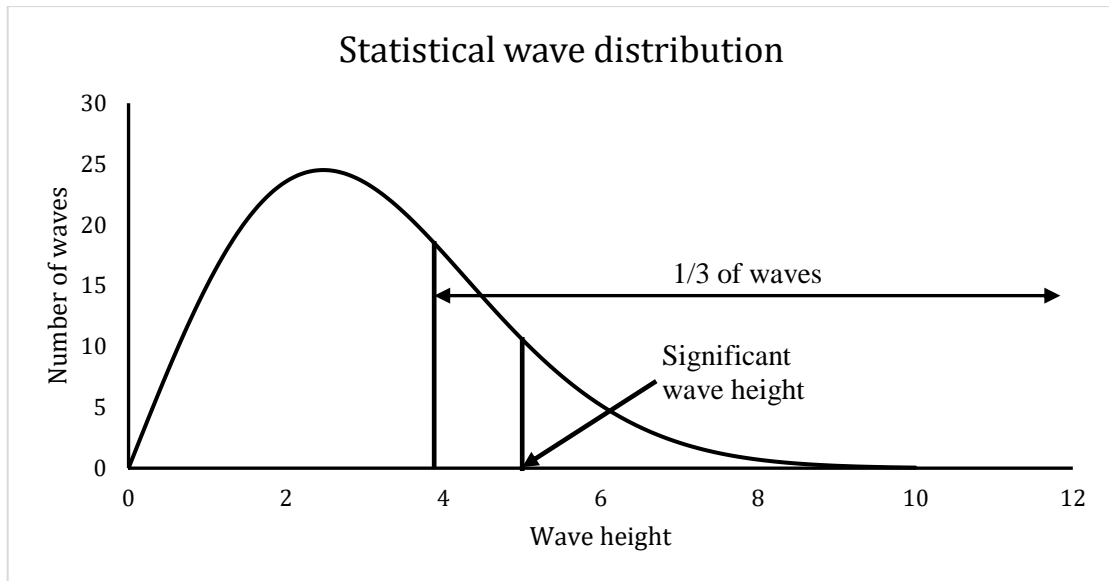


Figure 6.1 Statistical wave distribution illustrating the concept of significant wave height

From field measurements, statistical values of the significant wave height for extreme wave cases in certain return periods can be obtained.

### 6.1.3 Wind generated waves

Though waves are also generated through other means, there is no doubt that the wind contributes most to waves in large water bodies. The role of wind in the generation of waves continues to be an important subject in oceanographic research to fully understand the transfer of wind energy into wave energy.

The characteristics of wind generated waves were studied in detail by Bretschneider (1964). He devised a number of graphs to estimate the significant wave height and its associated period at the end of a fetch length for a given wind speed, duration and fetch (see figure 7.8 in Thomson (1981)). Such graphs also permit determination of the significant wave characteristics under fetch-limited and duration-limited conditions, if either the fetch or duration of the wind is insufficient to generated fully developed seas.

### 6.1.4 Wind generated current

Loads due to currents can be either wind induced or due to geographic water streams. From the site measurements, statistical current speed data together with the direction is needed to satisfy the pertinent load cases specified in DNV (2014). Unless data indicates otherwise, the wind generated current at still water level may be estimated as:

$$v_{wind0} = k \cdot U_0 \quad (6.2)$$

where  $k$  ranges from 0.015 to 0.03 and  $U_0$  is the 1-hour mean wind speed at 10 m height DNV (2014).



Similar to wind and wave loads, statistical values of the current velocities are obtained from field measurements for certain return periods.

## **6.2 Design input data for the codes**

The input data required for each code prior to modelling and analysing an OWT structure may vary slightly from one code to another. However, the general requirements are still maintained since all the codes run on virtually similar theories and principles (see Chapter 4). In this section, the various specifications required to analyse an OWT structure are discussed.

### **6.2.1 Geometry and material properties.**

This set of data describes blade, tower and substructure geometry which includes member sizes, section and material properties. For most codes like Bladed, Ashes and HAWC2; predefined blades can be used if required. However, if the user requires a turbine with blades other than those predefined then the entire blade geometry has to be rigorously modelled following the code's blade modeller. This is also true for the tower and substructure, which can be modelled using coordinates that define element topology. These coordinates represent the structural joints.

### **6.2.2 Aerodynamic data**

The appropriate wind spectrum has to be defined in order to set up the aerodynamic environment of the OWT, as shown in Section 4.2. Consequently, one has to state the mean wind speed together with the height at which the wind speed is defined. The air density, air viscosity, flow inclination and wind direction are also required. Longitudinal, lateral and vertical intensity factors for turbulence may be required depending on the complexity of the model.

Where applicable, codes that employ Blade Element Momentum (BEM) theory to model aerodynamic loads require the user to state the value of the aerodynamic coefficients. Some go ahead to combine the BEM theory with drag effects in a similar fashion to Morrison's equation. In that case, the drag coefficient needs to be provided for aerodynamic loads.

### **6.2.3 Hydrodynamic data**

Wave characteristics are fundamental when it comes to describing the hydrodynamic environment of the OWT structure as discussed in Section 4.3. This, however, depends on the nature of the waves (regular or irregular) and requires that the appropriate wave type is selected. For deterministic wave models, the wave height and period have to be specified. The JONSWAP/Pierson Moskowitz function requires one to define the significant wave height, peak spectral period and peak factor. In some codes though the user is allowed to define a wave spectrum from scratch. In all cases, the wave direction is required.

Depending on the hydrodynamic loading model that the code uses, a number of coefficients need to be specified including the mean water depth. Morison equation requires the hydrodynamic and drag inertia coefficients.

The current velocity and type are required as an input in the model. The direction (angle) at which the current arrives at the OWT has to be defined.

The salinity, temperature, viscosity and density of the water are required since these have a direct effect on the flow characteristics.

#### **6.2.4 Initial and boundary conditions**

Initial conditions include the initial angular blade rotation speed, the initial structural orientation and the initial wave profile. The initial wind conditions should be specified too.

Boundary conditions between different structural parts and at the support should be specified in order to obtain a whole set of coupled results.

#### **6.2.5 Soil interaction data**

Some codes describe the foundation boundary conditions simply as a fixed or pinned node, while others are capable of presenting a system of soil interaction of the forms described in Section 4.1.

#### **6.2.6 Computational specifications**

This set of input data includes convergence criteria, analysis time step, analysis method (linear and nonlinear) and the preferred iteration method.

#### **6.2.7 Summary**

Table 6.1 summarises the main input data required in order to run an OWT simulation.

Table 6.1 Summary of input data

Input group			Comments
Geometric data	Turbine configuration	Number of blades Blade-Rotor orientation Nacelle orientation Hub orientation Rotor-Yaw orientation	
	Blade geometry	Length/span Mounting angles Segment chord Aerodynamic twist Segment thickness	
	Tower and substructure geometry	Joint nodes and coordinates Element topology	
	Tower and substructure member cross section properties	Young's modulus Shear modulus Density Cross section sizes Damping ratio	
Hydrodynamic data	Wave characteristics	Wave spectrum model Modifications if any Significant wave height Peak spectral period Peak shape factor (JONSWAP) Lower frequency limit Upper frequency limit Wave direction of approach	Waves may be regular or irregular and that will determine which wave model is appropriate.
	Hydro loading	Hydro loading model Drag coefficient Inertia coefficient Marine growth density	
	Currents	Current velocity Current direction Reference depth	
	Sea characteristics	Maximum water depth Mean water depth	
Aerodynamic data	Wind characteristics	Wind spectrum model Mean wind speed Wind direction Wind height reference Flow inclination	
	Turbulence	Turbulence intensity	
Foundation data	Flexible foundation	Stiffness matrix	
		Damping matrix	
		Mass matrix	
		Translation and degrees of freedom	
		Apparent fixity length	
	Soil spring stiffness		
Fixed foundation	Base nodes and Boundary conditions		
Earthquake data	Earthquake dynamics	Earth quake spectrum model Earthquake duration	If the OWT is to be built in a seismically active region.

## 7 Case Study and Code Comparison

In this chapter, three codes were used to simulate various types of OWT foundations. The chapter includes a pre-study of the jacket structure used in OC4 and a case study to compare results of a tripod and a gravity base structure. The results from each code were used to study the differences and similarities between the codes. In addition, the wind turbine model (RNA and tower) used in the comparison studies is briefly discussed in Section 7.2. For more details on this turbine model, the reader is referred to Jonkman et al. (2009).

### 7.1 Pre-study

This exercise was done prior to the actual case study with the main purpose of ensuring familiarity with the software before using them on actual case studies. The exercise was based on the models and results of the OC4 project. For more details about OC4 project, readers are referred to Vorpahl et al. (2011).

The same jacket structure studied in OC4 was defined in both FAST and ASHES with identical tower and turbine configurations. To be consistent with the study, the same load cases and corresponding initial conditions were defined in both software. The structural model was assumed to be fixed at the bottom as the one in OC4 project. In other words, soil-pile interaction was not considered in the model. The results obtained from the models and OC4 study are shown as follows with related comments.

#### 7.1.1 Pre-Study with OC4 Load Case 2.1

With this load case, the codes are compared when there is no wind action on the structure and water stands still. Same conditions were defined and since there were no horizontal forces acting on the structure only the forces in axial (vertical) direction were extracted at this phase. The calculated vertical forces at the mudline obtained from both programs are shown in Figure 7.1.

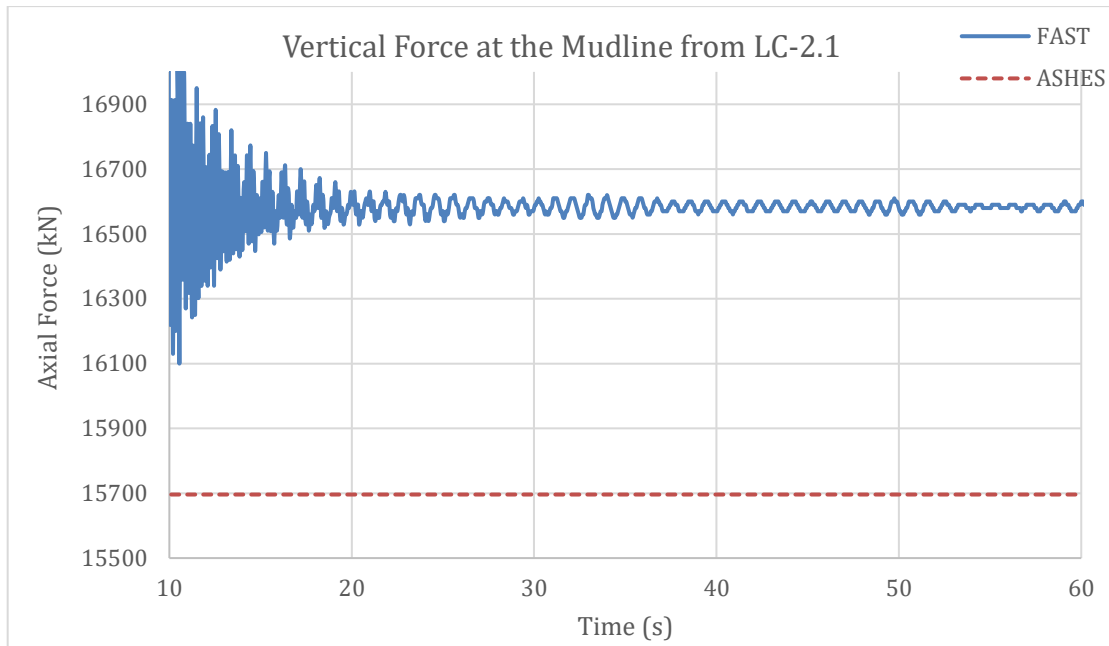


Figure 7.1 Vertical force at the mudline from load case 2.1

There is a small difference between the two results, but both results are still in the range of the results obtained in OC4 studies which is approximately between 15600 and 17200 kN.

### 7.1.2 Pre-Study with OC4 Load Case 2.3a

In this load case, the attention was given to wave and buoyancy effect. No wind was defined in the models and waves were modelled considering 6m wave height and 10s wave period. In this load case, both axial (vertical) and shear force at the mudline were extracted and compared.

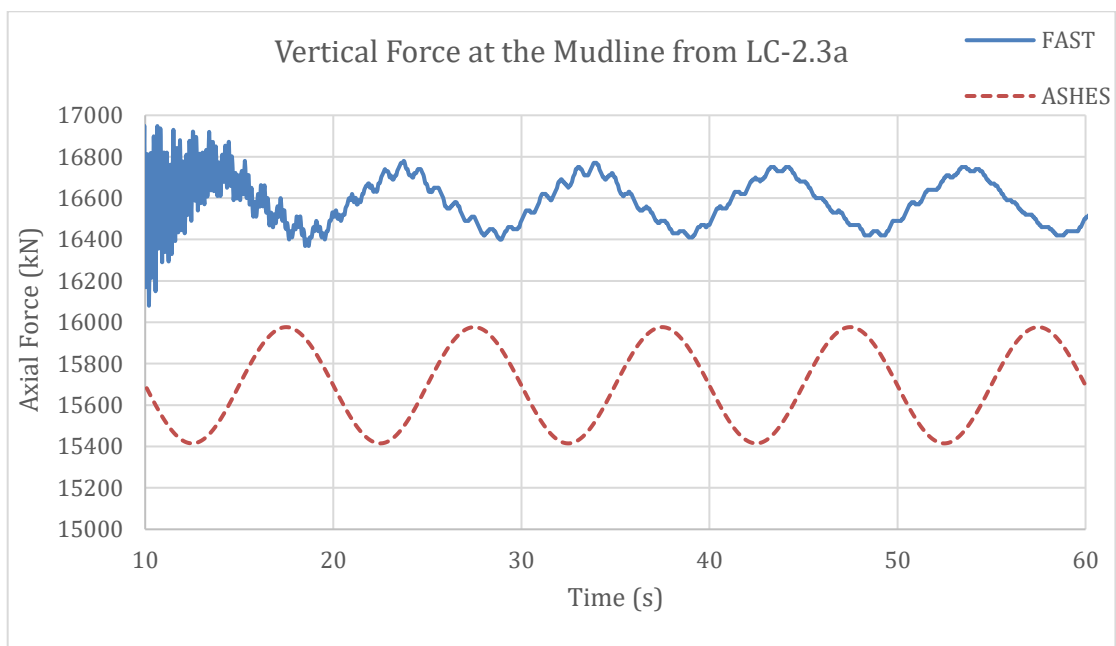


Figure 7.2 Vertical force at the mudline from load case 2.3a

The vertical force results from both analyses show coherence with the results from OC4. The buoyancy force due to the waves causes the oscillation in the axial force at the mudline. In OC4, the vertical force results for all simulation codes fluctuate approximately between 15400 and 17400kN.

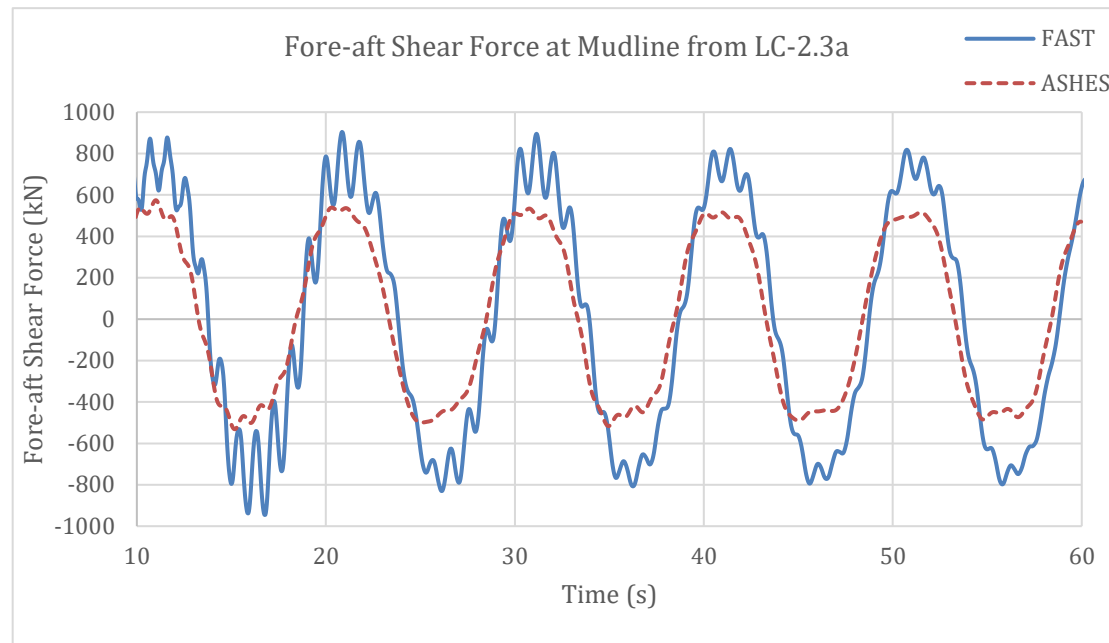
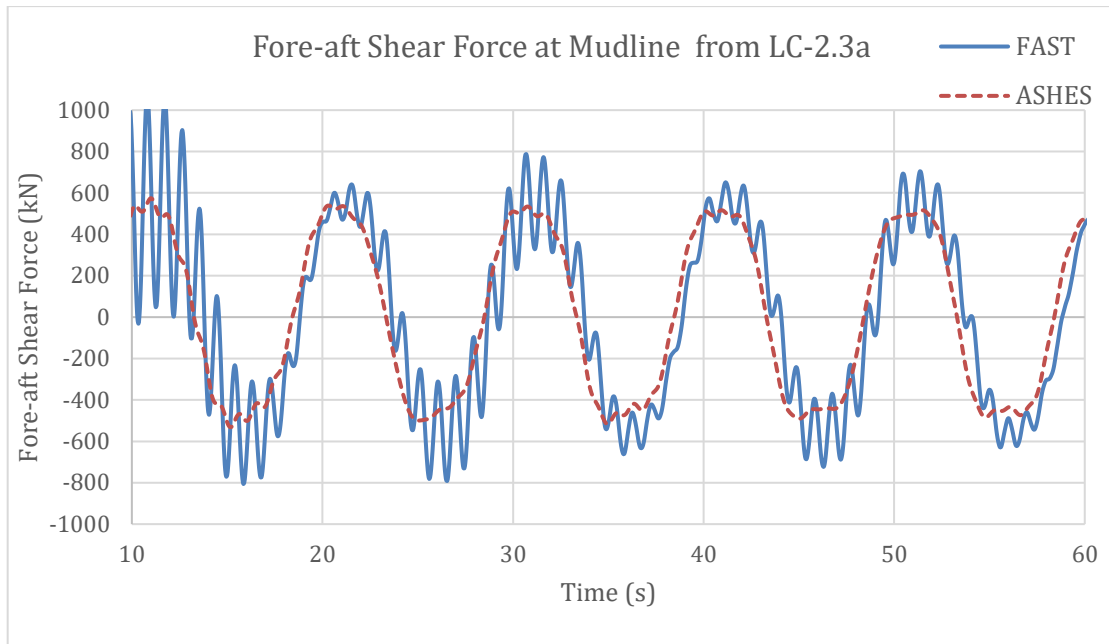


Figure 7.3 Fore-aft shear force at mudline from load case 2.3a

The shear force obtained from ASHES is considerably smaller than FAST. The main reason behind this difference is the additional horizontal force originated from the interaction between marine growth and wave action. In ASHES, it is not possible to define marine growth yet, therefore, the shear force at mudline is smaller than FAST and the rest of the codes studied in OC4. However, both results are quite similar to the results gotten from OC4 study. Moreover, it can be seen from the results obtained from both analyses that the ripples around the peaks in the graphs are vanishing with time due to the fact that the structure reaches the steady-state conditions and follows the excitation force rather than natural vibration.

### 7.1.3 Special case of OC4 Load Case 2.3a

This case was created to verify if the marine growth-wave interaction was the actual reason behind the difference between the fore-aft shear force results as it was stated in Section 7.1.2. The method followed here was removing the marine growth definition from FAST and adding the corresponding mass to the structure to get the same structural mass in both models. In the previous FAST model used in Section 7.1.2, the marine growth was included in the model to obtain comparable results with OC4 study even though it was not possible to do it in ASHES. In Figure 7.4 and Figure 7.5, FAST results were calculated without defining the marine growth as described above. Apart from that, the results shown from ASHES are the same with those in Section 7.1.2.



*Figure 7.4 Fore-aft shear force at mudline from load case 2.3a without marine growth in FAST*

As shown in Figure 7.4, without defining marine growth, the shear force at the mudline obtained from FAST was reduced and became similar to the result obtained by ASHES. Therefore, as expected, the difference in shear force results in the previous calculations were due to marine growth-wave interaction. On the other hand, modifying the mass properties of the structure seemed to change the dynamic response of the turbine. Likewise, since the marine growth surface was removed from the structure, the volume of the structure decreased and consequently the buoyancy force was reduced. This lead to an increase in the vertical force at the mudline in the FAST analysis as shown in Figure 7.5.

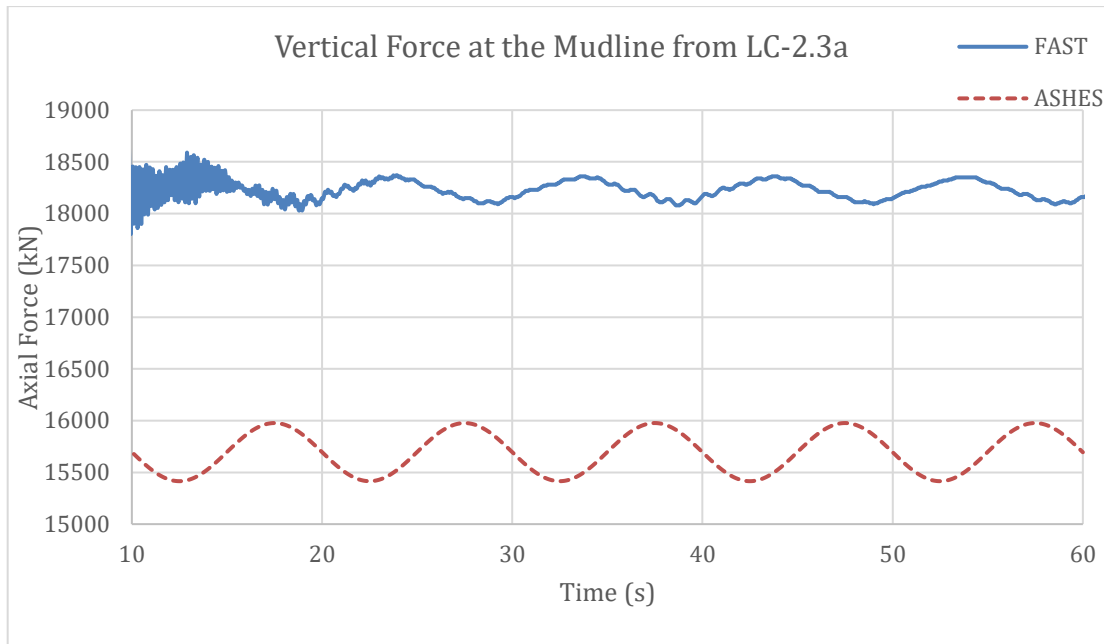


Figure 7.5 Vertical force at mudline from load case 2.3a without marine growth in FAST

## 7.2 RNA and tower definitions used in the studies

### 7.2.1 NREL 5MW Wind turbine model

This turbine model was developed by the National Renewable Energy Laboratory (NREL) funded through the U.S Department of Energy (DOE). It features representative specifications of a typical land and sea-based multi-megawatt turbine suitable for deployment in deep waters. Because of the cost of offshore support structures, the NREL decided that a minimum power rating of 5 MW for each turbine is required to warrant feasibility of an OWT power project.

According to Jonkman et al. (2009), the 5 MW baseline was chosen based on past successful studies that used similar turbine models and specifications. For instance:

- The scope of the floater concepts for offshore wind turbines was built on 5 MW unit specifications and assumptions (Musial et al. cited in Jonkman et al. 2009).
- The rotor diameter of 128 m featured in unpublished DOE offshore cost studies, which is a representative blade size of a 5-to-6 MW wind turbine.
- Wind Partnerships for Advanced Component Technology (WindPACT) considered systems rated up to 5 MW in their studies.
- The conceptual design calculations in the Recommendations for Design of Offshore Wind Turbines were based on a 5 MW rating turbine.
- A 6 MW rating turbine was used in the Dutch Offshore Wind Energy Converter (DOWEC) project.
- The largest wind turbine prototypes were each 5 MW rated, at the time the NREL model was developed.

The gross properties of chosen for the NREL 5 MW baseline wind turbine by Jonkman et al. (2009) are summarised in Table 7.1.



Table 7.1 NREL 5 MW Wind Turbine properties.

Rating	5 MW
Rotor Orientation, Configuration	Upwind, 3 Blades
Control	Variable Speed, Collective Pitch
Drivetrain	High speed, Multiple-Stage Gearbox
Rotor, Hub Diameter	126 m, 3 m
Hub Height	90 m
Cut-In, Rated, Cut-Out Wind speed	3 m/s, 11.4 m/s, 25 m/s
Cut-In, Rated Rotor speed	6.9 rpm, 12.1 rpm
Rated Tip Speed	80 m/s
Overhand, Shaft Tilt, Precone	5 m, 5 °, 2.5 °
Rotor Mass	110000 kg
Nacelle Mass	240000 kg
Tower Mass	347460 kg
Coordinate Location of Overall CM	(-0.2 m, 0.0 m, 64.0 m)

## 7.2.2 Tower

In the following comparison studies, a tubular steel tower was defined between the foundation and RNA. Similar to the tower used in OC3 study, the tower has a length of 77.6 meters, base diameter of 6 meters and top diameter of 3.87 meters. The details of the tower are outlined in Table 7.2

Table 7.2 Tower properties used in the comparison studies

<b>Geometry</b>	
Length	77.6 m
Base Diameter	6 m
Base Wall Thickness	0.03 m
Top Diameter	3.87 m
Top Wall Thickness	0.016 m
<b>Material Properties of Steel</b>	
Density	7850 kg/m <sup>3</sup>
Young Modulus	2.1E+11 Pa
Shear Modulus	8.1E+10 Pa
Poisson's Ratio	0.3

## 7.3 Definition of load cases

This section presents a set of load cases considered in the comparison studies. Following load cases provide a stepwise examination of possible differences in the simulation codes due to different methods and approaches utilised in the analysis. In order to work with realistic environmental conditions in this project, specific site measurement data for the east of Hanö was taken into account from Gyllenram et al.

(2009) to generate the load cases. The location of the area is shown in Figure 7.6 (Google Maps, 2016). Blekinge Offshore AB, the proprietors of the Blekinge offshore site, assigned SMHI with a task to measure environmental conditions.

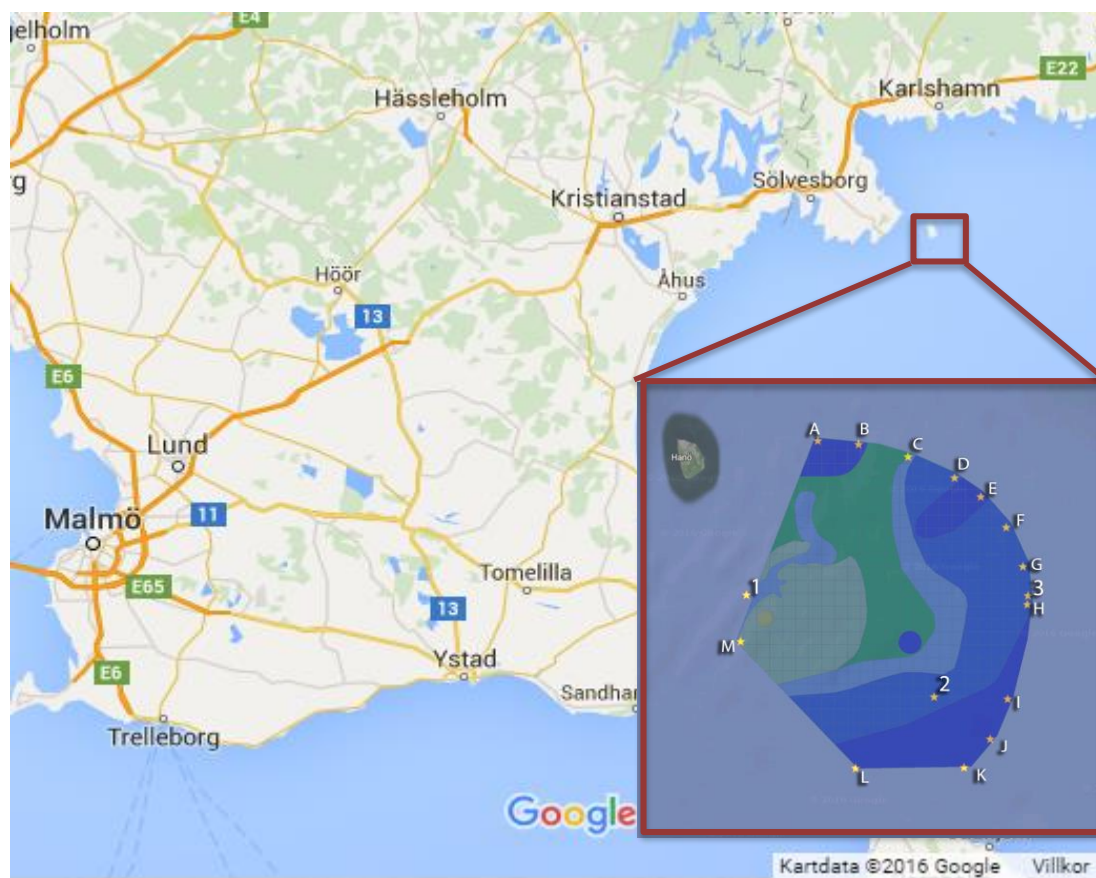


Figure 7.6 The location of the measured area

Load cases considered in the analyses are summarised in Table 7.3.

Table 7.3 Load cases used in comparison studies

Load Case	Wind Condition	Wave Condition	Current	Water Level
Load Case 1	No wind	No Wave	No Current	No Water
Load Case 2	No Wind	No Wave	50-year Current	MWL
Load Case 3	No Wind	50-year Wave	No Current	MWL
Load Case 4	Mean Wind Speed	No Wave	No Current	MWL
DNV-OS-J101 (2014) Load Case 1.1	$V_{in} < U_{10, hub} < V_{out}$	Wind generated specific wave height	Wind generated current	MWL
DNV-OS-J101 (2014) Load Case 6.1c	$1.1U_{10-50-yr}$	50-year Wave	50-year Current	50-year sea level

Load case 1 was meant to check if the geometry and mass definitions of the structure were defined correctly in the models before proceeding with more complex cases. Load cases 2 and 3 examine the results of the codes for hydrodynamic loadings. However, in ASHES it is not yet possible to define sea currents, therefore, only FAST and FOCUS6 were studied in load case 2. Load case 4 was included in this project to investigate the structural response of the model to wind loading for each simulation code. Since the wind turbine is parked under extreme wind conditions, load case 4 accounts for a constant wind load corresponding to the mean wind speed to inspect the aerodynamic response of the simulation codes including the dynamic effect of the rotor during power production.

To include standard load cases and inspect the codes with combined environmental effects, load case 1.1 and 6.1c from DNV (2014) were selected. Load case 1.1 deals with external loads to which the OWT structure is exposed during power production which is a typical load case for fatigue analysis. In design phases, DNV prescribes an investigation of the structural behaviour in several wind loadings from the minimum wind speed for which the turbine can produce energy to the maximum. However, the scope of this thesis does not include a structural design, therefore, only the mean wind speed at hub height was taken into account in this load case. Apart from that, load case 6.1c was chosen to examine results in extreme conditions for a 50-year return period.

### 7.3.1 Environmental effects measured from the site.

The environmental effects used in the comparison study were obtained from the Blekinge site-investigation report by Gyllenram et al. (2009) of SMHI. They were used to describe the load cases in Table 7.3 and are summarised in Table 7.4. The sea-current data shown was obtained from point B (see Figure 7.6) as shown in the investigation report, since the location of this point satisfied the requirements for mean water depth. However, the mean sea level in the comparison studies was taken as 35 and 45 meters in gravity base and tripod structure models respectively instead of the 25 m planned sea depth by Blekinge Offshore AB.

Table 7.4 Environmental effects measured from Blekinge offshore site

<b>Environmental condition</b>	
Mean sea level	35-45 m
Mean wind speed	8.6 m/s at 70.5m height
Wind generated significant wave height	1.49 m based on a fetch of approx. 180 km and the prevailing mean wind speed. See Figure 7,8 in Thomson (1981)
Wind generated wave period	4.84 s
Wind generated current	Estimated using Eq. 6.3. 15.9 cm/s
50-year significant wave height	6.5 m in the north east direction
50-year wave period	7.8 s
50-year wind speed	51.9 m/s at 90 m height
50-year sea Level	35-45 m
50-year current	89 cm/s in the north east direction

Considering the environmental data shown in Table 7.4, the corresponding load cases are outlined in Table 7.5.

*Table 7.5 Studied load cases according to the environmental data measured from Blekinge offshore site*

<b>Load Case</b>	<b>Wind Condition</b>	<b>Wave Condition</b>	<b>Current</b>	<b>Water Level</b>
Load Case 1	-	-	-	-
Load Case 2	-	-	0.89 m/s	MWL
Load Case 3	-	H=6.5 m T=7.8 s	-	MWL
Load Case 4	8.79 m/s	-	-	MWL
DNV-OS-J101 (2014) Load Case 1.1	8.79 m/s	H=1.49 m T=4.84 s	0.159 m/s	MWL
DNV-OS-J101 (2014) Load Case 6.1c	57.09 m/s	H=6.5 m T=7.8 s	0.89 m/s	50-year sea level

## 7.4 Comparison study for tripod structure

### 7.4.1 Description of the structure

The support structure used here is a symmetric tripod. The choice of this support structure was driven by a number of factors ranging from feasibility to technical aspects. In the third phase of the OC3 project, where a tripod structure was studied using several simulation codes, the support structure was modelled as bottom fixed disregarding any soil-pile interaction. Likewise, soil-pile interaction was disregarded in this project. More details about the OC3 project can be found in Jonkman and Musial (2010). Since ASHES was not included in the OC3 project, it was decided in this thesis to study a tripod structure in ASHES along with FOCUS6 and FAST.

The structure has a 45-meter tripod foundation under water and a 10-meter transition piece that starts at the sea level and connects the tubular tower to the foundation. The details of the tripod structure are outlined in Table 7.6 and Table 7.7.

*Table 7.6 Material properties of tripod structure*

<b>Material Properties of Steel</b>	
Density	7850 kg/m <sup>3</sup>
Young Modulus	2.1E+11 Pa
Shear Modulus	8.1E+10 Pa
Poisson's Ratio	0.3

Table 7.7 Geometry of the tripod structure

Part	Length (m)	Diameter (m)	Thickness (m)
Transition Structure	10		
Top Wall		6	0.04
Base Wall		6	0.04
Central Column	37		
Top Wall		6	0.068
Base Wall		4	0.028
Diagonal Braces	32.28	1.2	0.032
Interior Braces	19.785	0.8	0.028
Exterior Braces	40.624	0.8	0.016
Piles	20	4	0.04

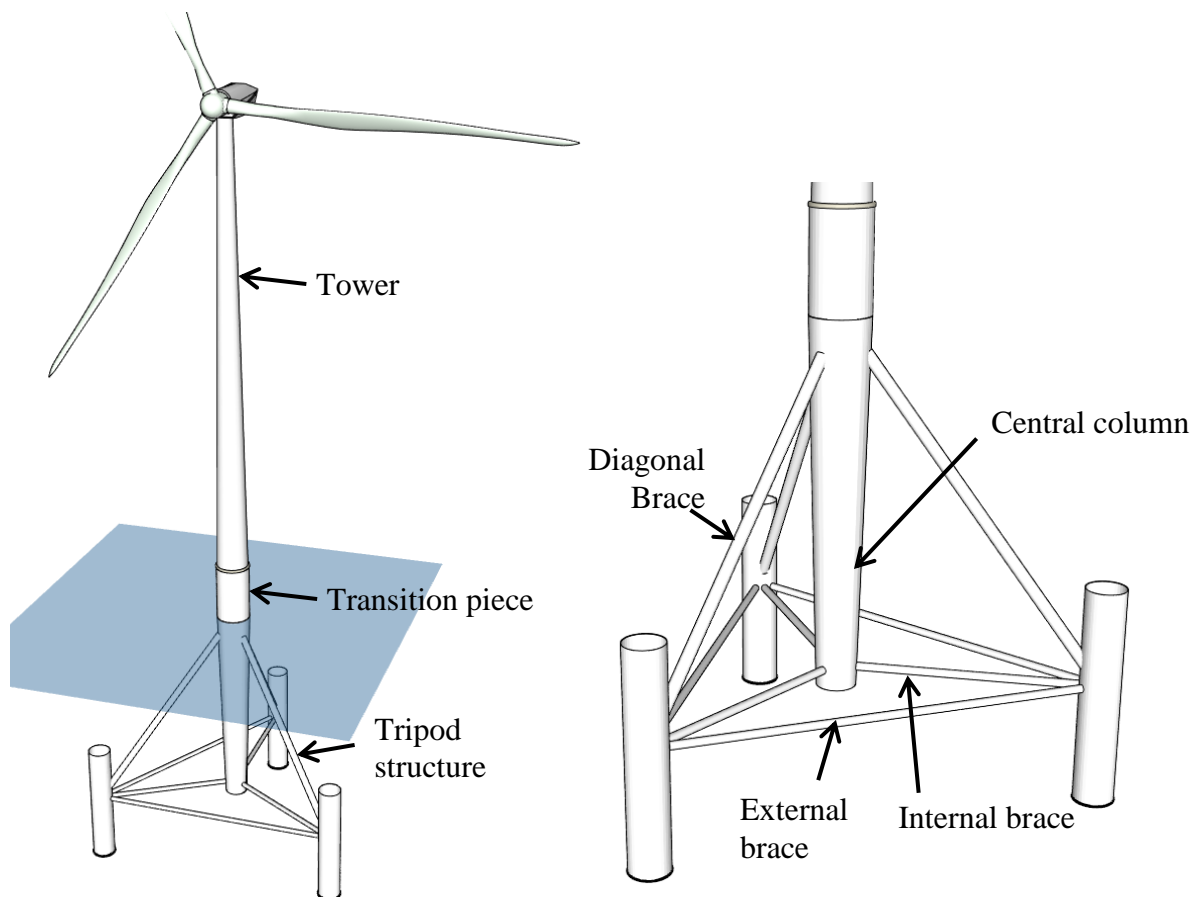


Figure 7.7 Illustration of the tripod structure

## 7.4.2 Modelling the support structure

In this section, the methods followed to model the tripod structure in the simulation codes are presented. The tripod structure was modelled in FAST, ASHES and FOCUS6 in the same way as much as possible to avoid distinctions in the results coming from the differences in the model itself. In ASHES and FOCUS6, it was not possible to define a tapered section in a space frame foundation automatically, therefore, the central column of the tripod structure was divided into 5 members following the diameter and wall thickness defined in Table 7.7. Even though FAST is able to define tapered sections, the structure was modelled in the same way in all three simulation codes as described in the previous sentence.

Moreover, ASHES, is not yet able to define marine growth on the members beneath the sea level. Since comparing results from two different simulation codes would not give any hints to observe which one is more precise, the effect of marine growth on the results was excluded in this comparison. In a similar way, filled members also cannot be defined in ASHES yet and therefore were disregarded in this study.

The transition piece (the part between the tripod foundation and the tower, see Figure 7.7) in the tripod model is made of steel and defined as a part of the foundation in FAST and FOCUS6. However, the transition piece in ASHES is very stiff by the definition of the software itself and cannot be omitted in all space frame foundation models. Therefore, to obtain the same hub height in all three simulation codes, the transition piece part of the tripod foundation was subtracted from the model in ASHES and a stiff transition piece stipulated by the software was added instead. The effect of this will be discussed comprehensively in the results.

## 7.4.3 Soil interaction in the model

As mentioned in the description, this study focused on a fixed foundation in which the soil-pile interaction was ignored. In such a model, the foundation legs were cantilevered at the mudline.

## 7.4.4 Results

### 7.4.4.1 Results from load case 1

It can be seen from Figure 7.8 that there is a very good agreement between the codes. All codes gave a vertical reaction force slightly greater than 12350 kN in an acceptable range. Since the tapered sections of the tripod structure were modelled in the same way for all three codes, it was expected to have very similar results.

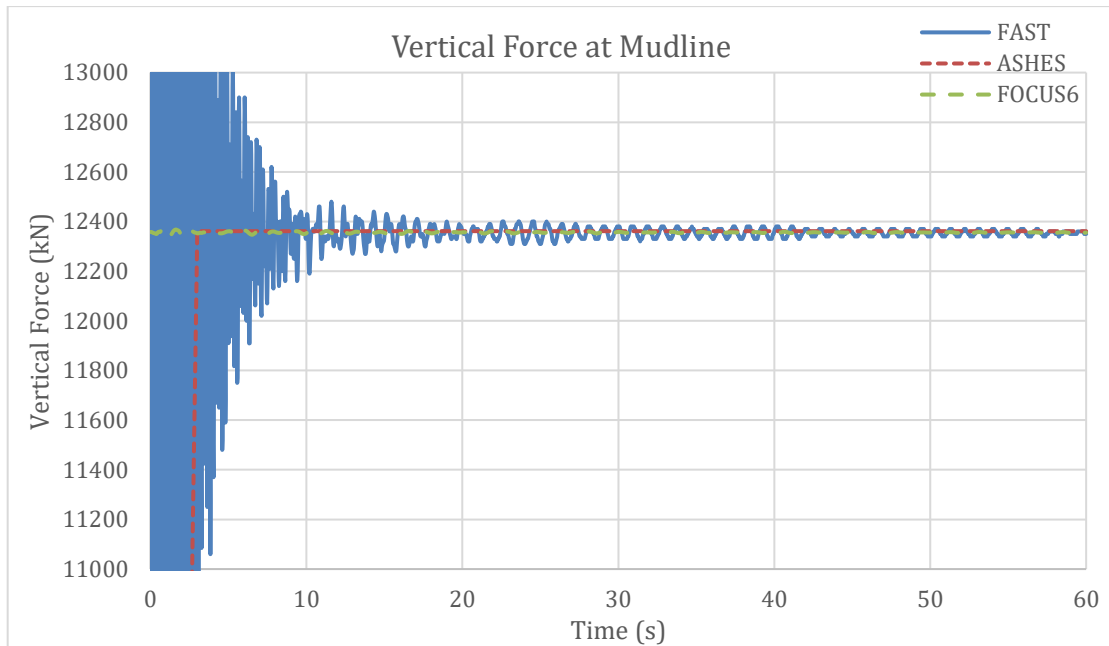


Figure 7.8 Vertical force at mudline for load case 1

#### 7.4.4.2 Results from load case 2

The fore-aft shear force results at the mudline are presented in Figure 7.9. There is a slight difference in the results even though the same current profile was selected in both codes but the difference is still acceptable. Additionally, FAST results fluctuate more compared to FOCUS6 results, but it can also be observed from the diagram that the response gently tends to reach steady-state.

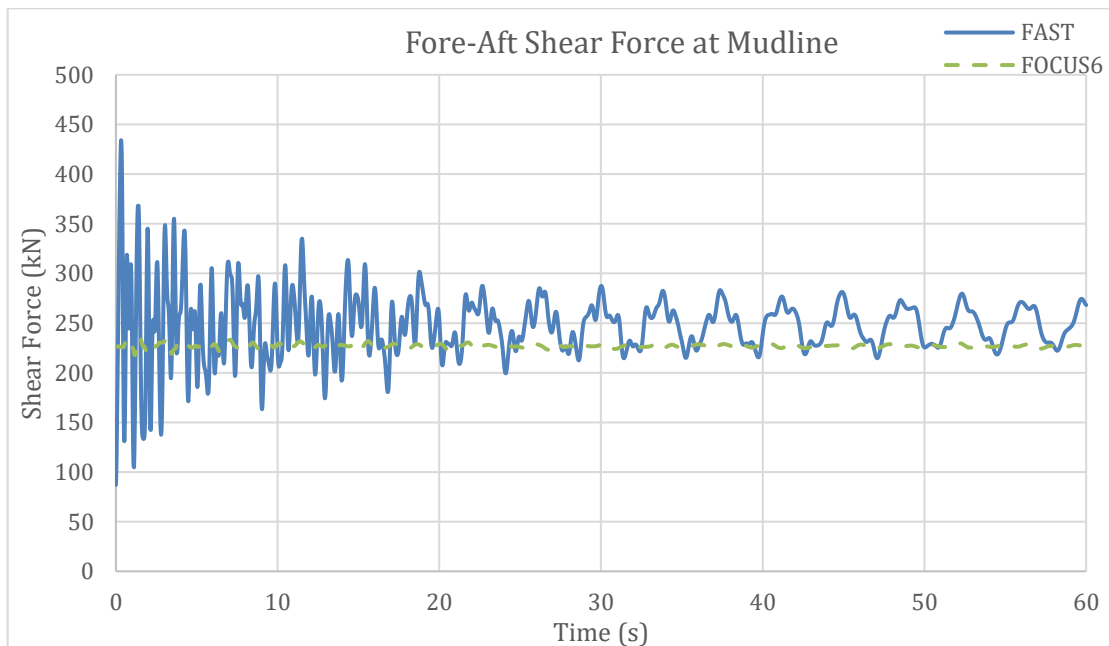


Figure 7.9 Fore-aft shear force at mudline for load case 2

#### 7.4.4.3 Results from load case 3

FAST and FOCUS6 are able to construct wave loads with both Morison Equation and Potential Flow Theory, however, it is not possible to use Potential Flow Theory in ASHES. Therefore, to obtain comparable results between codes, only Morison Equation was used to calculate the wave loads in FAST and FOCUS6 too. Apart from that, the drag coefficient  $C_d$  and inertia coefficient  $C_m$  in hydrodynamic load calculations were selected as 1 and 2 respectively.

Altogether, Figure 7.10 shows the fore-aft shear force results at mudline. After taking a glance at the figure, one can easily observe that there is an incoherence in the periods of the results from ASHES. However, the difference is only in periods in this case. The amplitudes from all three codes are around 1750 kN differing by +/- 75 kN which shows a good agreement between each other. In addition, the results from FAST initiates with ripples that vanish with time depending on how calculation is initialised in the code.

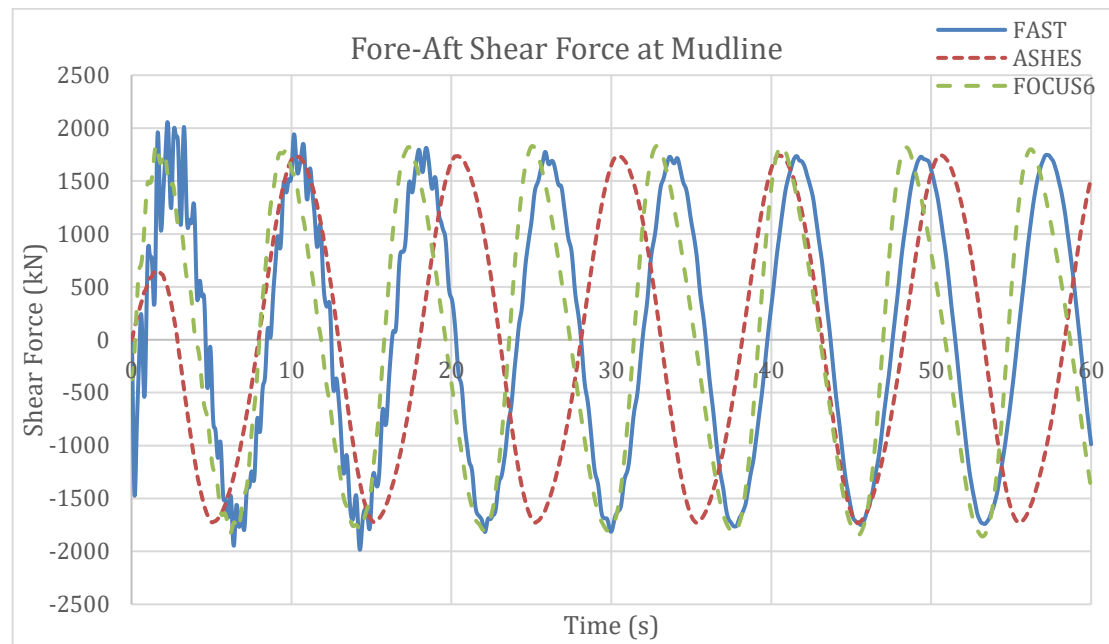


Figure 7.10 Fore-aft shear force at mudline for load case 3

#### 7.4.4.4 Results from load case 4

In this load case, BEM theory was used in the calculations with hub loss, tip loss corrections. Apart from that, the effect of the wind load on the tower was excluded in these calculations to observe the structural behaviour under wind loads acting only on the blades and hub. However, this effect was included in the subsequent load cases 5 and 6.

It can be observed from Figure 7.11 that the shear force results from all participant simulation codes show coherence with each other. The results converge to a shear force of around 480 kN showing a very good agreement. Still, there is a difference in the way of load application in the code.



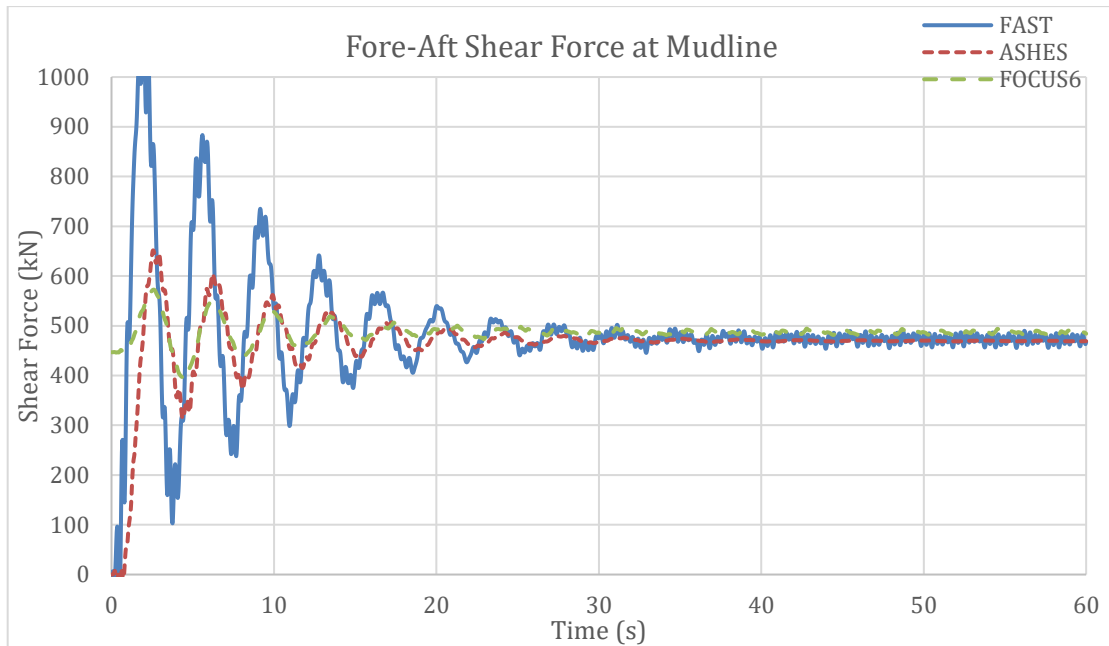


Figure 7.11 Fore-aft shear force at mudline for load case 4

In the tower top fore-aft deflections (Figure 7.12), FAST and FOCUS6 results show a good match. FAST result fluctuates about 37.5 cm whereas FOCUS6 result fluctuates about 38.5 cm. However, ASHES result converges to 33 cm. The main cause of this is the difference in the transition piece definitions between the codes. As explained in Section 7.4.2, the transition piece in ASHES was obligatorily modelled as if it was infinitely stiff, whereas in FAST and FOCUS6 the part was modelled as elastic. Considering that, a stiffer response in ASHES result was normal to encounter.

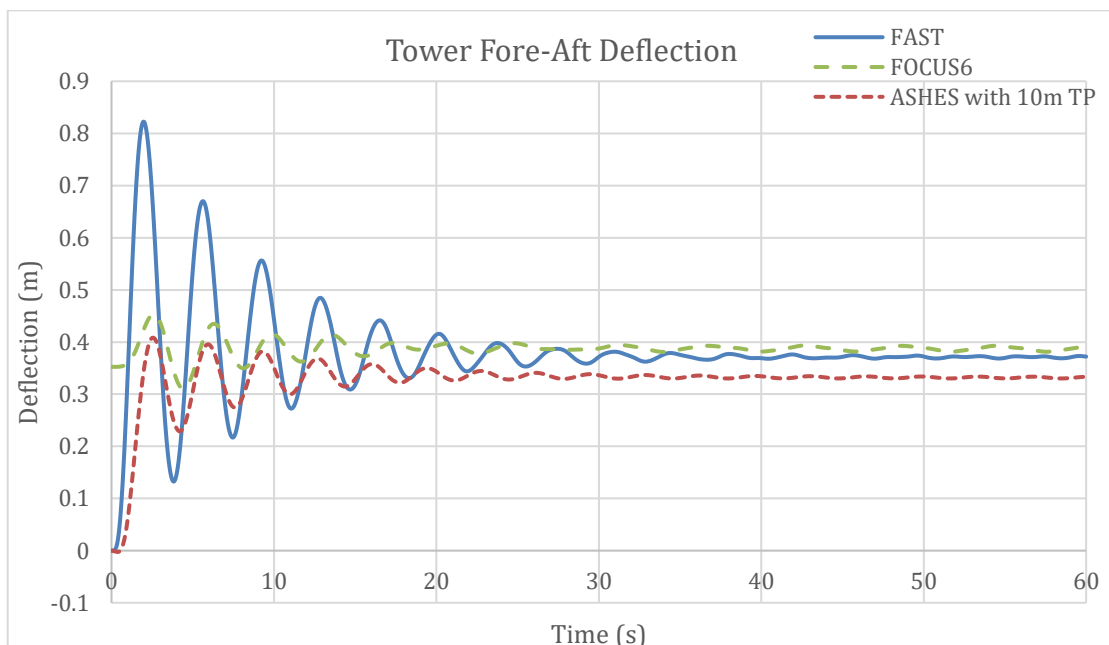


Figure 7.12 Tower top fore-aft deflection for load case 4

To avoid the effect of this stiff transition piece definition in ASHES, the height of the transition piece was reduced to 0.1 meter and the remaining (9.9 meters) part was

added into the tripod geometry to have the same hub height as in other models from FAST and FOCUS6. Nonetheless, during the analysis with these changes, a big localisation of rotation in the transition piece was witnessed. In other words, the model behaved as if the transition piece was a pin. The developers reported a bug in the transition piece definition that the software defines the actual stiffness of the transition piece according to its height. Hence, it had shown extremely flexible results with 0.1-meter height. So the problem here became to find the convenient transition piece for ASHES. By ‘convenient transition piece’, here the aim was to find the equivalent transition piece height in ASHES that gives the same response as in the other simulation codes without giving too stiff or flexible results to continue the comparison study. Deflection itself could not be the only criteria to find out the convenient transition piece in ASHES but the period of the response too.

A number of models with different transition piece height were created in ASHES and the corresponding tower top deflections and periods are presented in Figure 7.13. Both deflection and period in the results provide comprehensive arguments about the behaviour. For instance, one can easily say that the result with 1-meter transition piece is too flexible and the result is out of range. In addition, it can be observed that with increasing transition piece height, the results are converging and the difference in each result is getting smaller. However, the only way to find the convenient height was to compare the results with FAST and FOCUS6 where the periods of the results are 3.57 and 3.61 seconds respectively.

It can be observed from Figure 7.13 and Figure 7.14 that the result with a 4-meter transition piece shows consistency with both FAST and FOCUS6 in terms of period and deflection. The deflection result is slightly above 37.5 cm, which is very close to the FAST results but remains between the results from FOCUS6 and FAST. Moreover, considering there is just 1 cm difference, the results are considered acceptable. In the following load cases, a 4-meter transition piece was used in all ASHES models.

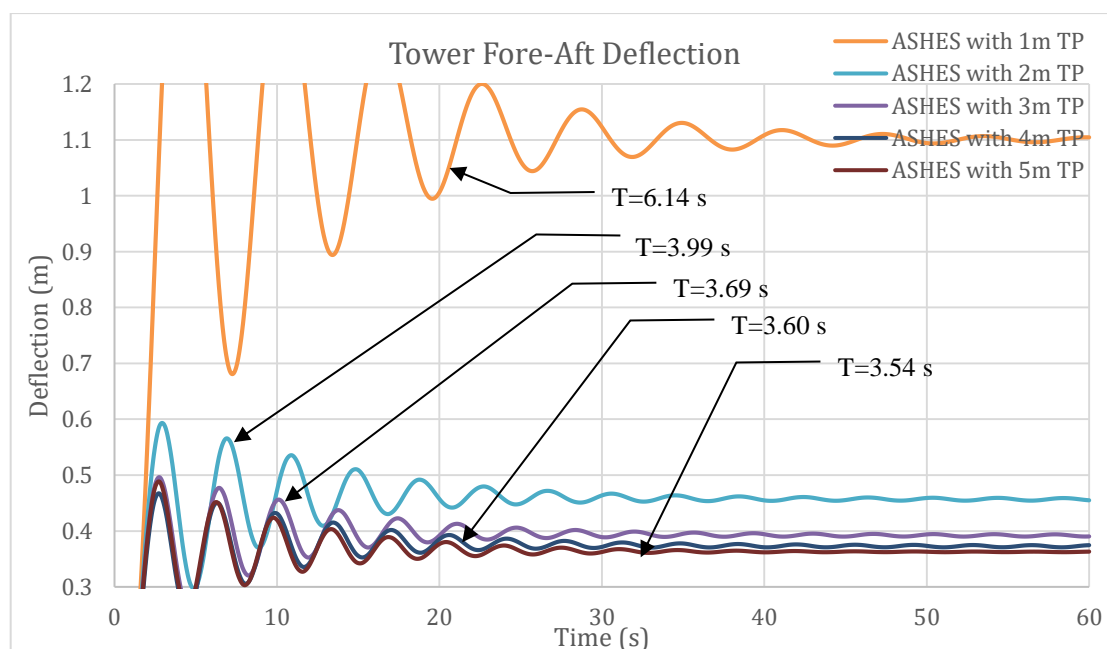


Figure 7.13 The effect of transition piece height in ASHES to deflection

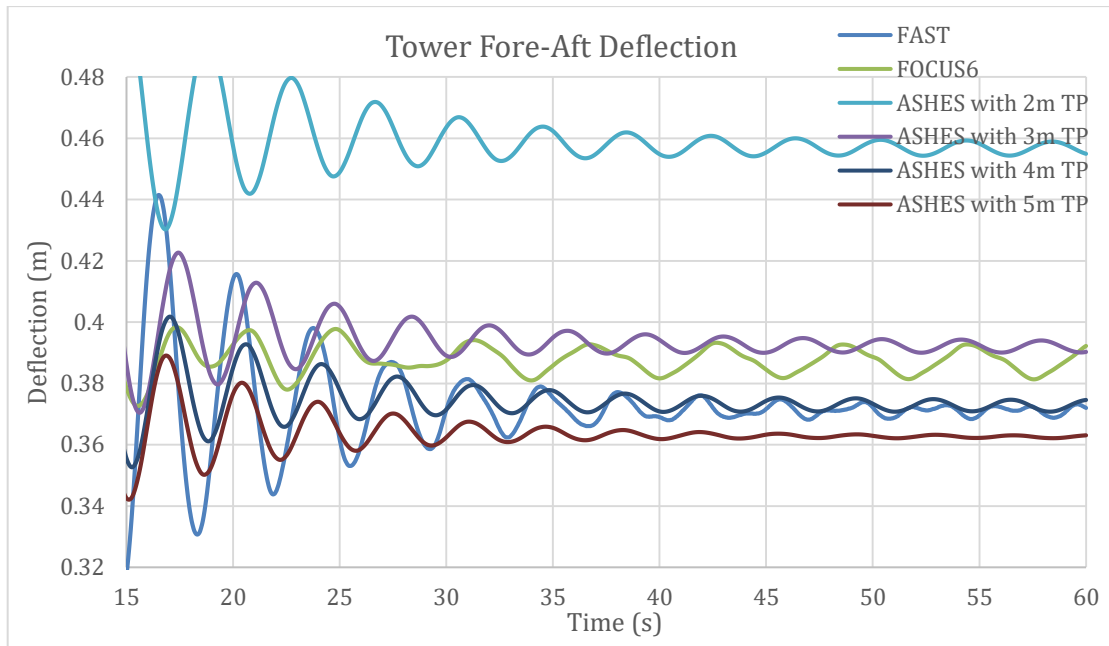


Figure 7.14 Comparison of ASHES results with FAST and FOCUS6

Furthermore, the fore-aft moment results are presented in Figure 7.15. After steady state loading, the results are seen to converge to nearly 65000 kNm differing by +/- 1000 kNm. Considering the height of the structure and the difference in shear force, the results are acceptable.

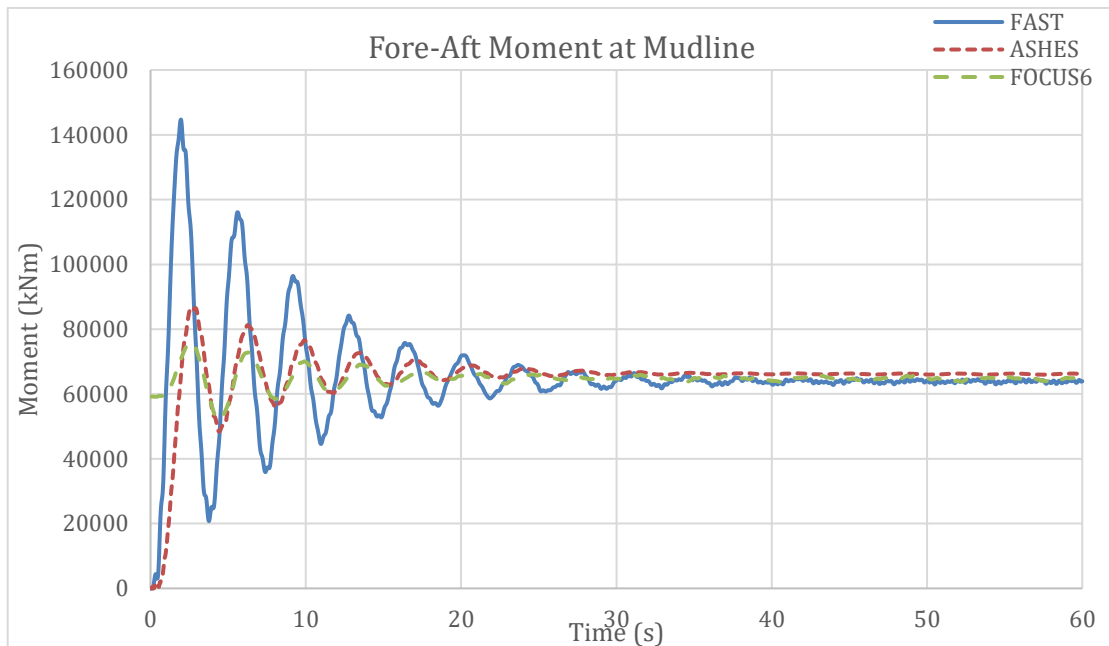


Figure 7.15 Fore-aft moment at mudline for load case 4

#### 7.4.4.5 Results from DNV load case 1.1

The results for the fore-aft shear force at the mudline for DNV load case 1.1 are plotted in Figure 7.16. There is a small but visible variation in the shear force amplitudes: FAST and FOCUS6 show a shear force result going up and down between nearly +/- 900 kN, but the result from ASHES remains under 850 kN. Apart

from that, there is a small difference in the average of the shear force as well, but this difference is undoubtedly because of the fact that currents were not defined in ASHES.

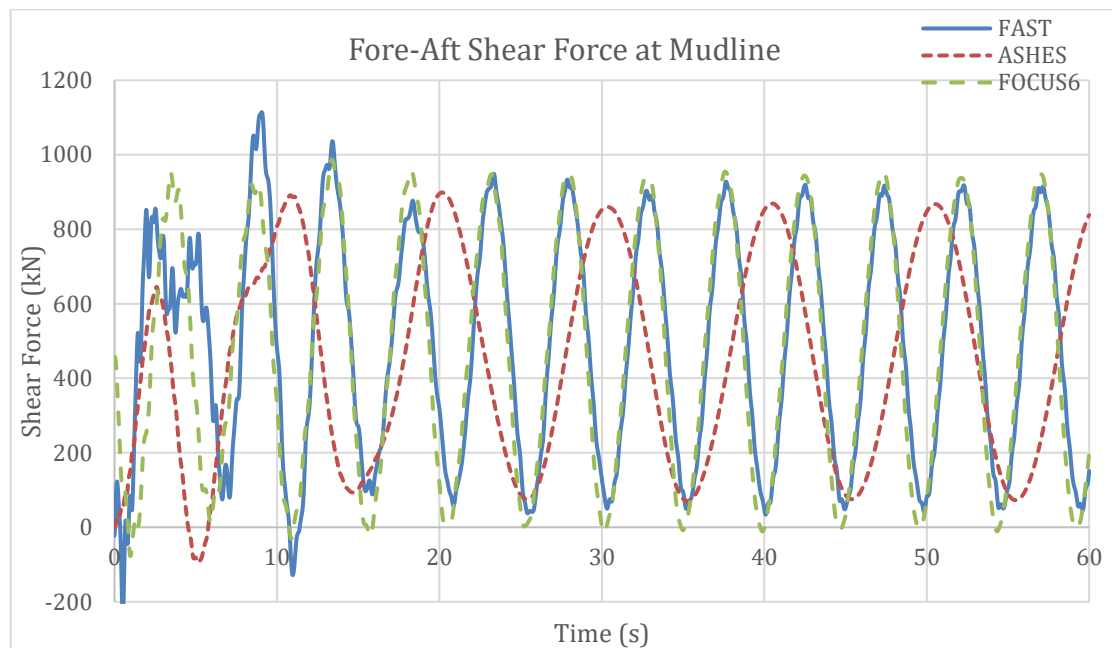


Figure 7.16 Fore-aft shear force at mudline for DNV load case 1.1

It can be observed from Figure 7.17 that the tower top fore-aft deflection results show consistency in all three simulation codes. As explained in the previous load case, here the results from the ASHES model with 4-meter transition piece were taken into account.

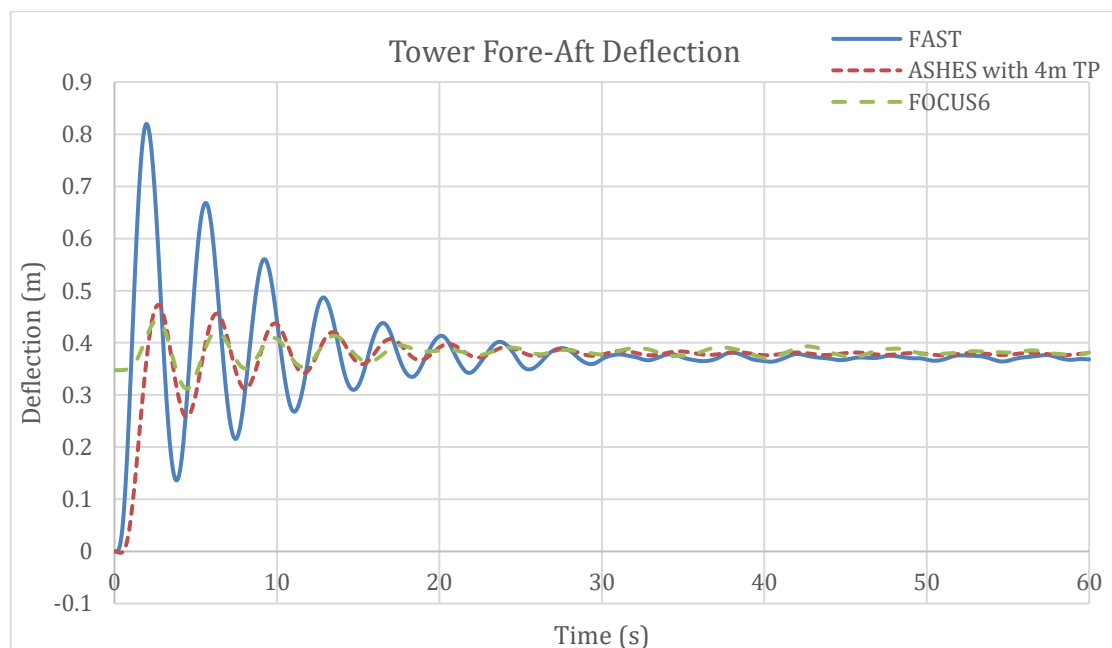


Figure 7.17 Tower fore-aft deflection for DNV load case 1.1

The moment results at the mudline are presented in Figure 7.18. Considering the different amplitudes in the shear force results, it is ordinary to have bigger difference in the moment results due to the amplification factor of the moment arm owing to the structure's height.

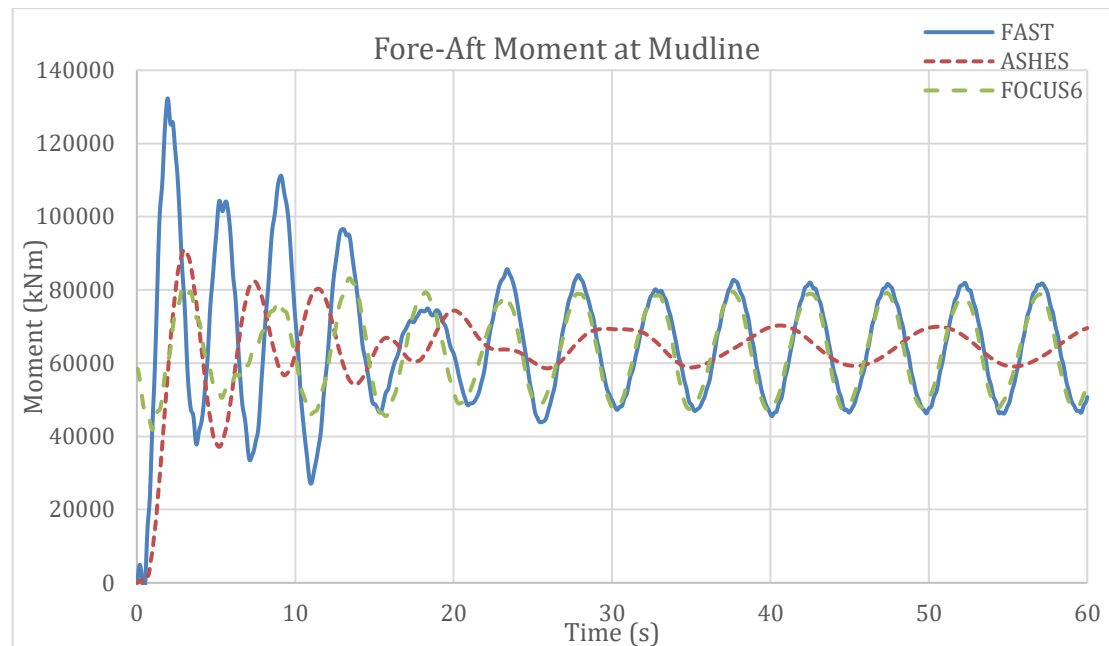


Figure 7.18 Fore-aft moment at mudline for DNV load case 1.1

#### 7.4.4.6 Results from DNV load case 6.1c

The shear force results as shown in Figure 7.19 show consistency at the beginning of the analysis. However, an unusual instability problem took place in the blades in ASHES and therefore the ASHES results were truncated to avoid unrealistic extreme response in the diagram. Apart from that, there is a good agreement between all three simulation codes.

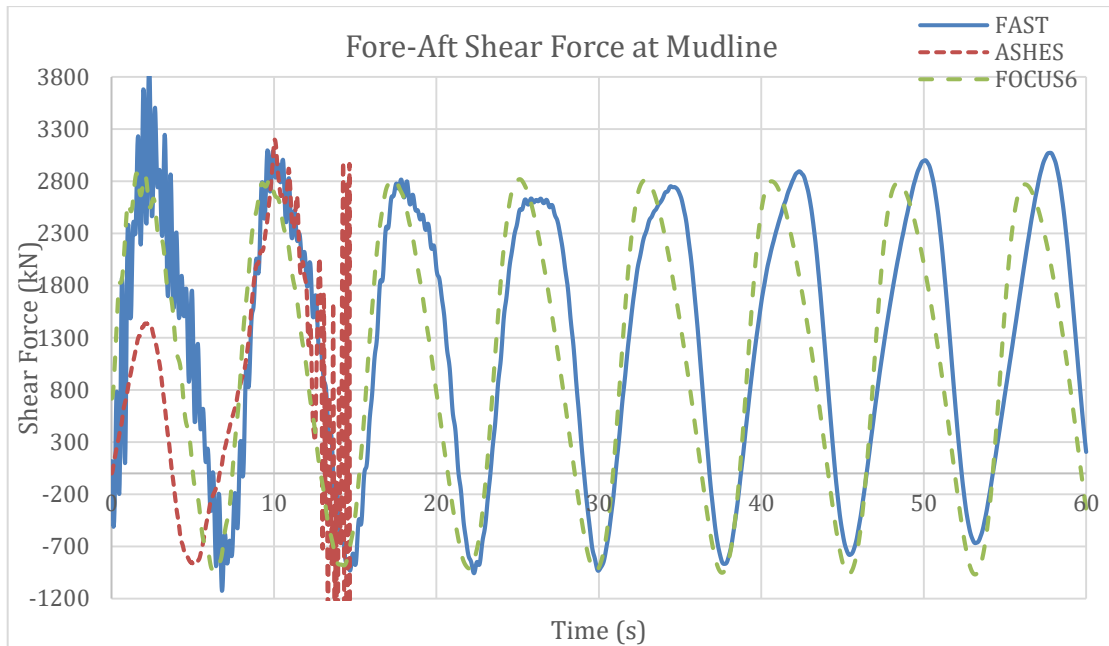


Figure 7.19 Fore-aft shear force at mudline for DNV load case 6.1c

The moment results shown in Figure 7.20 have small distinctions, and the ASHES results were truncated because of the same reason explained before. The irregularities in the results might be because of the complex extreme loading condition.

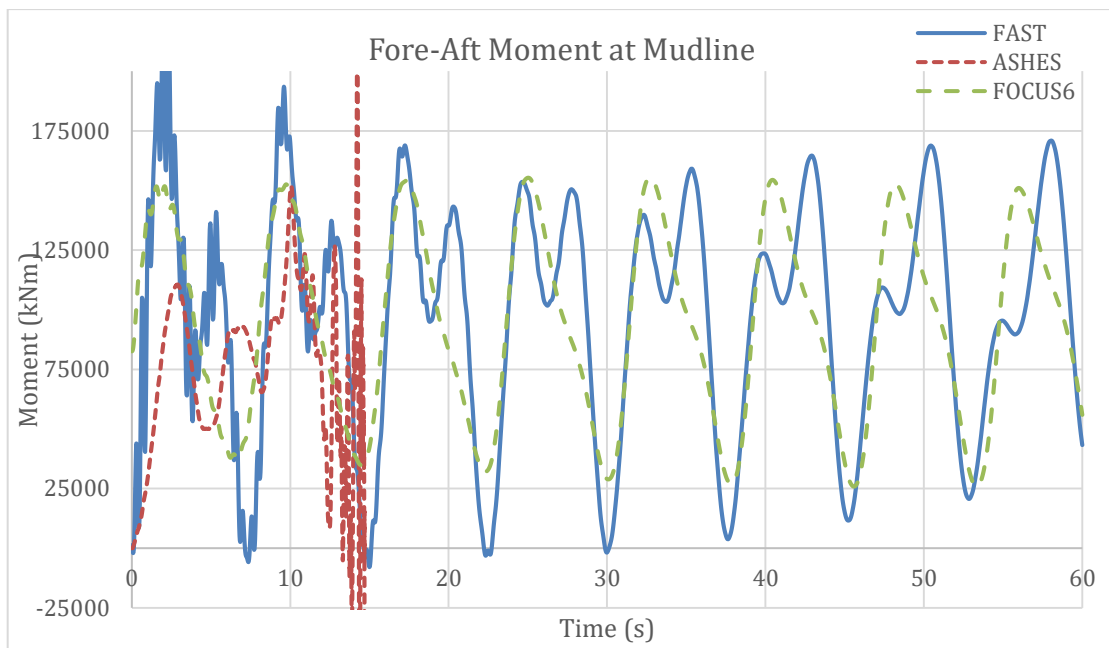


Figure 7.20 Fore aft moment at mudline for DNV load case 6.1c

Tower fore-aft deflection results are shown in Figure 7.21. FAST results remain slightly under the results from ASHES and FOCUS6. In addition, the average of ASHES results is slightly higher than that of the FOCUS6 results. However, although it is not possible to see the response for a longer time because of the instability problem in the blades, the steady-state response of ASHES might be even closer to the FOCUS6 results.

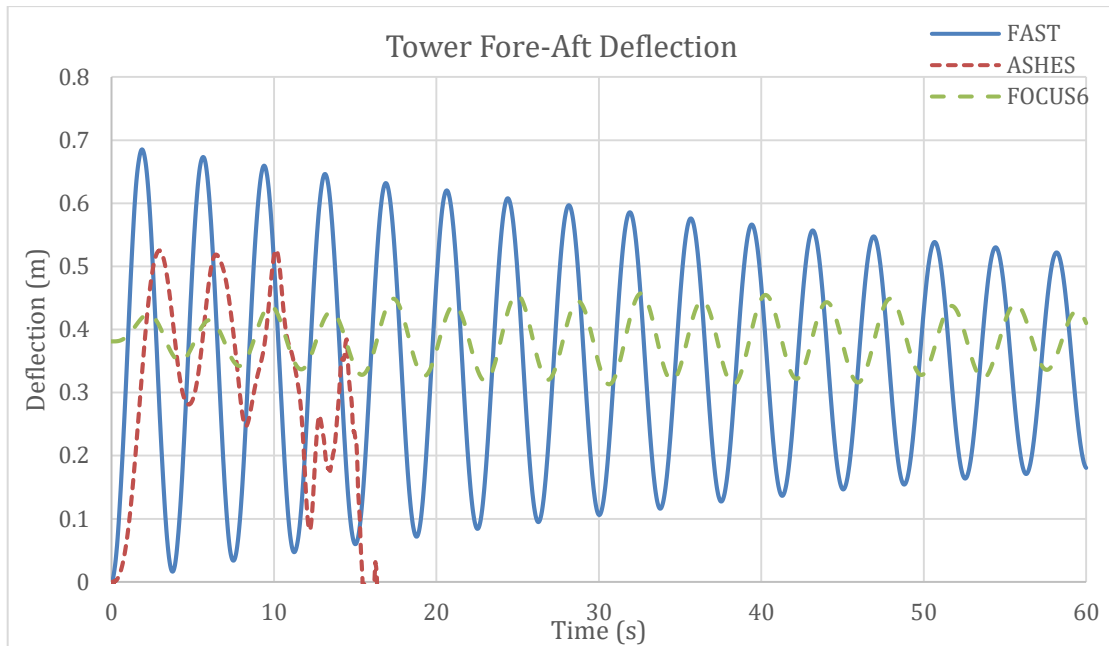


Figure 7.21 Tower fore aft deflection for DNV load case 6.1c

## 7.5 Comparison study for the gravity base structure

### 7.5.1 Description of the structure

The OWT was also analysed with a gravity base foundation, which could be a suitable solution for the planned offshore wind farm of Blekinge Offshore AB. Furthermore, its geometry was selected to meet the requirements for the environmental conditions laid out in the site investigation report by Gyllenram et al. (2009).

Figure 7.22 is an illustration of the OWT tower and its gravity base. In principle, the gravity base is a hollow reinforced concrete drum with a solid base plate. It is divided into a conical section that resides below the mean water level and a cylindrical section which rises up to a height of 10 meters above the mean water level. The steel tower settles at the top of this cylindrical section. In order to counteract the effect of buoyancy, it is possible to fill the hollow section of this gravity base with dense fluid or ballast. The geometry of the base structure is summarised in Table 7.8.

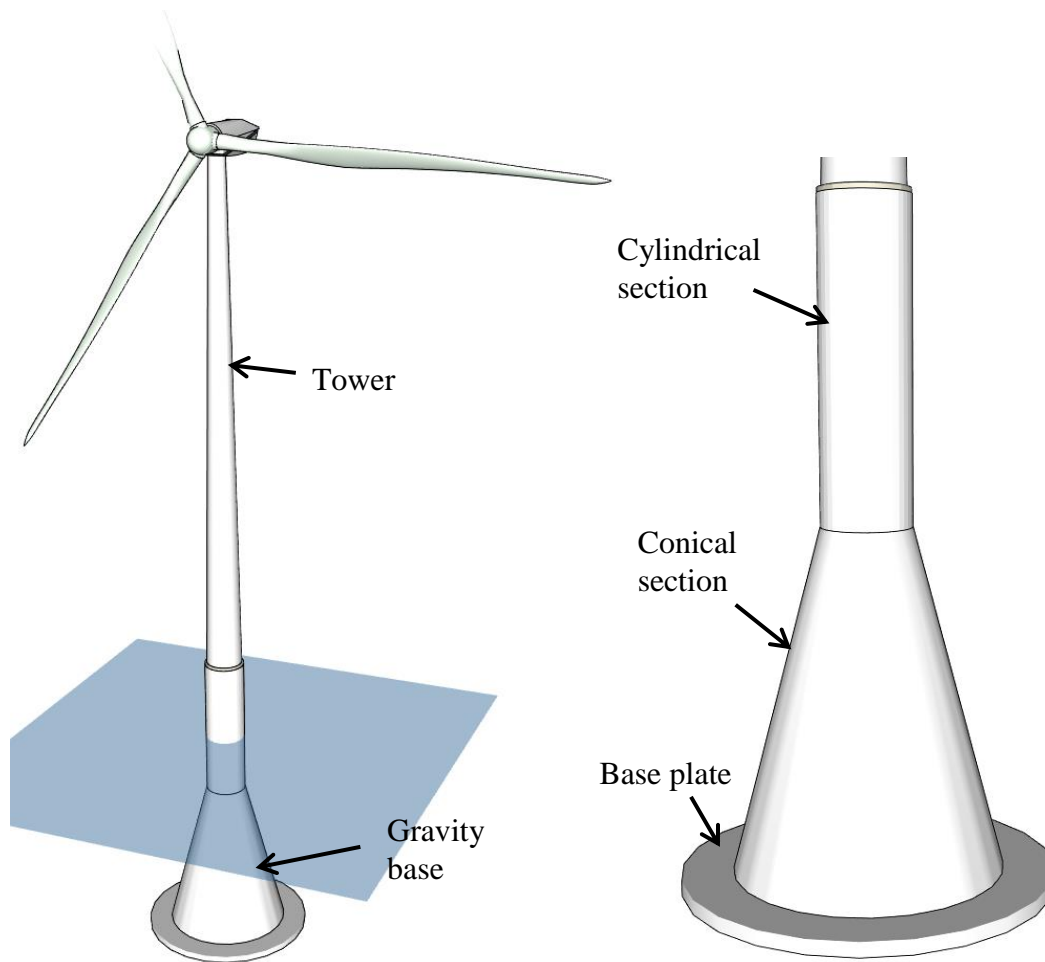


Figure 7.22 Illustration of the gravity base structure

Table 7.8 Geometry of the gravity base structure

Part	Height (m)	Outer Diameter (m)	Thickness (m)
Base plate	1	25	3.5
Conical section	23		
Bottom of cone		18	0.75
Top of cone		6	0.75
Cylindrical section	21	6	0.75

The material properties for the gravity base are summarised in Table 7.9

Table 7.9 Material properties for the gravity base

Material Properties of Concrete	
Density	2500 kg/m <sup>3</sup>
Young Modulus	3.6E+10 Pa
Shear Modulus	2.1E+10 Pa
Poisson's Ratio	0.2



## **7.5.2 Modelling the support structure**

The support structure was modelled element-wise in all of the three simulation codes. This means that the structure was assumed to be composed of numerous elemental cylinders that were assembled to form the entire system. In the tapered part of the structure, the element radius was allowed to decrease sequentially as the foundation gained height.

In FAST and ASHES, the structure was automatically divided into its sub elements by virtue of the number of elements defined by the user. FOCUS6 however, could not carry this out automatically and therefore the elements were described manually.

In practice, the hollow part of the concrete drum is often filled with either water or suitably dense material. However, here the drum was modelled as unfilled since the version of ASHES used in this project was not equipped with this capability.

It is often typical to see a transition piece in OWT support structures as extensively discussed in the tripod model as well as the jacket model. On the other hand, gravity systems have little regard for a transition piece and therefore the gravity base model in this project did not include a transition piece. Lastly, similar to the tripod model, marine growth was disregarded.

## **7.5.3 Soil interaction in the model**

Similar to the tripod model, the gravity base was assumed to be firmly fixed on the sea bed although in reality there is a reasonable degree of flexibility. This flexibility was ignored.

## **7.5.4 Results**

### **7.5.4.1 Results from load case 1**

From Figure 7.23, the average weight of the structure at steady state in FAST is seen to be 32709 kN which is approximately similar to the output from FOCUS6. On the hand, both the Calfem and ASHES models weighed approximately 32660 kN. This proximity of results was expected because the model assembly procedure for all the programs is similar. The tapered part of the structure was divided into the same number of elements.

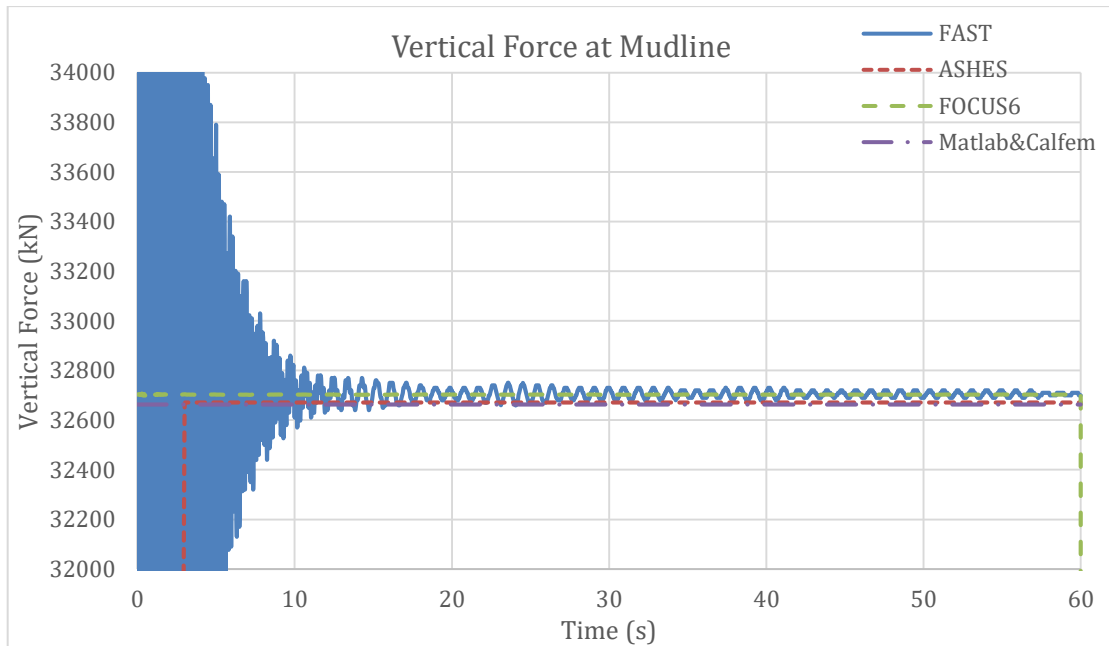


Figure 7.23 Vertical force at the mudline for load case 1

The initial oscillations associated with FAST results originated from the internal vibrations of the structure prior to reaching steady state conditions. The steady state internal vibrations are also present in the FOCUS6 result, but cannot be seen due to the resolution of the graph. However, while the oscillations in FOCUS6 are steady right from the start of the simulation, the result in ASHES gradually grows from zero to the maximum steady load without oscillating. This gradual change can only be seen if the resolution of the graph is increased, as shown in Figure 7.24.

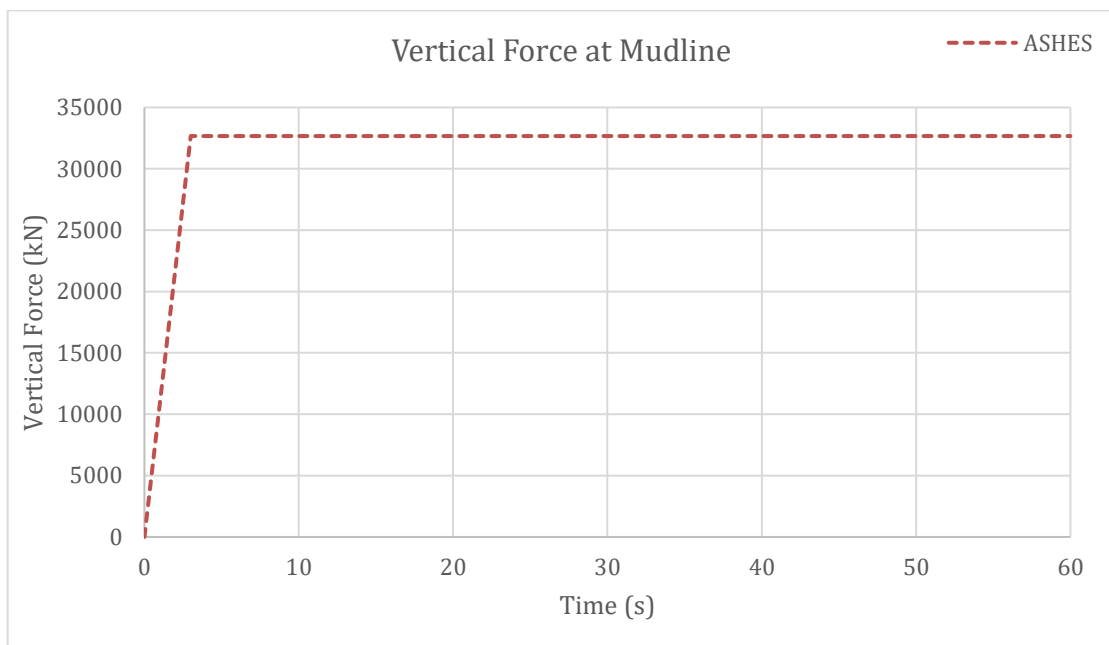


Figure 7.24 ASHES results for the vertical force at the mudline for load case 1

#### 7.5.4.2 Results from load case 2

On their own, currents produce a relatively small load effect as clearly seen in Figure 7.25. However, there was a difference of about 50kN in the average shear force due to currents in FOCUS6 and FAST.

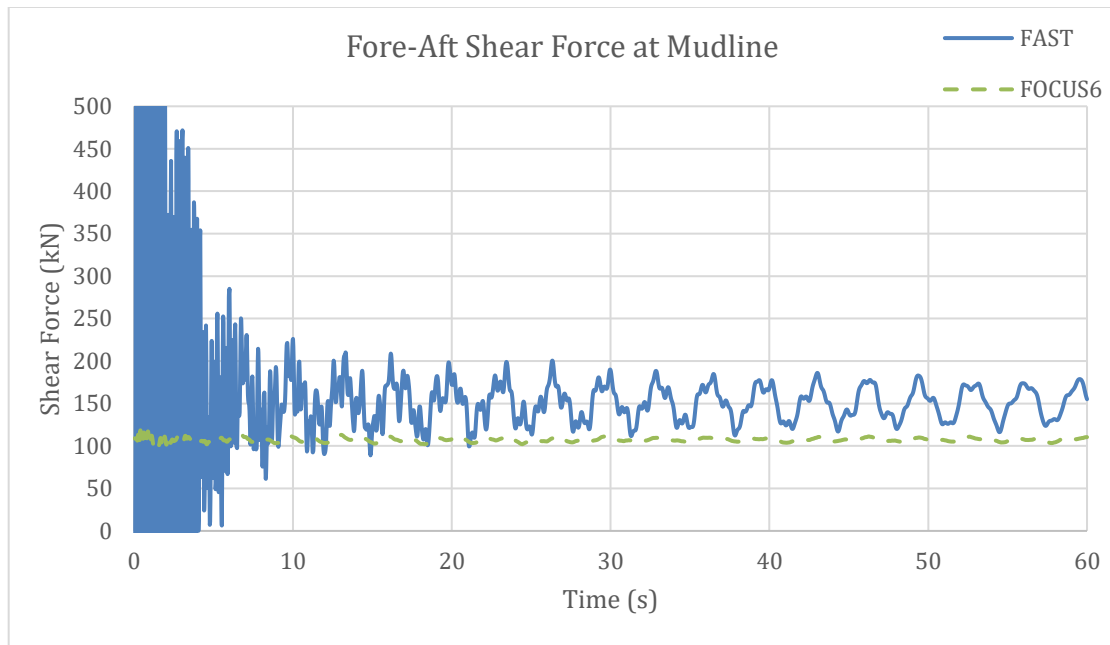


Figure 7.25 Fore-Aft shear force at the mudline for load case 2

#### 7.5.4.3 Results from load case 3

Figure 7.26 show resemblance in amplitude for FOCUS6 and FAST. The difference in phase angle was considered insignificant since it remains consistent. However, ASHES shows marked differences in both amplitude and phase angle.

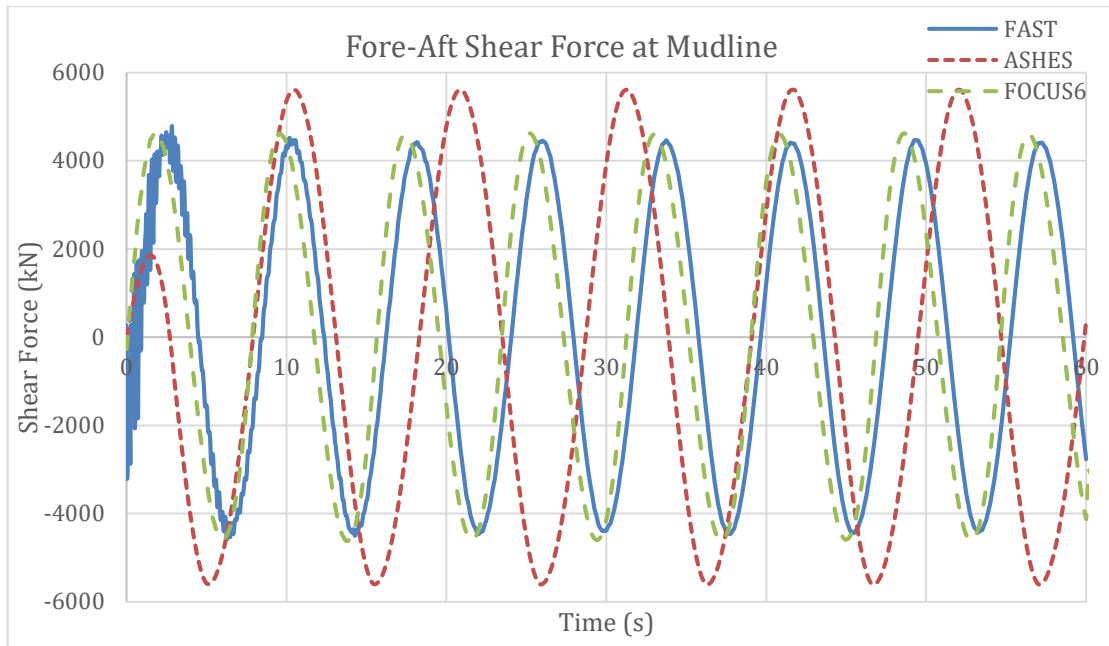


Figure 7.26 Fore-Aft shear force at the mudline, for load case 3

#### 7.5.4.4 Results from load case 4

Load case 4 also presents the results from the Matlab code in addition to FAST, ASHES and FOCUS6, as a means to verify that the structure was deflecting as expected.

It can be seen from Figure 7.27 and Figure 7.28, the average deflection results range from 0.28 m to 0.3m. It was considered acceptable since all the codes produced results conforming to this range over the entire simulation time.

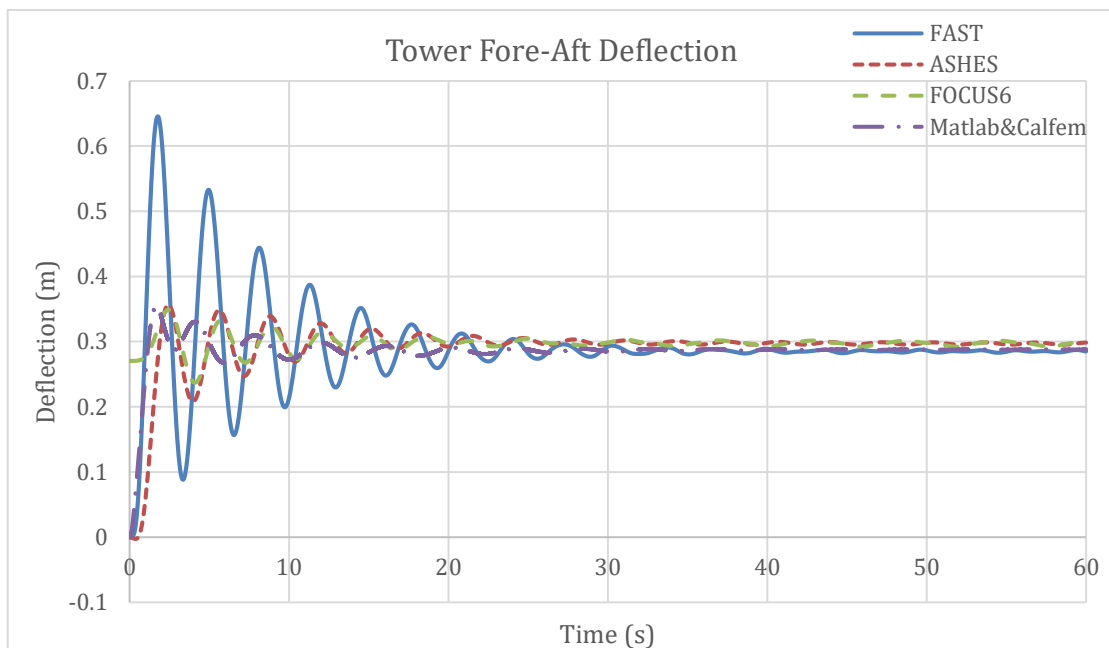


Figure 7.27 Fore-Aft tower deflection for load case 4

Similar to the deflection, the shear force results in Figure 7.28 showed similarity over the entire simulation time. The average shear force value according to Figure 7.28 is 480 kN.

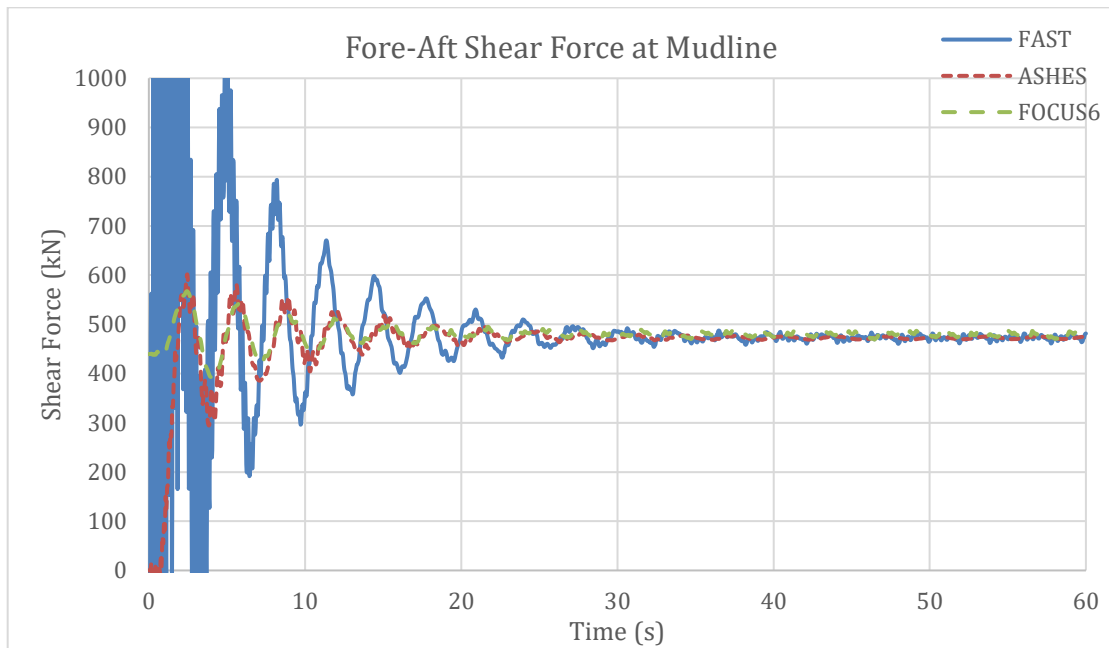


Figure 7.28 Fore-Aft Shear force at the mudline for load case 4

The fore-aft bending results in Figure 7.29 followed the same manner as the shear force results explained before. The average bending moment is seen to be approximately 60000 kNm according to Figure 7.29.

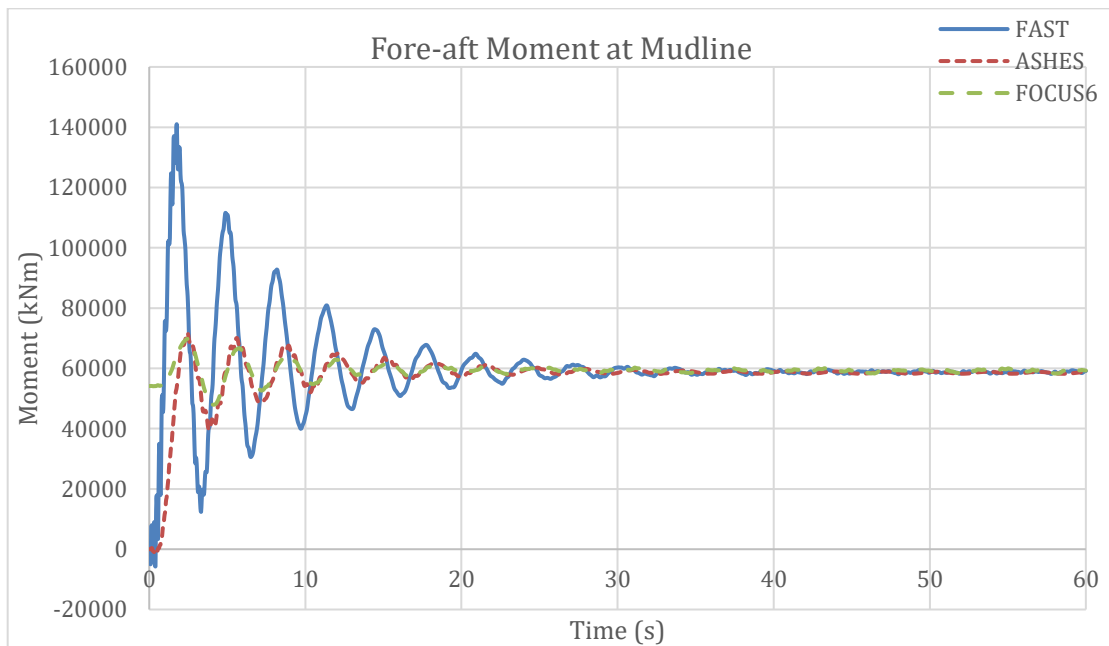


Figure 7.29 Fore-Aft bending moment at the mudline for load case 4

#### 7.5.4.5 Results from DNV load case 1.1

Disregarding the initial oscillations shown in the FAST results, the deflection results shown in Figure 7.30 remain consistent over the entire simulation time. The average deflection is seen to be approximately 0.3 m.

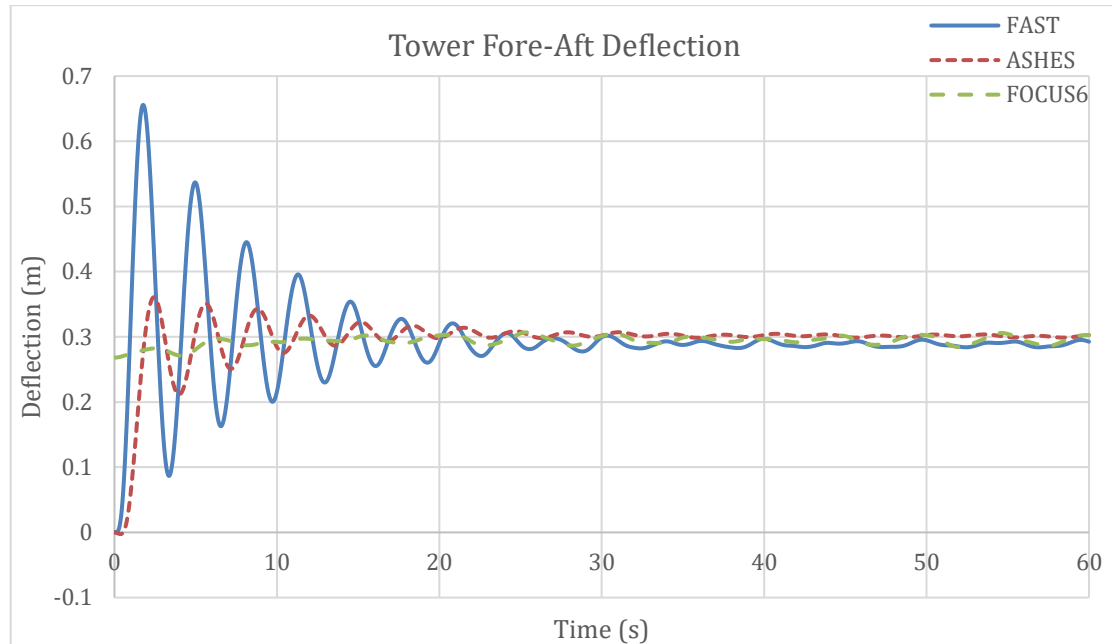


Figure 7.30 Fore-Aft tower deflection for DNV load case 1.1

The fore-aft shear force results from FAST and FOCUS6 produced some minor deviation in amplitude. Figure 7.31 shows an approximate difference of 160 kN in amplitude between FOCUS6 and FAST. However, it is worth noting that this gap in results remains fairly consistent for most of the simulation.

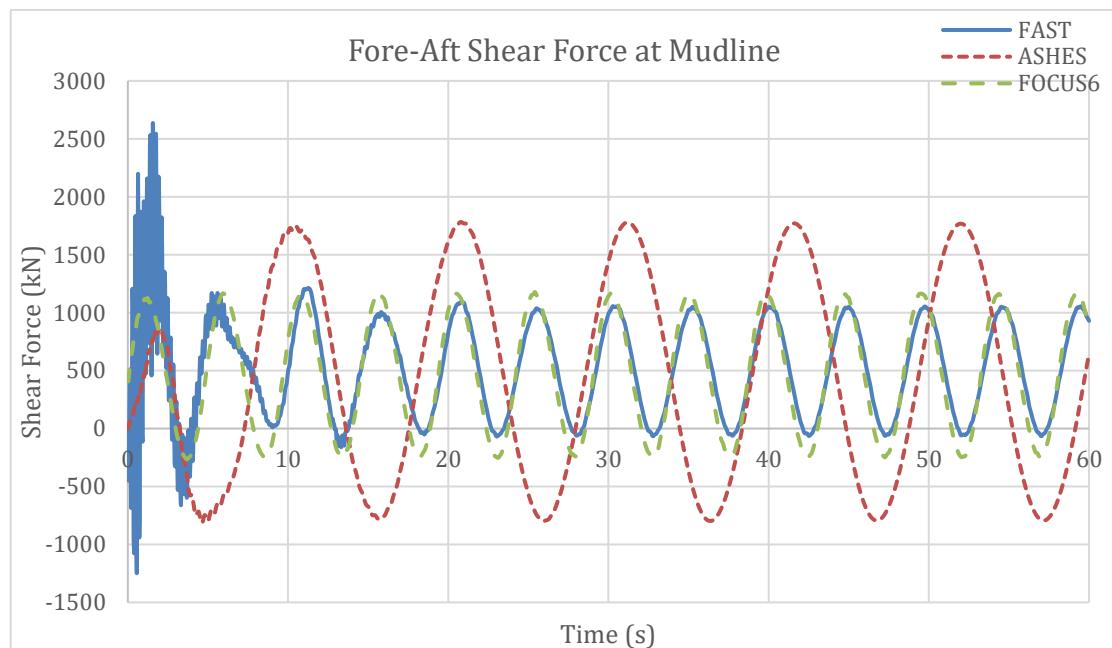


Figure 7.31 Fore-Aft shear force at the mudline for DNV load case 1.1

The gap exhibited between shear force results for FOCUS6 and FAST is also exhibited in the fore-aft moment at the mudline. As shown in Figure 7.32, the results indicate a difference of about 3560 kNm in the amplitude. However, this difference is seen to remain consistent for the entire simulation time once steady state conditions are attained. Interestingly, results for ASHES have much the same amplitude as the FAST results even though, the amplitude in shear force was evidently different.

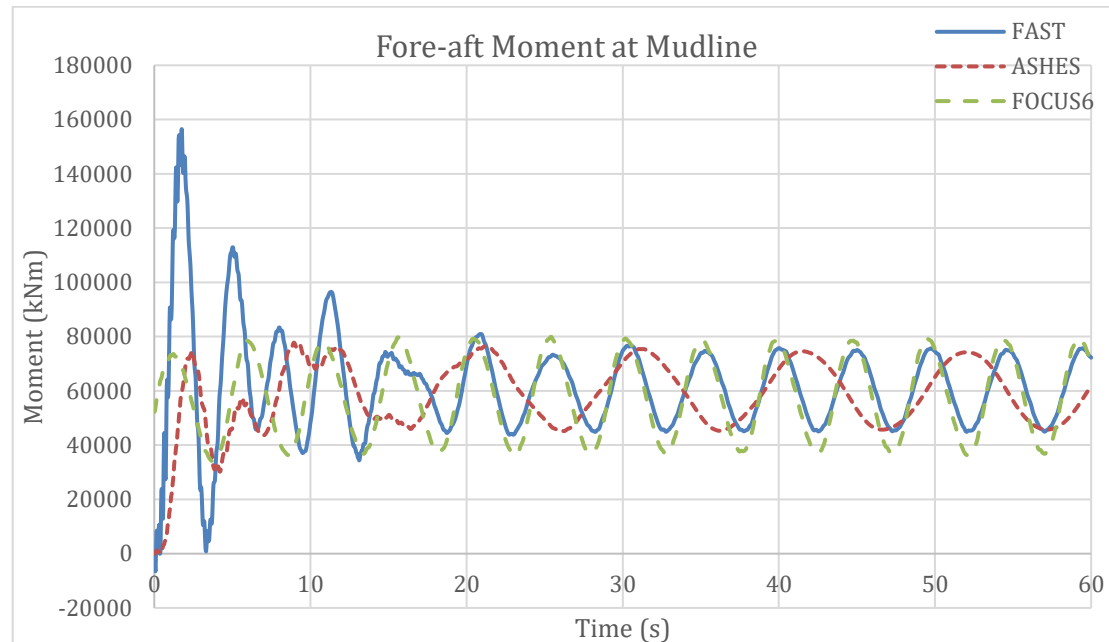


Figure 7.32 Fore-Aft bending moment at the mudline for DNV load case 1.1

#### 7.5.4.6 Results from DNV load case 6.1c

All ASHES results for DNV load case 6.1c were truncated at 15 seconds, due to model instability that developed beyond 15 seconds of simulation. This instability phenomenon was observed in only this load case.

The FAST results are seen to oscillate with higher amplitudes than FOCUS6 and ASHES. Figure 7.33 shows that these oscillations are dumping out as the simulation proceeds. It is worth noting that the average deflection seen in the FAST results is not far off from what FOCUS6 produces, with just a difference of 0.02 m. The average deflection shown by ASHES results is approximately 0.305 m, which is slightly more than the FOCUS6 results. Again, this gap remains consistent for a considerable amount of the simulation time.

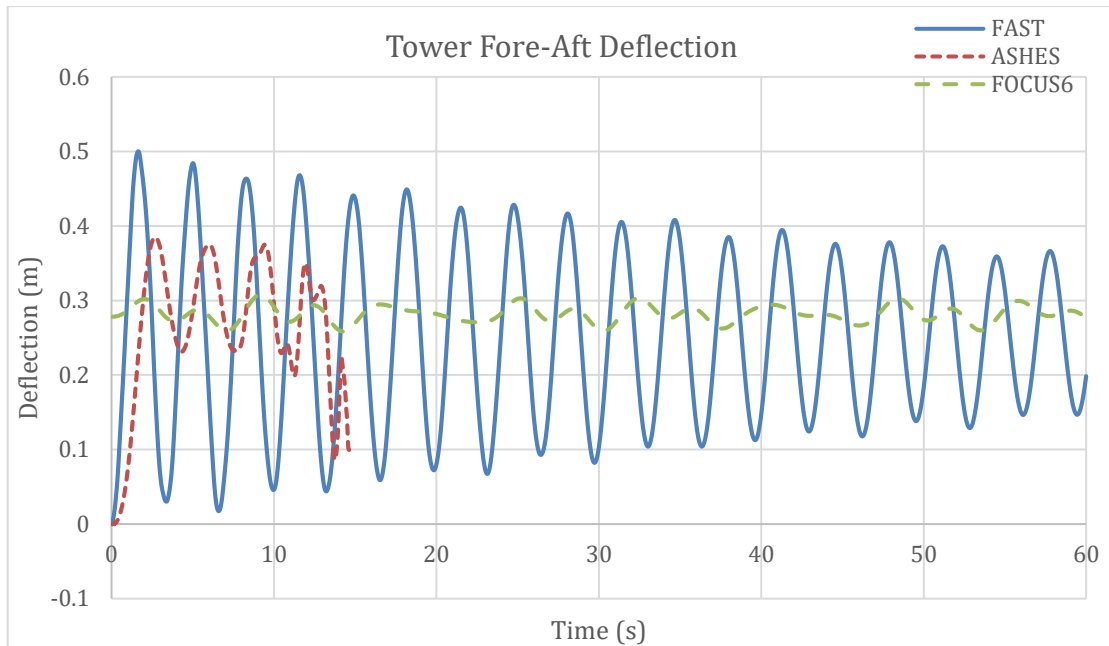


Figure 7.33 Fore-Aft tower deflection for DNV load case 6.1c

The fore-aft shear force results shown in Figure 7.34 indicate a fluctuating difference in FOCUS6 and FAST output. This was expected given that extreme loads were studied in this load case and each program handles such extreme loading differently.

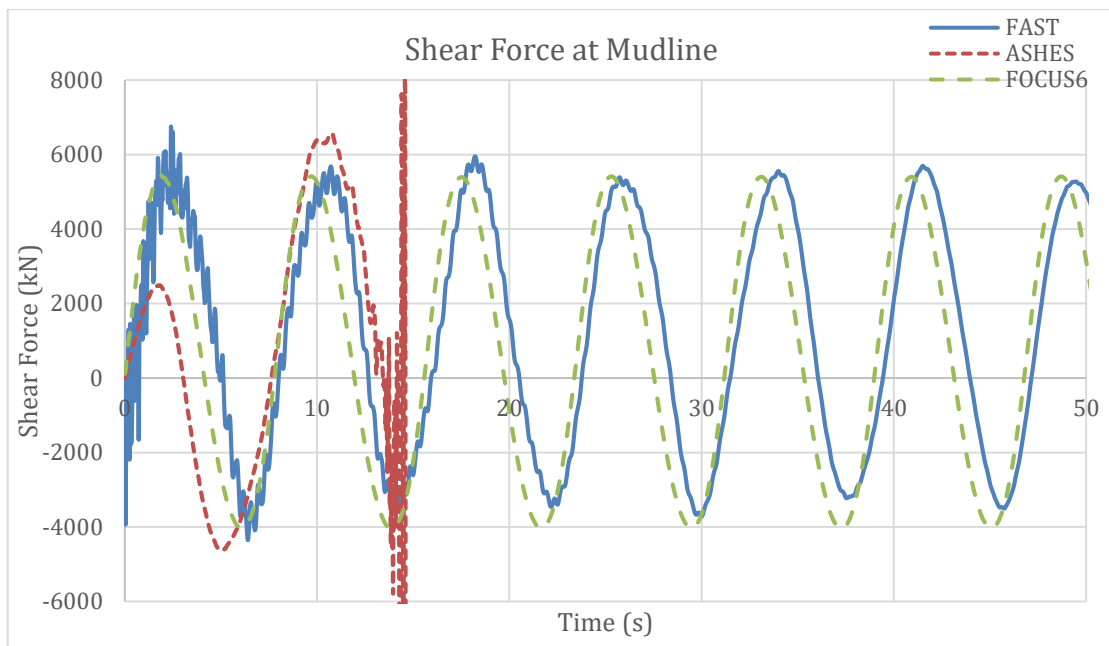


Figure 7.34 Fore-Aft shear for at the mudline for DNV load case 6.1c



The fore-aft moment results at the mudline shown in Figure 7.35 highlights the distinctions in the way these programs handle such extreme environmental conditions. Even though the amplitude seen in the FOCUS6 results is close to that produced by FAST, the irregularity of the oscillation in the FAST results is very evident. On the other hand, the FOCUS6 oscillations remain fairly regular. On the contrary, the irregularity in ASHES oscillations seems to keep growing until the model becomes unstable. It is fair to say though, that the average fore-aft bending moment results for FOCUS6 and FAST are similar, approximately 74500 kN. The average for ASHES is also seen to be close to FAST and FOCUS6.

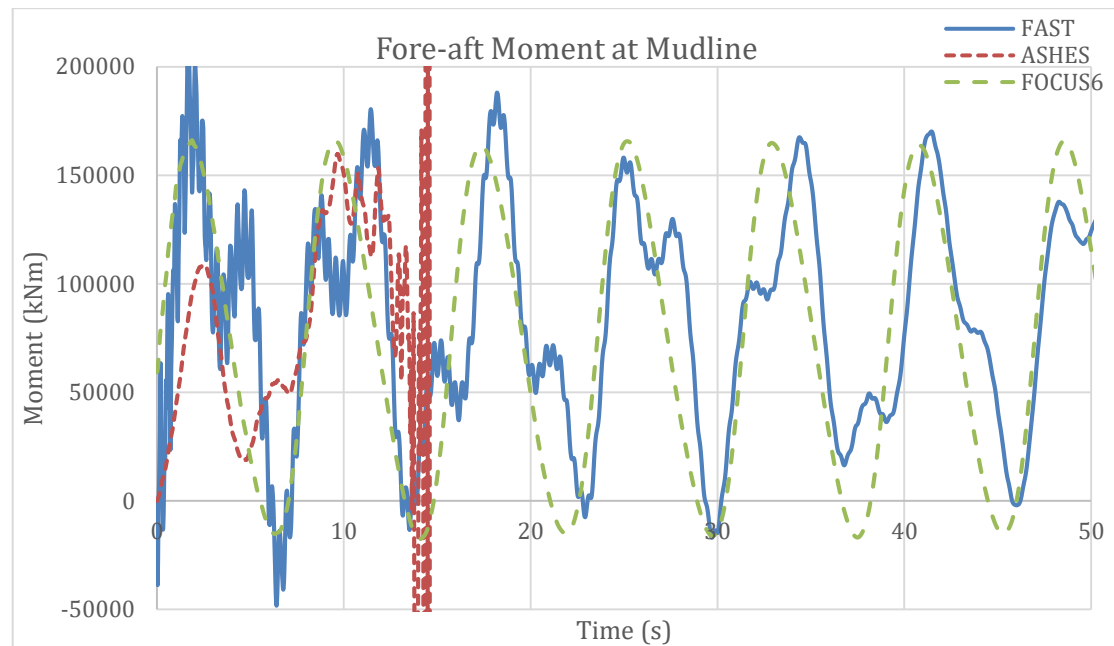


Figure 7.35 Fore-Aft bending moment at the mudline for DNV load case 6.1c

## 8 Discussion

This chapter discusses the results of the simulations of the tripod and gravity base support structures and presents the observations made. The differences and similarities between the code results are discussed in Section 8.1 from one load case to another, in each case highlighting possible reasons behind discrepancies. In addition, the results are discussed from a design point of view in Section 8.2. A summary of the load cases and the respective environmental conditions is shown in Table 8.1.

Table 8.1 Studied load cases and corresponding environmental condition

Load Case	Wind Condition	Wave Condition	Current	Water Level
Load Case 1	-	-	-	-
Load Case 2	-	-	0.89 m/s	MWL
Load Case 3	-	H=6.5 m T=7.8 s	-	MWL
Load Case 4	8.79 m/s	-	-	MWL
DNV-OS-J101 (2014) Load Case 1.1	8.79 m/s	H=1.49 m T=4.84 s	0.159 m/s	MWL
DNV-OS-J101 (2014) Load Case 6.1c	57.09 m/s	H=6.5 m T=7.8 s	0.89 m/s	50-year sea level

As mentioned in Section 7.3, load cases 1 to 4 were only used to consecutively check the simulation codes in terms of the hydrodynamic and aerodynamic responses hence they are not typical design load cases. However, from these load cases, it was then possible to observe the dominant environmental conditions in the results as discussed later on in Section 8.2.

### 8.1 Comparison of the simulation codes

A study of the structural weight in load case 1 showed consistent results from all simulation codes for both the tripod and gravity base models. Furthermore, for the gravity base system, the results were verified with an additional model created in Matlab with Calfe toolbox. This confirmed that in both structure types, the model assembly was correct prior to studying more complex load cases.

Load case 2 was a case of more complexity than load case 1. Again, the agreement between the simulation codes was evident despite the minor difference in the results. However, as one might note, this load case did not include results from ASHES because it is not yet able to model sea currents. In addition, FOCUS6 is limited to the simple uniform current model whereas FAST is able to describe all possible current models (Section 4.4). Therefore, to get comparable results between FAST and FOCUS6, the uniform current model was adopted in FAST even though it was unrealistic to use it for such deep waters.

From load case 3, an issue was detected in ASHES: even if the wave period was changed in the user interface, the software still took a certain time period (approximately 10.2 seconds) into account. The developers intend to fix this issue in the next release of the software. In the tripod model, this did not affect the amplitude of the result. However, there was a considerable increase of the amplitude of the gravity base result. This was probably attributed to the massive shape of the gravity base structure; nevertheless, it requires further investigation. The ripples observed in the results from FAST can be ignored since they are vanishing with time and are caused by minor start-up transients. Apart from that, the results showed a good agreement between each simulation code.

The aero-elastic response of the tripod and gravity base structures coming from load case 4 produced consistent fore-aft shear force results in all three simulation codes. However, there was a difference in the way the simulation codes apply the aerodynamic loads at the beginning of the simulation. It was observed that FOCUS6 initialises with a static equilibrium load and therefore the shear force and the tower deflection start from a certain value. Moreover, in ASHES, the load is ramped up gradually over the first few steps to minimise the sudden impact of the aerodynamic load. However, FAST applies the load abruptly at the start and therefore the result from FAST has very big oscillations at the beginning of the analysis. Nevertheless, all the codes converge at the same shear force and as mentioned before, start-up transients can normally be neglected.

Moreover, in load case 4, the tower deflection results from ASHES in the tripod model were found to be sensitive to the height of the transition piece (see Section 7.4.4.4). The developers aim to correct this in the transition piece definition in the next release of the program. However, for the gravity base model, the deflection results were consistent for all simulation codes. Similar to load case 1, these deflection results were also verified with the Matlab-Calfem model.

DNV load case 1.1 involved typical fatigue conditions. The results of the fore-aft deflection in both structures showed that the waves and currents have negligible effect on the deflection of the tower top because of the fact that almost similar results were obtained with load case 4.

In both structures, the shear force results from DNV load case 1.1 produced a number of interesting observations. Unlike in load case 3 of the tripod, here the difference in the wave period between ASHES and the rest caused a difference in the respective amplitudes of the results. However, it is important to note that the result might be sensitive to the wave height as well. On the hand, for the gravity base structure, the difference observed in the amplitudes in load case 3 was also observed in this load case too.

The moment results for the tripod structure from DNV load case 1.1 were obtained as expected considering the difference in the shear force results. However, due to the high moment arm of the geometry, the difference is magnified by the height of the structure in the moment results. On the contrary, the moment results for the gravity base were unexpected in comparison to the analogous shear force results. Although, the amplitude of the shear force results from ASHES was higher than the other

results, the corresponding moment amplitude from ASHES turned out to be lower. This might be because of the shape of the gravity base foundation though.

The extremities associated with DNV load case 6.1c resulted into model instabilities in the blades of the ASHES model for both structures. After a point, the blades showed unrealistic blade deformations which resulted into an unrealistic structural response. The developers were made aware of this issue and therefore probable fixes can be expected in the coming versions. Beside the instability and the wave period issues in ASHES, the shear force results from all three show consistent agreement. The moment results from FAST showed more irregularity at the beginning of the simulation but the behaviour became more regular with time. However, FOCUS6 results did not show a noticeable change with time because of the principle it adopts to apply the steady-state load at the beginning of the analysis as explained earlier on. Since ASHES results were truncated because of the instability issue, it was not possible to check possible irregularities in the results.

Prior to the blade instability, the ASHES deflection results were very similar to those seen from FOCUS6 in both structures. However, there was a slight difference seen in the FAST results. In terms of oscillation, the FAST results showed more resilience against the damping effects that were observed in the previous load cases. This might be due to the high wind speed, which eventually undermined all possible damping in the structure.

## **8.2 Discussion of the results from a design vantage point**

As discussed in the Section 2.4, wind turbines are highly dynamic structures which suffer from both cyclic and extreme loading conditions. Therefore, there are two main challenges in OWT foundation design namely, fatigue limits and ultimate limits. It is worth noting that the engineer should also consider serviceability limits in the design. Hence, this section aims at discussing the results of this study from the design point of view.

Fatigue design is not only governed by the amplitude of the result but also the number of load cycles. This implies that the dominant loads in fatigue design are those responsible for the oscillations in the results. From the results of this thesis project, this seemed to be mainly due to the waves. However, it is important to remember that only constant wind action was considered in this thesis. For instance, Figure 7.10, that represents the shear force results from load case 3, shows considerably big oscillations from a negative point to a positive one with a mean shear of zero. However, the shear force profiles due to the currents and wind oscillate about a certain value without changing the signs as seen in Figure 7.9 and Figure 7.11. The oscillations here were seen to be less pronounced than those from the waves. Although one can argue that the reason for this might be because of the steady wind and current loads, the possibility is very high that even with cyclic wind loading the magnitude of the oscillations does not exceed that from waves. For that reason, waves were deemed to be the dominant environmental factor in fatigue design. It should also be noted that the cyclic behaviour of moment results also has to be considered in fatigue design, not just the shear.

Design for ultimate limits on the other hand is only dependent on the magnitude of the results. In fact, ultimate limit design considers the external loads on the structure in terms of axial force, shear force and moment respectively.

The dominating load for shear force response at the mudline in ultimate limit state is highly dependent on the geometry of the structure and specific environmental conditions. From Figure 7.10, it can be seen that the maximum shear force value due to the waves is considerably larger than the value due to the currents as shown in Figure 7.9. In addition, one can also see that the shear force due to the wind as shown in Figure 7.11 is considerably low compared to that from the waves. However, the wind speed used to obtain the results shown in Figure 7.11 was the mean value. Therefore, it is possible that wind can dominate the design if higher wind speeds are applied.

The dominating load for the moment at the mudline in ultimate limit state is also highly dependent on the geometry of the structure as well as the environmental conditions. Although, there is a considerable correlation between shear force and moment, the leverage of the loads also has a big effect on the moment results. Similar to the shear response, waves again cause oscillations in the moment results about a mean value of zero, whereas wind results have small oscillations about a certain value. For instance, it can be observed from Figure 7.15 for load case 4 and Figure 7.18 for DNV load case 1.1 that the mean values of the moment results are the same, the only difference being the oscillations in Figure 7.18. Therefore, one can argue that the wind dictates the average moment whereas the waves dictate the amplitude of the moment oscillations. In this case, wind governs the moment results. However, generally it is hard to presume the dominant environmental action for moment results, since the leverage of the wind action to the base is dependent on the height of the structure.

The design of the structure in serviceability limit state depends on vibrations and deformations of the structure. In this project however, only tower top deflection response was studied in different load cases, not the vibration. In addition, there is no big difference in the tower top deflection results shown in Figure 7.15 and Figure 7.17 for load case 4 and DNV load case 1.1 respectively, even though the latter case includes the waves and currents yet the former case has only the wind. This implies that the deflection at tower top is mainly due to the wind. However, when it comes to vibration, a steady cyclic load may cause a considerable effect on the serviceability. Hence, the wave action might dominate the serviceability limits in vibration, of course the dynamic effects of the wind on vibration (such as dynamic stall) are ignored.

In summary, considering the environmental data and the geometry of the structures studied in this project, the dominating actions varied for different design requirements. For instance, waves had a dominant effect in the shear force results at the mudline compared to the rest. Moreover, due to the cyclic nature of the wave loads, waves were deemed to be the determining environmental action in fatigue design and vibrations. On the other hand, wind had a considerable effect on the tower top deflection and the moment results at the mudline. Currents however, had a little effect on shear and moment results at the mudline compared to waves and wind. They merely amplified the shear and moment results.

## 9 Conclusion and Future Recommendations

### 9.1 Conclusion

There are numerous foundation solutions for offshore wind turbines (OWTs) as revealed by the literature study conducted. These solutions are specific depending on ground conditions, water depth and other environmental situations. The literature study also introduced the various principles, methods and load models used in OWT design. Past literature showed that extensive research has been conducted to develop OWT simulation codes. From this, one can observe that some simulation codes are more advanced than the others in terms of being able to describe complex foundation types and loads. This provided a proper basis for the classification of OWT simulation codes which outlines the similar and different principles adopted by each code.

Some simulation codes were examined through case studies with two different foundation structures, including tripod and gravity base to practically establish their capabilities and limitations. These case studies revealed that the codes differ in various ways, for instance: mode of modelling the structure, way of describing environmental loads and analysing models. In addition, the simulation codes showed variety in the application of the environmental loads, which eventually affect the response of the structural model. One should note however that the differences also might depend on the type of the foundation being modelled.

Comparison of different results indicated that a limitation of a code to model a given environmental condition may result into a number of variations in the output. For instance, a limitation in the way a code models hydrodynamic loads may result into a variation in the shear force results which at the same time affects the moment results at the base. In fact, the code limitations seen in this project were easily detected only because comparisons were made between codes.

In general terms, there was a good agreement between the results from the simulation codes and one might be driven to conclude that all simulation codes produce similar results. However, this would be an over simplified judgement given that only three simulation codes were studied in this project. A better conclusion may be drawn if more codes were to be studied. In specific terms though, the differences seen between the codes varied between different load cases as discussed in Section 8.1. For instance, the relatively simple load cases (load case 1 to 4) did not show pronounced differences in the code results, however, the more complex load cases (DNV load case 6.1c) brought out more marked variations.

Simulation code development has evolved over many years to include new demands in foundation types, modelling procedure and overall user friendliness. Currently, all codes are at different stages of development and therefore have different levels of capabilities. For instance, FAST has very developed load models, turbine control modules and ability to describe complex structures. FOCUS6 on the other hand, has advanced load case definition modules which might be very helpful in the design process. For ASHES, the well-developed user interface makes the modelling process and result extraction considerably easy. A conclusion is that further development in the future versions of these simulation codes will only serve to improve the process of OWT simulation and design by allowing for more realistic model definitions.

All in all, this project showed that the choice of the simulation code might be dependent on the type of foundation structure to be designed. Moreover, the study proved that the environmental conditions also play an important role in the selection of suitable simulation codes for a given project. For instance, one might look at how the type of structure depends on the water depth which then defines the theory appropriate to calculate the hydrodynamic loads acting on the structure. Therefore, it is important to assess the suitability and capability of the simulation code to be used before modelling the structure.

## **9.2 Future recommendations**

In this project, due to a restricted timeline, only three simulation codes were studied in detail. Nonetheless, including more simulation codes with different theories and principles adopted would bring more interesting discussions. For instance, comparing simulation codes employing Morison Equations and Potential Flow Theory could give good arguments not only regarding the choice of simulation codes but also of the theories used.

Because of the same reason as mentioned above, design aspects of the simulation codes were not studied in this project. To exemplify, the supported design codes in terms of load combinations, meeting the modelling requirements specified in the codes of practice etc. Hence, examining the simulation codes considering the requirements in the codes of practice would add a different point of view to the assessment.

Apart from that, only the fixed foundation model was used in all comparison studies. It would be very interesting to examine the simulation codes for such models with flexible foundations as well as comparing different flexible foundation models in different simulation codes.

In addition, the results of this project may open many new horizons for possible future studies. For instance, the difference in wave period in load case 3 only affects the shear force results in the gravity base model, but not in the tripod model. The reason behind this might be the bold diameter or the considerable conical shape of the gravity base foundation. One way to examine this could be by studying the same load case with a straight monopile foundation in all three (or more) simulation codes starting with a considerably tiny section and comparing the results for every increment in the diameter of the section. According to the response one can bring good arguments such as: if the shear forces would not show differences in big-sized monopile foundations, then one can argue that the variation that occurred in this study was because of the shape of the gravity base foundation and may lead to deep discussions of the application of the principle adopted in hydrodynamic loading.

## 10 References

- 4C Offshore LTD, 2016. Monopiles Support Structures. Available at: <http://www.4coffshore.com/windfarms/monopiles-support-structures-aid4.html> [Accessed February 11, 2016].
- Abhinav, K.A. & Saha, N., 2015. Dynamic analysis of an offshore wind turbine including soil effects. *Procedia Engineering*, 116(1), pp.32–39. Available at: <http://dx.doi.org/10.1016/j.proeng.2015.08.261>.
- Airy, G.B., 1845. *Tides and Waves*. , pp.241 – 396.
- Andrew, S.E. & Todd, R.D., 1996. ADAMS\_WT Advanced Development-Version 1\_4 and Beyond. , pp.1–11.
- Anon, 2016. OneWind. Available at: <http://www.onewind.de/OneWindStudent.html> [Accessed April 4, 2016].
- API, 2007. Recommended Practice for Planning , Designing and Constructing Fixed Offshore Platforms — Working Stress Design. *Api Recommended Practice*, 24-WSD(December 2000), p.242. Available at: <http://scholar.google.com/scholar?hl=en&btnG=Search&q=intitle:Recommended+Practice+for+planning,+designing+and+constructing+fixed+Offshore+Platforms+-+Working+stress+design#0>.
- Bai, Y. & Jin, W.-L., 2016. *Loads and Dynamic Response for Offshore Structures*, Available at: <http://linkinghub.elsevier.com/retrieve/pii/B9780080999975000071>.
- Bertrand, Y.A., 2002. Middelgrunden offshore wind farm, off the coast of Copenhagen, Denmark (55°41' N, 12°40' E).
- Bhattacharya, S., 2014. Challenges in Design of Foundations for Offshore Wind Turbines. *Engineering & Technology Reference*, pp.1–9. Available at: <http://digital-library.theiet.org/content/reference/10.1049/etr.2014.0041>.
- Bretschneider, C.L., 1964. Generation of Waves by Wind State of the Art. *International Summer Course Lunteren*, p.160.
- Cassidy, M.J., Taylor, R.E. & Houlsby, G.T., 2001. Analysis of jack-up units using a Constrained New Wave methodology. *Applied Ocean Research*, 23, pp.221–234.
- Crampsie, S., 2014. Offshore windfarms stretch manufacturing supply chains. Available at: <http://eandt.theiet.org/magazine/2014/05/windfarm-foundations.cfm> [Accessed February 25, 2016].
- D.Winkelaar, 1992. Program for Three-Dimensional Wind Simulation. , (December), pp.1–76.
- Dean, R.G., 1965. Stream function representation of nonlinear ocean waves. *Journal of Geophysical Research*, 70(18), pp.4561–72.
- Det Norske Veritas, 2014. Dnv-Os-J101. *Design of offshore wind turbine structures*, (June).
- DNV, 2010. Environmental Conditions and Environmental Loads October 2010. , (October). Available at: <http://www.dnv.com>.
- DNV GL, 2014a. Bladed Theory Manual. , Version 4.(1), pp.1–134.
- DNV GL, 2014b. Bladed User Manual. , Version 4.(1), pp.1–209.
- DNV GL, 2016. No Title. , p.1.
- Eecen, P., 2003. Wind Waves: Forces due to waves on offshore wind turbines. , (September), p.45.
- El-Reedy, M.A., 2012. *Chapter 2 – Offshore Structure Loads and Strength*, Available at: <http://www.sciencedirect.com/science/article/pii/B978012385475900002X>.



- van Engelen, T.G. & Braam, H., 2004. TURBU Offshore, computer program for frequency-domain analysis of horizontal-axis offshore wind turbines - Implementation. , (September).
- Fenton, J.D., 1988. The numerical solution of steady water wave problems. *Computers and Geosciences*, 14(3), pp.357–368.
- Gyllenram, W., Lindahl, S. & Lindberg, A., 2009. Designunderlag havsbaserad vindkraft , Hanöbukten.
- Hansen, a C. & Laino, D.J., 2002. USER ’ S GUIDE to the Wind Turbine Aerodynamics Computer Software AeroDyn. , pp.1–60.
- Hasselmann, K. et al., 1973. Measurements of Wind-Wave Growth and Swell Decay during the Joint North Sea Wave Project (JONSWAP). *Ergänzungsheft zur Deutschen Hydrographischen Zeitschrift Reihe*, A(8)(8 0), p.p.95.
- Henderson, A.R., Zaaier, M.B. & Camp, T.R., 2003. Hydrodynamic Loading on Offshore Wind Turbines. *Theory Of Ordered Sets And Its Applications*, 2(April), pp.1–15. Available at: [http://www.lr.tudelft.nl/fileadmin/Faculteit/LR/Organisatie/Afdelingen\\_en\\_Leerstoelen/Afdeling\\_AEWE/Wind\\_Energy/Research/Publications/Publications\\_2003/doc/Zaaier\\_OWEMES2003\\_Hydro.pdf](http://www.lr.tudelft.nl/fileadmin/Faculteit/LR/Organisatie/Afdelingen_en_Leerstoelen/Afdeling_AEWE/Wind_Energy/Research/Publications/Publications_2003/doc/Zaaier_OWEMES2003_Hydro.pdf).
- Hillmer, B. et al., 2007. Aerodynamic and Structural Design of MultiMW Wind Turbine Blades beyond 5MW. *Journal of Physics: Conference Series*, 75, p.012002.
- IEC, 2005. IEC 61400-1 Wind Turbines - Part 1: Design requirements. *Iec 61400*, 2005, pp.1–92. Available at: <http://homes.civil.aau.dk/rrp/BM/BM8/r.pdf>.
- IEC, 2009. International Standard IEC 61400-3 Wind turbines - Part 3: Design requirements for offshore wind turbines.
- Ingram, G., 2011. Wind Turbine Blade Analysis using the Blade Element Momentum Method. Version 1.1. *October*, (c), pp.1–21.
- J.M. Jonkman, G.J. Hayman, B.J. Jonkman, R.R.D., AeroDyn v15 User’s Guide and Theory Manual.
- Jonkman, B. & Jonkman, J., 2015. FAST v8.12.00a-bjj. , pp.1–42.
- Jonkman, J. et al., 2009. Definition of a 5-MW reference wind turbine for offshore system development. *Contract*, (February), pp.1–75. Available at: [http://tethys-development.pnnl.gov/sites/default/files/publications/Jonkman\\_et\\_al\\_2009.pdf](http://tethys-development.pnnl.gov/sites/default/files/publications/Jonkman_et_al_2009.pdf).
- Jonkman, J. & Musial, W., 2010. Offshore code comparison collaboration (OC3) for IEA task 23 offshore wind technology and deployment. *Contract*, 303(December), pp.275–3000.
- Jonkman, J.M. & Buhl, M.L.J., 2005. FAST User’s Guide. *Acta Psychiatrica Scandinavica*, 123(6), pp.407–8. Available at: <http://www.ncbi.nlm.nih.gov/pubmed/21564034>.
- Jonkman, J.M., Robertson, A.N. & Hayman, G.J., HydroDyn User ’ s Guide and Theory Manual HydroDyn User ’ s Guide and Theory Manual.
- Kaiser, M.J. & Snyder, B.F., 2012. Offshore Wind Energy Cost Modeling - Installation and Decommissioning. *Offshore Wind Energy Cost Modeling*. Available at: <http://www.springerlink.com/index/10.1007/978-1-4471-2488-7>.
- Knowledge Centre WMC, 2016. WMC FOCUS6. Available at: <https://www.wmc.eu/focus6.php> [Accessed February 24, 2016].
- Larsen, T.J. & Hansen, A.M., 2007. *How 2 HAWC2 , the user ’ s manual*, Risø National Laboratory, Technical University of Denmark.
- Lindenburg, C., 2005. PHATAS Release “NOV-2003” and “APR-2005” USER ’ S MANUAL. , (May).

- Lindenburg, C. & Holierhoek, J.G., 2013. Blademode v2.2 : User Manual. , pp.1–136.
- Lucas, C. & Guedes Soares, C., 2015. On the modelling of swell spectra. *Ocean Engineering*, 108, pp.749–759. Available at: <http://dx.doi.org/10.1016/j.oceaneng.2015.08.017>.
- Malhotra, S., 2010. Selection , Design and Construction of Offshore Wind Turbine Foundations.
- MARINTEK, 2009. Modelling of piles in USFOS. , pp.1–15. Available at: [http://www.usfos.no/manuals/usfos/users/documents/Modelling\\_of\\_Piles.pdf](http://www.usfos.no/manuals/usfos/users/documents/Modelling_of_Piles.pdf).
- MARINTEK, 1999a. USFOS User’s Manual - Program Concepts. , pp.1–4. Available at: [http://www.usfos.no/manuals/usfos/users/documents/Usfos\\_UM\\_02.pdf](http://www.usfos.no/manuals/usfos/users/documents/Usfos_UM_02.pdf).
- MARINTEK, 1999b. USFOS User’s Manual - Program Concepts. , pp.1–4.
- Matha, D. et al., 2010. Model Development and Loads Analysis of a Wind Turbine on a Floating Offshore Tension Leg Platform. *European Offshore Wind Conference*, (February), pp.1–10. Available at: <http://www.nrel.gov/docs/fy10osti/46725.pdf>.
- Le Mehaute, B., 1976. *An Introduction to Hydrodynamics and Water waves*, New York: Springer Science+ Business Media New York.
- Modelica-Association, 2012. Modelica® -A Unified Object-Oriented Language for Systems Modeling Language Specification Version 3.3. Available at: <http://www.modelica.org/>.
- Moriarty, P.J. & Hansen, a C., 2005. AeroDyn Theory Manual. *Renewable Energy*, 15(January), pp.500–36313. Available at: <http://www.nrel.gov/docs/fy05osti/36881.pdf>.
- Passon, P. & Branner, K., 2013. Load calculation methods for offshore wind turbine foundations. *Ships and Offshore Structures*, 5302(May 2014), pp.1–17. Available at: <http://www.tandfonline.com/doi/abs/10.1080/17445302.2013.820108>.
- Passon, P. & Kühn, M., 2005. State-of-the-art and development needs of simulation codes for offshore wind turbines. *Copenhagen Offshore Wind 2005 Conference and ...*, pp.1–12. Available at: [http://www.ieawind.org/task\\_23/Subtask\\_2S\\_docs/PPT\\_Risoe/Copenhagen\\_2005-State\\_of\\_the\\_art\\_and\\_development\\_needs\\_of\\_simulation\\_codes\\_for\\_offshore\\_wind\\_turbines.pdf](http://www.ieawind.org/task_23/Subtask_2S_docs/PPT_Risoe/Copenhagen_2005-State_of_the_art_and_development_needs_of_simulation_codes_for_offshore_wind_turbines.pdf).
- Peeringa, J.M., 2013. CurrentROWS manual: Random linear Ocean Waves Simulation on a steady uniform current. , (November), pp.1–49.
- Peeringa, J.M., 2005. Stream Function program user manual. , (February).
- Pierson, W.J.J. & Moskowitz, L., 1964. A Proposed Spectral Form for Fully Developed Wind Seas Based on the Similarity Theory of S. A. Kitaigorodskii. *Journal of Geophysical Research*, 69(24), pp.5181–5190. Available at: [http://adsabs.harvard.edu/cgi-bin/nph-data\\_query?bibcode=1964JGR....69.5181P&link\\_type=EJOURNAL\papers2://publication/doi/10.1029/JZ069i024p05181](http://adsabs.harvard.edu/cgi-bin/nph-data_query?bibcode=1964JGR....69.5181P&link_type=EJOURNAL\papers2://publication/doi/10.1029/JZ069i024p05181).
- Ramachandran, K. et al., 2013. A Numerical Model for a Floating TLP Wind Turbine A numerical model for a floating TLP wind turbine Department of Wind Energy Technical University of Denmark.
- Robertson, A., Jonkman, J. & Musial, W., 2014. IEA Wind Task 30 Offshore Code Comparison Collaboration Continued - Final Management Report.
- Savenije, F. & Peeringa, J., 2009. Aero-elastic simulation of offshore wind turbines in the frequency domain. *Ecnnl*. Available at: <http://www.ecn.nl/docs/library/report/2009/e09060.pdf>.

- Simis, 2015. User Manual ASHES 2.1.
- Sintef Group, 2010. USFOS Hydrodynamics. , pp.1–95. Available at:  
[http://usfos.no/manuals/usfos/theory/documents/Usfos\\_Hydrodynamics.pdf](http://usfos.no/manuals/usfos/theory/documents/Usfos_Hydrodynamics.pdf).
- SINTEF marintek & NTNU, 2016. USFOS non-linear static and dynamic analysis of space frame structures. Available at: <http://www.usfos.no/> [Accessed February 24, 2016].
- Skaare, B. et al., 2006. Integrated dynamic analysis of floating offshore wind turbines. *Proceedings of the International Conference on Offshore Mechanics and Arctic Engineering - OMAE*, 2006.
- Statoil, 2008. StatoilHydro to build first full scale offshore floating wind turbine. [www.statoilhydro.com](http://www.statoilhydro.com). Available at:  
[http://www.statoil.com/en/NewsAndMedia/News/2008/Downloads/hywind\\_04.jpg](http://www.statoil.com/en/NewsAndMedia/News/2008/Downloads/hywind_04.jpg) [Accessed February 11, 2016].
- Thomassen, P.E. et al., 2012. A Novel Tool for FEM Analysis of Offshore Wind Turbines With Innovative Visualization Techniques. , 4, pp.374–379.
- Thomson, R.E., 1981. *Oceanography of the British Columbia Coast*,
- Tromans, P.S., Anaturk, A.R. & Hagemeyer, P., 1991. A New Model for the Kinematics of Large Ocean Waves - Application as a Design Wave. *First International Offshore and Polar Engineering Conference*.
- Usfos, Usfos Download.
- Vahdati, M. et al., 2011. Dynamic stall for a Vertical Axis Wind Turbine in a two-dimensional study. *Fluid Dynamics*, pp.4225–4232. Available at:  
<http://www.ep.liu.se/http://dx.doi.org/10.3384/ecp110574225>.
- Van Der Tempel, J. et al., 2011. *Offshore environmental loads and wind turbine design : impact of wind, wave, currents and ice*, Woodhead Publishing Limited. Available at:  
<http://www.sciencedirect.com/science/article/pii/B9781845695804500156>.
- Vertikal Press, 2013. First Genie S-3800 in Europe. [www.vertikal.net](http://www.vertikal.net). Available at:  
<http://www.vertikal.net/en/news/story/16605/> [Accessed February 25, 2016].
- Vorpahl, F. et al., 2007. A Flexible Aeroelastic Simulation Approach for Offshore Wind Turbines. *European Offshore Wind, Berlin*.
- Vorpahl, F., Popko, W. & Kaufer, D., 2011. Description of a basic model of the “UpWind reference jacket” for code comparison in the OC4 project under IEA Wind Annex XXX. *Fraunhofer Institute for Wind ...*, 1, pp.1–14. Available at:  
[http://www.iwes.fraunhofer.de/en/publications/list\\_of\\_publication/publikationen\\_veroeffentlichungengesamt/2011/description\\_of\\_a\\_basic\\_model\\_of\\_the\\_upwind\\_reference\\_jacket\\_for\\_code\\_comparison/jcr:content/pressrelease/linklistPar/download/file.res/UpWindReferenceJacket](http://www.iwes.fraunhofer.de/en/publications/list_of_publication/publikationen_veroeffentlichungengesamt/2011/description_of_a_basic_model_of_the_upwind_reference_jacket_for_code_comparison/jcr:content/pressrelease/linklistPar/download/file.res/UpWindReferenceJacket).
- White, F.M., 2003. *Fluid Mechanics* 4th Editio. P. Holman, Jack & J. Lloyd, eds., Rhode Island: WCB & McGraw-Hill.
- Zaaijer, M.B., 2006. Foundation modelling to assess dynamic behaviour of offshore wind turbines. *Applied Ocean Research*, 28(1), pp.45–57.
- Zarafshan, A. & Hall, R., 2015. Design Considerations for Iffshore Wind Energy Support Structures. In pp. 1741–1747.

# 11 Appendices

## 11.1 Appendix 1 – Matlab code for gravity base model

```
%-----%
% MASTERS THESIS: ASSESSMENT OF SIMULATION CODES FOR OWT FOUNDATIONS
% DYNAMIC ANALYSIS OF AN OWT STRUCTURE WITH A CONCRETE GRAVITY BASE
% ÖMER FARUK HALICI & HILLARY MUTUNGI
% MSc STRUCTURAL ENGINEERING - CHALMERS UNIVERSITY OF TECHNOLOGY
% MAY 2016
%-----%
clc
clear
close all
%-----%
%INPUT
%-----%
t_c1=3.5;
t_c2=0.75;
t_s1=0.030;
t_s2=0.016;

eq_t=[393e3 -3.44e6]; %Force vector at tower top,i.e [Fx, Fz] in
Newtons
eq=[0 0];

rho_c=2500; %Density of concrete
rho_s=7850; %Density of steel
E_c=36e9; %E modulus of concrete
E_s=210e9; %E modulus of steel

H_t=77.6; % Tower height in meters
Htap_f=23; % Height of tapered foundation in meters
Hpad_f=1; % Height of foundation pad in meters
H_f=21; % Height of uniform part of foundation in meters
H_s=H_f+Hpad_f+Htap_f;

nel_t=16; % Number of Tower elements
neltap_f=23; % Number of elements in tapered part of foundation
nelu_f=21; % Number of elements in uniform part of foundation
nel_pad=1; % Number of elements in foundation pad
nel_f=nelu_f+nel_pad+neltap_f; %Total number of elements in
foundation

el_t= H_t/nel_t; % Element length in tower
eltap_f= Htap_f/neltap_f; % Element length in tapered foundation
el_f= H_f/nelu_f; % Element length in foundation
elpad_f= Hpad_f/nel_pad; % Element length in tapered foundation

nnodes_pad=nel_pad+1; % Number of nodes in pads
nnodes_t=nel_t+1; % Number of nodes in tower
nnodes_f=nel_f+1; % Number of nodes in foundation
nnodes=nnodes_f+nnodes_t-1; % Number of nodes in OWT structure

%-----%
%-----%
% FOUNDATION MODEL
%-----%
%-----%
Dout_f=zeros(nel_f,1);
```

```

Din_f=zeros(nel_f,1);
A_f=zeros(nel_f,1);
I_f=zeros(nel_f,1);

Dout_b1=25;
Dout_b2=18-0.13;
Dout_t1=6;

Dout_f(1)=Dout_b1;
Din_f(1)=Dout_b1-2*t_c1;
A_f(1)=pi/4*Dout_f(1)^2-pi/4*Din_f(1)^2;
I_f(1)=pi/4*((Dout_f(1)/2)^4-(Din_f(1)/2)^4);

for i=neltap_f-nelu_f:neltap_f+nel_pad;
    Dout_f(i)=Dout_b2-2*((i-2)*eltap_f*Dout_t1/Htap_f);
    Din_f(i)=Dout_f(i)-2*t_c2;
    A_f(i)=pi/4*Dout_f(i)^2-pi/4*Din_f(i)^2;
    I_f(i)=pi/4*((Dout_f(i)/2)^4-(Din_f(i)/2)^4);
end

for k=neltap_f+nel_pad+1:nel_f;
    Dout_f(k)=Dout_t1;
    Din_f(k)=Dout_f(k)-2*t_c2;
    A_f(k)=(pi/4)*Dout_f(k)^2-pi/4*Din_f(k)^2;
    I_f(k)=(pi/4)*((Dout_f(k)/2)^4-(Din_f(k)/2)^4);
end

end

%-----%
%-----%
% TOWER MODEL
%-----%
%-----%

Dout_t=zeros(nel_t,1);
Din_t=zeros(nel_t,1);
A_t=zeros(nel_t,1);
I_t=zeros(nel_t,1);

Dout_t1=6; Dout_t2=3.87;
Din_t1=Dout_t1-2*t_s1; Din_t2=Dout_t2-2*t_s2;
Dout_t(1)=Dout_t1;Din_t(1)=Din_t1;
A_t(1)=pi/4*Dout_t1^2-pi/4*Din_t1^2;
I_t(1)=pi/4*((Dout_t1/2)^4-(Din_t1/2)^4);

for i=2:nel_t;
    Dout_t(i)=Dout_t1-(i*el_t*(Dout_t1-Dout_t2)/H_t);
    Din_t(i)=Din_t1-(i*el_t*(Din_t1-Din_t2)/H_t);
    A_t(i)=pi/4*Dout_t(i)^2-pi/4*Din_t(i)^2;
    I_t(i)=pi/4*((Dout_t(i)/2)^4-(Din_t(i)/2)^4);
end

end

i=[];
k=[];

%-----%
%-----%
% COORDINATES AND TOPOLOGY
%-----%
%-----%

Coord=zeros(nnodes,2);
Dof=zeros(nnodes,3);

```

```

Edof=zeros (nnodes-1,7);

% Node coordinates-----
y1=0;
for i=1:nnodes_pad;
Coord(i,2)=y1;
y1=y1+elpad_f;
end

y2=elpad_f+eltap_f;
for i=nnodes_pad+1:nnodes_f;
Coord(i,2)=y2;
y2=y2+elpad_f;
end

y3=H_s+el_t;
for k=nnodes_f+1:nnodes;
Coord(k,2)=y3;
y3=y3+el_t;
end

% Node degrees of freedom-----
for i=1:nnodes;
Dof(i,1)=3*i-2;
Dof(i,2)=3*i-1;
Dof(i,3)=3*i;
end

% Element degrees of freedom-----
for i=1:nnodes-1;
Edof(i,1)=i;
Edof(i,2)=Dof(i,1);
Edof(i,3)=Dof(i,2);
Edof(i,4)=Dof(i,3);
Edof(i,5)=Dof(i+1,1);
Edof(i,6)=Dof(i+1,2);
Edof(i,7)=Dof(i+1,3);
end

[Ex,Ey]=coordxtr (Edof,Coord,Dof,2);
figure
eldraw2 (Ex,Ey,[1 2 0])
hold

% Stiffness /Mass Matrix-----
K=zeros (max (max (Dof) ));
M=zeros (max (max (Dof) ));

for i=1:nel_pad;
A=A_f(i); E=E_c;I=I_f(i);m=rho_c*A;ep=[E A I m];
[Ke,Me]=beam2dedit (Ex(i,:),Ey(i,:),ep);
K=assem (Edof(i,:),K,Ke);
M=assem (Edof(i,:),M,Me);
end

for i=nel_pad+1:nel_f-nelu_f;
A=A_f(i); E=E_c;I=I_f(i);m=rho_c*A;ep=[E A I m];
[Ke,Me]=beam2dedit (Ex(i,:),Ey(i,:),ep);
K=assem (Edof(i,:),K,Ke);
M=assem (Edof(i,:),M,Me);
end

```

```

for i=nel_f-nel_u_f+1:nel_f;
    A=A_f(i); E=E_c;I=I_f(i);m=rho_c*A;ep=[E A I m];
    [Ke,Me]=beam2dedit (Ex(i,:),Ey(i,:),ep);
    K=assem(Edof(i,:),K,Ke);
    M=assem(Edof(i,:),M,Me);
end

for i=nel_f+1:nel_f+nel_t
    A=A_t(i-nel_f); E=E_s;I=I_t(i-nel_f);m=rho_s*A;ep=[E A I m];
    [Ke,Me]=beam2dedit (Ex(i,:),Ey(i,:),ep);
    K=assem(Edof(i,:),K,Ke);
    M=assem(Edof(i,:),M,Me);
end

%-----%
% STATIC ANALYSIS
%-----%
% Force matrix-----%
f=zeros(max(max(Dof)),1);
f(184)=eq_t(1);f(185)=eq_t(2);

% Boundary conditions-----
bc=[1 0;2 0;3 0];

[a,Q]=solveq(K,f,bc);
[Lamda,Eigenvec]=eigen(K,M,bc(:,1));
Freq=sqrt(Lamda);

Edb=extract(Edof,Eigenvec(:,1));
eldisp2(Ex,Ey,Edb,[2 3 0],2000);

Edb2=extract(Edof,Eigenvec(:,2));
eldisp2(Ex,Ey,Edb2,[2 3 0],2000);

Edb3=extract(Edof,Eigenvec(:,3));
eldisp2(Ex,Ey,Edb3,[2 3 0],2000);
%-----%
% TIME SERIES (DYNAMIC ANALYSIS) USING Newmark's method
%-----%

% Damping Matrix (Rayleigh Dampin)-----
% First eigenmode/freq
% Mr_1=Eigenvec(fdof,1)'*M(fdof,fdof)*Eigenvec(fdof,1);
a0=2*Freq(1)*Freq(2)/(Freq(1)+Freq(2));
a1=2/(Freq(1)+Freq(2));
% a0=0;
% a1=0.0023;
C=a0*M+a1*K;

% Wind load -----
BEM_Loads=importdata('BEM_Loads.txt')*1000;
Time=importdata('Time.txt');

% Controls for Newmark's method -----
gama=1/2;
beta=1/4;
h_new=0.0006;
niter=max(Time)/h_new;

fdof(:,1)=Dof(2,1):max(max(Dof));

```

```

P_t=zeros(length(fdof),1);

u=zeros(length(fdof),1,niter);
ud=zeros(length(fdof),1,niter);
udd=zeros(length(fdof),1,niter);
t=zeros(niter,1);

for i=1:niter
    P_t(max(max(Dof))-3-2)=BEM_Loads(i)*cosd(5);           % Horizontal
force component at the tower top
    P_t(max(max(Dof))-3-1)=eq_t(2)-BEM_Loads(i)*sind(5); % Vertical
force component at the tower top

    udd(:,1,i+1)=(M(fdof,fdof)+gama*C(fdof,fdof)+beta*(h_new^2)*K(fdof,fd
of))\ (P_t-K(fdof,fdof)*...
        u(:,1,i)-(C(fdof,fdof)+K(fdof,fdof)*h_new)*ud(:,1,i)-...
        (h_new*(1-gama)*C(fdof,fdof)+(h_new^2)*(1-
2*beta)*K(fdof,fdof))*udd(:,1,i)/2);

    u(:,1,i+1)=u(:,1,i)+ud(:,1,i)*h_new+((1-2*beta)*udd(:,1,i)+2*...
        beta*udd(:,1,i+1))*(h_new^2)/2;

    ud(:,1,i+1)=ud(:,1,i)+((1-gama)*udd(:,1,i)+gama*udd(:,1,i+1))*h_new;
    Time(i)
end

disp=zeros(length(BEM_Loads),1);
for i=1:length(BEM_Loads)
disp(i)=u(181,1,i);
end

% Plot deflection-time series -----
figure
plot(Time,disp*1000,'LineWidth',2)
xlabel('Time [s]')
title('Tower deflection')
ylabel('Deflection [mm]')

```



## 11.2 Appendix 2 – Fast input data for tripod structure model for DNV load case 6.1c

```

----- FAST v8.12.* INPUT FILE -----
Master's Thesis: Assessment of Simulation Codes for Offshore Wind Turbine Foundations - DNV load case 6.1c
----- SIMULATION CONTROL -----
False          Echo          - Echo input data to <RootName>.ech (flag)
"FATAL"        AbortLevel  - Error level when simulation should abort (string) {"WARNING", "SEVERE", "FATAL"}
              60      TMax      - Total run time (s)
              0.001  DT        - Recommended module time step (s)
              2      InterpOrder - Interpolation order for input/output time history (-) {1=linear, 2=quadratic}
              1      NumCrctn   - Number of correction iterations (-) {0=explicit calculation, i.e., no corrections}
              99999.9 DT_UJac   - Time between calls to get Jacobians (s)
              1E+06  UJacSclFact - Scaling factor used in Jacobians (-)
----- FEATURE SWITCHES AND FLAGS -----
              1      CompElast   - Compute structural dynamics (switch) {1=ElastoDyn; 2=ElastoDyn + BeamDyn for blades}
              1      CompInflow  - Compute inflow wind velocities (switch) {0=still air; 1=InflowWind; 2=external from
OpenFOAM}
              1      CompAero    - Compute aerodynamic loads (switch) {0=None; 1=AeroDyn v14; 2=AeroDyn v15}
              1      CompServo   - Compute control and electrical-drive dynamics (switch) {0=None; 1=ServoDyn}
              1      CompHydro   - Compute hydrodynamic loads (switch) {0=None; 1=HydroDyn}
              1      CompSub     - Compute sub-structural dynamics (switch) {0=None; 1=SubDyn}
              0      CompMooring  - Compute mooring system (switch) {0=None; 1=MAP++; 2=FEAMooring; 3=MoorDyn;
4=OrcaFlex}
              0      CompIce     - Compute ice loads (switch) {0=None; 1=IceFloe; 2=IceDyn}
----- INPUT FILES -----
"NRELOffshrBslne5MW_Tripod_ElastoDyn.dat"  EDFFile      - Name of file containing ElastoDyn input parameters
(quoted string)
"NRELOffshrBslne5MW_BeamDyn.dat"          BDBldFile(1) - Name of file containing BeamDyn input parameters for blade 1
(quoted string)
"NRELOffshrBslne5MW_BeamDyn.dat"          BDBldFile(2) - Name of file containing BeamDyn input parameters for blade 2
(quoted string)
"NRELOffshrBslne5MW_BeamDyn.dat"          BDBldFile(3) - Name of file containing BeamDyn input parameters for blade 3
(quoted string)

```

```

"NRELOffshrBslime5MW_InflowWind_Steady57.09mps.dat"    InflowFile      - Name of file containing inflow wind input
parameters (quoted string)
"NRELOffshrBslime5MW_Tripod_AeroDyn.dat"              AeroFile        - Name of file containing aerodynamic input parameters
(quoted string)
"NRELOffshrBslime5MW_Tripod_ServoDyn.dat"            ServoFile       - Name of file containing control and electrical-drive
input parameters (quoted string)
"NRELOffshrBslime5MW_Tripod_HydroDyn.dat"            HydroFile       - Name of file containing hydrodynamic input parameters
(quoted string)
"NRELOffshrBslime5MW_Tripod_SubDyn.dat"              SubFile         - Name of file containing sub-structural input parameters
(quoted string)
"unused"      MooringFile    - Name of file containing mooring system input parameters (quoted string)
"unused"      IceFile        - Name of file containing ice input parameters (quoted string)
----- OUTPUT -----
True          SumPrint      - Print summary data to "<RootName>.sum" (flag)
              1      SttsTime    - Amount of time between screen status messages (s)
              1000   ChkptTime  - Amount of time between creating checkpoint files for potential restart (s)
              0.04   DT_Out     - Time step for tabular output (s) (or "default")
              0      TStart     - Time to begin tabular output (s)
              1      OutFileFmt  - Format for tabular (time-marching) output file (switch) {1: text file
[<RootName>.out], 2: binary file [<RootName>.outb], 3: both}
True          TabDelim    - Use tab delimiters in text tabular output file? (flag) {uses spaces if false}
"ES10.3E2"    OutFmt        - Format used for text tabular output, excluding the time channel. Resulting field
should be 10 characters. (quoted string)

```

```

----- ELASTODYN v1.03.* INPUT FILE -----
Master's Thesis: Assessment of Simulation Codes for Offshore Wind Turbine Foundations - DNV load case 6.1c
----- SIMULATION CONTROL -----
False      Echo      - Echo input data to "<RootName>.ech" (flag)
           3  Method    - Integration method: {1: RK4, 2: AB4, or 3: ABM4} (-)
"DEFAULT"  DT      - Integration time step (s)
----- ENVIRONMENTAL CONDITION -----
           9.80665 Gravity - Gravitational acceleration (m/s^2)
----- DEGREES OF FREEDOM -----
True       FlapDOF1  - First flapwise blade mode DOF (flag)
True       FlapDOF2  - Second flapwise blade mode DOF (flag)
True       EdgeDOF   - First edgewise blade mode DOF (flag)
False      TeetDOF   - Rotor-teeter DOF (flag) [unused for 3 blades]
True       DrTrDOF   - Drivetrain rotational-flexibility DOF (flag)
True       GenDOF    - Generator DOF (flag)
True       YawDOF    - Yaw DOF (flag)
True       TwFADOF1  - First fore-aft tower bending-mode DOF (flag)
True       TwFADOF2  - Second fore-aft tower bending-mode DOF (flag)
True       TwSSDOF1  - First side-to-side tower bending-mode DOF (flag)
True       TwSSDOF2  - Second side-to-side tower bending-mode DOF (flag)
True       PtfmSgDOF - Platform horizontal surge translation DOF (flag)
True       PtfmSwDOF - Platform horizontal sway translation DOF (flag)
True       PtfmHvDOF - Platform vertical heave translation DOF (flag)
True       PtfmRDOF  - Platform roll tilt rotation DOF (flag)
True       PtfmPDOF  - Platform pitch tilt rotation DOF (flag)
True       PtfmYDOF  - Platform yaw rotation DOF (flag)
----- INITIAL CONDITIONS -----
           0  OopDefl  - Initial out-of-plane blade-tip displacement (meters)
           0  IPDefl  - Initial in-plane blade-tip deflection (meters)
           90 BlPitch(1) - Blade 1 initial pitch (degrees)
           90 BlPitch(2) - Blade 2 initial pitch (degrees)
           90 BlPitch(3) - Blade 3 initial pitch (degrees) [unused for 2 blades]
           0  TeetDefl - Initial or fixed teeter angle (degrees) [unused for 3 blades]

```

0	Azimuth	- Initial azimuth angle for blade 1 (degrees)
0	RotSpeed	- Initial or fixed rotor speed (rpm)
0	NacYaw	- Initial or fixed nacelle-yaw angle (degrees)
0	TTDspFA	- Initial fore-aft tower-top displacement (meters)
0	TTDspSS	- Initial side-to-side tower-top displacement (meters)
0	PtfmSurge	- Initial or fixed horizontal surge translational displacement of platform (meters)
0	PtfmSway	- Initial or fixed horizontal sway translational displacement of platform (meters)
0	PtfmHeave	- Initial or fixed vertical heave translational displacement of platform (meters)
0	PtfmRoll	- Initial or fixed roll tilt rotational displacement of platform (degrees)
0	PtfmPitch	- Initial or fixed pitch tilt rotational displacement of platform (degrees)
0	PtfmYaw	- Initial or fixed yaw rotational displacement of platform (degrees)
----- TURBINE CONFIGURATION -----		
3	NumBl	- Number of blades (-)
63	TipRad	- The distance from the rotor apex to the blade tip (meters)
1.5	HubRad	- The distance from the rotor apex to the blade root (meters)
-2.5	PreCone(1)	- Blade 1 cone angle (degrees)
-2.5	PreCone(2)	- Blade 2 cone angle (degrees)
-2.5	PreCone(3)	- Blade 3 cone angle (degrees) [unused for 2 blades]
0	HubCM	- Distance from rotor apex to hub mass [positive downwind] (meters)
0	UndSling	- Undersling length [distance from teeter pin to the rotor apex] (meters) [unused for 3 blades]
0	Delta3	- Delta-3 angle for teetering rotors (degrees) [unused for 3 blades]
0	AzimBlUp	- Azimuth value to use for I/O when blade 1 points up (degrees)
-5.0191	OverHang	- Distance from yaw axis to rotor apex [3 blades] or teeter pin [2 blades] (meters)
1.912	ShftGagL	- Distance from rotor apex [3 blades] or teeter pin [2 blades] to shaft strain gages [positive for upwind rotors] (meters)
-5	ShftTilt	- Rotor shaft tilt angle (degrees)
1.9	NacCMxn	- Downwind distance from the tower-top to the nacelle CM (meters)
0	NacCMyn	- Lateral distance from the tower-top to the nacelle CM (meters)
1.75	NacCMzn	- Vertical distance from the tower-top to the nacelle CM (meters)
-3.09528	NcIMUxn	- Downwind distance from the tower-top to the nacelle IMU (meters)
0	NcIMUyn	- Lateral distance from the tower-top to the nacelle IMU (meters)
2.23336	NcIMUzn	- Vertical distance from the tower-top to the nacelle IMU (meters)

```

1.96256  Twr2Shft  - Vertical distance from the tower-top to the rotor shaft (meters)
  87.6   TowerHt   - Height of tower above ground level [onshore] or MSL [offshore] (meters)
   10    TowerBsHt - Height of tower base above ground level [onshore] or MSL [offshore] (meters)
   0     PtfmCMxt  - Downwind distance from the ground level [onshore] or MSL [offshore] to the platform CM
(meters)
   0     PtfmCMyt  - Lateral distance from the ground level [onshore] or MSL [offshore] to the platform CM
(meters)
   10    PtfmCMzt  - Vertical distance from the ground level [onshore] or MSL [offshore] to the platform CM
(meters)
   10    PtfmRefzt - Vertical distance from the ground level [onshore] or MSL [offshore] to the platform
reference point (meters)
----- MASS AND INERTIA -----
   0     TipMass(1) - Tip-brake mass, blade 1 (kg)
   0     TipMass(2) - Tip-brake mass, blade 2 (kg)
   0     TipMass(3) - Tip-brake mass, blade 3 (kg) [unused for 2 blades]
  56780  HubMass   - Hub mass (kg)
 115926  HubIner   - Hub inertia about rotor axis [3 blades] or teeter axis [2 blades] (kg m^2)
 534.116 GenIner   - Generator inertia about HSS (kg m^2)
240000   NacMass   - Nacelle mass (kg)
2.60789E+06 NacYIner - Nacelle inertia about yaw axis (kg m^2)
   0     YawBrMass - Yaw bearing mass (kg)
   0     PtfmMass  - Platform mass (kg)
   0     PtfmRIner - Platform inertia for roll tilt rotation about the platform CM (kg m^2)
   0     PtfmPIner - Platform inertia for pitch tilt rotation about the platform CM (kg m^2)
2.48448E+06 PtfmYIner - Platform inertia for yaw rotation about the platform CM (kg m^2)
----- BLADE -----
   17    BldNodes  - Number of blade nodes (per blade) used for analysis (-)
"NRELOffshrBsline5MW_Blade.dat"  BldFile(1) - Name of file containing properties for blade 1 (quoted string)
"NRELOffshrBsline5MW_Blade.dat"  BldFile(2) - Name of file containing properties for blade 2 (quoted string)
"NRELOffshrBsline5MW_Blade.dat"  BldFile(3) - Name of file containing properties for blade 3 (quoted string)
[unused for 2 blades]
----- ROTOR-TEETER -----
   0     TeetMod   - Rotor-teeter spring/damper model {0: none, 1: standard, 2: user-defined from routine
UserTeet} (switch) [unused for 3 blades]

```

```

0 TeetDmpP - Rotor-teeter damper position (degrees) [used only for 2 blades and when TeetMod=1]
0 TeetDmp - Rotor-teeter damping constant (N-m/(rad/s)) [used only for 2 blades and when TeetMod=1]
0 TeetCDmp - Rotor-teeter rate-independent Coulomb-damping moment (N-m) [used only for 2 blades and
when TeetMod=1]
0 TeetSSStP - Rotor-teeter soft-stop position (degrees) [used only for 2 blades and when TeetMod=1]
0 TeetHStP - Rotor-teeter hard-stop position (degrees) [used only for 2 blades and when TeetMod=1]
0 TeetSSSp - Rotor-teeter soft-stop linear-spring constant (N-m/rad) [used only for 2 blades and when
TeetMod=1]
0 TeetHSSp - Rotor-teeter hard-stop linear-spring constant (N-m/rad) [used only for 2 blades and when
TeetMod=1]
----- DRIVETRAIN -----
100 GBoxEff - Gearbox efficiency (%)
97 GBRatio - Gearbox ratio (-)
8.67637E+08 DTTorSpr - Drivetrain torsional spring (N-m/rad)
6.215E+06 DTTorDmp - Drivetrain torsional damper (N-m/(rad/s))
----- FURLING -----
False Furling - Read in additional model properties for furling turbine (flag) [must currently be FALSE]
"unused" FurlFile - Name of file containing furling properties (quoted string) [unused when Furling=False]
----- TOWER -----
20 TwrNodes - Number of tower nodes used for analysis (-)
"NRELOffshrbSline5MW_Tripod_ElastoDyn_Tower.dat" TwrFile - Name of file containing tower properties (quoted
string)
----- OUTPUT -----
True SumPrint - Print summary data to "<RootName>.sum" (flag)
2 OutFile - Switch to determine where output will be placed: {1: in module output file only; 2: in
glue code output file only; 3: both} (currently unused)
True TabDelim - Use tab delimiters in text tabular output file? (flag) (currently unused)
"ES10.3E2" OutFmt - Format used for text tabular output (except time). Resulting field should be 10
characters. (quoted string) (currently unused)
0 TStart - Time to begin tabular output (s) (currently unused)
1 DecFact - Decimation factor for tabular output {1: output every time step} (-) (currently unused)
1 NTwGages - Number of tower nodes that have strain gages for output [0 to 9] (-)
20 TwrGagNd - List of tower nodes that have strain gages [1 to TwrNodes] (-) [unused if NTwGages=0]
3 NB1Gages - Number of blade nodes that have strain gages for output [0 to 9] (-)

```

```

5,          9,          13   BldGagNd   - List of blade nodes that have strain gages [1 to BldNodes] (-)
[unused if NBlGages=0]
      OutList   - The next line(s) contains a list of output parameters. See OutListParameters.xlsx for a
listing of available output channels, (-)
"OoPDefl1, IPDefl1, TwstDefl1" - Blade 1 out-of-plane and in-plane deflections and tip twist
"BldPitch1"                    - Blade 1 pitch angle
"Azimuth"                      - Blade 1 azimuth angle
"RotSpeed, GenSpeed"           - Low-speed shaft and high-speed shaft speeds
"TwHt1TPxi, TwHt1TPyi, TTDspTwst" - Tower-top fore-aft and side-to-side displacements and top twist
"Spn2MLxb1, Spn2MLyb1"         - Blade 1 local edgewise and flapwise bending moments at span station 2 (approx.
50% span)
"RootFxcl, RootFycl, RootFzcl" - Out-of-plane shear, in-plane shear, and axial forces at the root of blade 1
"RootMxcl, RootMycl, RootMzcl" - In-plane bending, out-of-plane bending, and pitching moments at the root of
blade 1
"RotTorq, LSSGagMya, LSSGagMza" - Rotor torque and low-speed shaft 0- and 90-bending moments at the main bearing
"YawBrFxp, YawBrFyp, YawBrFzp" - Fore-aft shear, side-to-side shear, and vertical forces at the top of the tower
(not rotating with nacelle yaw)
"YawBrMxp, YawBrMyp, YawBrMzp" - Side-to-side bending, fore-aft bending, and yaw moments at the top of the tower
(not rotating with nacelle yaw)
END of input file (the word "END" must appear in the first 3 columns of this last OutList line)
-----

```

```

----- ELASTODYN V1.00.* TOWER INPUT FILE -----
Master's Thesis: Assessment of Simulation Codes for Offshore Wind Turbine Foundations - DNV load case 6.1c
----- TOWER PARAMETERS -----
17  NTwInpSt   - Number of input stations to specify tower geometry
1   TwrFADmp(1) - Tower 1st fore-aft mode structural damping ratio (%)
1   TwrFADmp(2) - Tower 2nd fore-aft mode structural damping ratio (%)
1   TwrSSDmp(1) - Tower 1st side-to-side mode structural damping ratio (%)
1   TwrSSDmp(2) - Tower 2nd side-to-side mode structural damping ratio (%)
----- TOWER ADJUSTMUNT FACTORS -----
1   FASStunr(1) - Tower fore-aft modal stiffness tuner. 1st mode (-)
1   FASStunr(2) - Tower fore-aft modal stiffness tuner. 2nd mode (-)
1   SSStTunr(1) - Tower side-to-side stiffness tuner. 1st mode (-)
1   SSStTunr(2) - Tower side-to-side stiffness tuner. 2nd mode (-)
1   AdjTwMa    - Factor to adjust tower mass density (-)
1   AdjFAST    - Factor to adjust tower fore-aft stiffness (-)
1   AdjSSSt    - Factor to adjust tower side-to-side stiffness (-)
----- DISTRIBUTED TOWER PROPERTIES -----
HtFract      TMassDen      TwFASTif      TwSSStif
(-)          (kg/m)          (Nm^2)        (Nm^2)
0           4416.875067  5.26409E+11  5.26409E+11
0.0625      4193.058832  4.77839E+11  4.77839E+11
0.125      3974.950194  4.32692E+11  4.32692E+11
0.1875      3762.549152  3.90804E+11  3.90804E+11
0.25       3555.855706  3.52015E+11  3.52015E+11
0.3125      3354.869857  3.16169E+11  3.16169E+11
0.375      3159.591604  2.83115E+11  2.83115E+11
0.4375      2970.020947  2.52704E+11  2.52704E+11
0.5         2786.157887  2.24793E+11  2.24793E+11
0.5625      2608.002424  1.99241E+11  1.99241E+11
0.625      2435.554557  1.75912E+11  1.75912E+11
0.6875      2268.814286  1.54676E+11  1.54676E+11
0.75       2107.781612  1.35403E+11  1.35403E+11
0.8125      1952.456534  1.1797E+11   1.1797E+11

```



```

0.875 1802.839053 1.02257E+11 1.02257E+11
0.9375      1658.929168 88148831301 88148831301
1      1520.72688      75532575601 75532575601
----- TOWER FORE-AFT MODE SHAPES -----
0.9329      TwFAM1Sh(2) - Mode 1. coefficient of x^2 term
0.1613      TwFAM1Sh(3) -      . coefficient of x^3 term
-0.1103     TwFAM1Sh(4) -      . coefficient of x^4 term
0.1472      TwFAM1Sh(5) -      . coefficient of x^5 term
-0.1311     TwFAM1Sh(6) -      . coefficient of x^6 term
-0.8758     TwFAM2Sh(2) - Mode 2. coefficient of x^2 term
1.2147     TwFAM2Sh(3) -      . coefficient of x^3 term
0.7442     TwFAM2Sh(4) -      . coefficient of x^4 term
0.0588     TwFAM2Sh(5) -      . coefficient of x^5 term
-0.1419     TwFAM2Sh(6) -      . coefficient of x^6 term
----- TOWER SIDE-TO-SIDE MODE SHAPES -----
0.9181     TwSSM1Sh(2) - Mode 1. coefficient of x^2 term
0.1896     TwSSM1Sh(3) -      . coefficient of x^3 term
-0.1532     TwSSM1Sh(4) -      . coefficient of x^4 term
0.1853     TwSSM1Sh(5) -      . coefficient of x^5 term
-0.1398     TwSSM1Sh(6) -      . coefficient of x^6 term
-1.0120     TwSSM2Sh(2) - Mode 2. coefficient of x^2 term
0.9950     TwSSM2Sh(3) -      . coefficient of x^3 term
1.0828     TwSSM2Sh(4) -      . coefficient of x^4 term
-0.2720     TwSSM2Sh(5) -      . coefficient of x^5 term
0.2062     TwSSM2Sh(6) -      . coefficient of x^6 term

```

```

----- BEAMDYN V1.01.* INPUT FILE -----
NREL 5MW blade
----- SIMULATION CONTROL -----
False          Echo          - Echo input data to "<RootName>.ech" (flag)
2              analysis_type - 1: Static analysis; 2: Dynamic analysis
0.0           rhoinf         - Numerical Damping Parameter for Generalized-alpha integrator
2             quadrature    - 1: Gauss; 2: Trapezoidal
DEFAULT       refine        - Refinement factor for quadrature 2. DEFAULT = 1
DEFAULT       n_fact         - Factorization frequency: The Jacobian is computed every n_fact steps in N-R
iteration. DEFAULT = 5
DEFAULT       DTBeam        - Time step size
DEFAULT       NRMax         - Max number of iterations in Newton-Ralphson algorithm
DEFAULT       stop_tol      - Tolerance for stopping criterion
----- GEOMETRY PARAMETER -----
1              member_total  - Total number of member (-)
49             kp_total      - Total number of key point (-)
1      49          - Member number; Number of key points in this member
      kp_xb      kp_yb      kp_zb      initial_twist
      (m)        (m)        (m)        (deg)
0.000000  0.000000  0.000000  13.308000
0.000000  0.000000  0.199875  13.308000
0.000000  0.000000  1.199865  13.308000
0.000000  0.000000  2.199855  13.308000
0.000000  0.000000  3.199845  13.308000
0.000000  0.000000  4.199835  13.308000
0.000000  0.000000  5.199825  13.308000
0.000000  0.000000  6.199815  13.308000
0.000000  0.000000  7.199805  13.308000
0.000000  0.000000  8.201025  13.308000
0.000000  0.000000  9.199785  13.308000
0.000000  0.000000  10.199775  13.308000
0.000000  0.000000  11.199765  13.181000
0.000000  0.000000  12.199755  12.848000

```

0.000000	0.000000	13.200975	12.192000
0.000000	0.000000	14.199735	11.561000
0.000000	0.000000	15.199725	11.072000
0.000000	0.000000	16.199715	10.792000
0.000000	0.000000	18.200925	10.232000
0.000000	0.000000	20.200290	9.672000
0.000000	0.000000	22.200270	9.110000
0.000000	0.000000	24.200250	8.534000
0.000000	0.000000	26.200230	7.932000
0.000000	0.000000	28.200825	7.321000
0.000000	0.000000	30.200190	6.711000
0.000000	0.000000	32.200170	6.122000
0.000000	0.000000	34.200150	5.546000
0.000000	0.000000	36.200130	4.971000
0.000000	0.000000	38.200725	4.401000
0.000000	0.000000	40.200090	3.834000
0.000000	0.000000	42.200070	3.332000
0.000000	0.000000	44.200050	2.890000
0.000000	0.000000	46.200030	2.503000
0.000000	0.000000	48.201240	2.116000
0.000000	0.000000	50.199990	1.730000
0.000000	0.000000	52.199970	1.342000
0.000000	0.000000	54.199950	0.954000
0.000000	0.000000	55.199940	0.760000
0.000000	0.000000	56.199930	0.574000
0.000000	0.000000	57.199920	0.404000
0.000000	0.000000	57.699915	0.319000
0.000000	0.000000	58.201140	0.253000
0.000000	0.000000	58.699905	0.216000
0.000000	0.000000	59.199900	0.178000
0.000000	0.000000	59.699895	0.140000
0.000000	0.000000	60.199890	0.101000
0.000000	0.000000	60.699885	0.062000

```

0.000000  0.000000  61.199880  0.023000
0.000000  0.000000  61.500000  0.000000
----- MESH PARAMETER -----
5          order_elem    - Order of interpolation (basis) function (-)
----- MATERIAL PARAMETER -----
"NRELOffshrBsline5MW_BeamDyn_Blade.dat" BldFile - Name of file containing properties for blade
----- PITCH ACTUATOR PARAMETERS -----
False      UsePitchAct   - Whether a pitch actuator should be used (flag)
200        PitchJ        - Pitch actuator inertia (kg-m^2) [used only when UsePitchAct is true]
2.0E+7     PitchK        - Pitch actuator stiffness (kg-m^2/s^2) [used only when UsePitchAct is true]
5.0E+5     PitchC        - Pitch actuator damping (kg-m^2/s) [used only when UsePitchAct is true]
----- OUTPUTS -----
True       SumPrint     - Print summary data to "<RootName>.sum" (flag)
"ES10.3E2" OutFmt       - Format used for text tabular output, excluding the time channel. Resulting field
should be 10 characters. (quoted string)
0         NNodeOuts     - Number of nodes to output to file [0 - 9] (-)
1,2,3,4,5,6 OutNd      - Nodes whose values will be output (-)
          OutList      - The next line(s) contains a list of output parameters. See OutListParameters.xlsx
for a listing of available output channels, (-)
"RootFxr, RootFyr, RootFzr"
"RootMxr, RootMyr, RootMzr"
"TipTDxr, TipTDyr, TipTDzr"
"TipRDxr, TipRDyr, TipRDzr"
END of input file (the word "END" must appear in the first 3 columns of this last OutList line)
-----

```

```

----- InflowWind v3.01.* INPUT FILE -----
Steady 57.09 m/s wind
-----
False      Echo      - Echo input data to <RootName>.ech (flag)
          1  WindType  - switch for wind file type (1=steady; 2=uniform; 3=binary TurbSim FF; 4=binary Bladed-
style FF; 5=HAWC format; 6=User defined)
          0  PropogationDir - Direction of wind propogation (meteoroligical rotation from aligned with X (positive
rotates towards -Y) -- degrees)
          1  NWindVel   - Number of points to output the wind velocity (0 to 9)
          0  WindVxiList - List of coordinates in the inertial X direction (m)
          0  WindVyiList - List of coordinates in the inertial Y direction (m)
          90 WindVzList - List of coordinates in the inertial Z direction (m)
===== Parameters for Steady Wind Conditions [used only for WindType = 1] =====
          57.09 HWindSpeed - Horizontal windspeed
          90  RefHt      - Reference height for horizontal wind speed
          0  PLeXP      - Power law exponent
===== Parameters for Uniform wind file [used only for WindType = 2] =====
"Wind/08ms.wnd"  Filename      - Filename of time series data for uniform wind field.
          90  RefHt      - Reference height for horizontal wind speed
          125.88 RefLength - Reference length for linear horizontal and vertical sheer
===== Parameters for Binary TurbSim Full-Field files [used only for WindType = 3] =====
"Wind/08ms.wnd"  Filename      - Name of the Full field wind file to use (.bts)
===== Parameters for Binary Bladed-style Full-Field files [used only for WindType = 4] =====
"unused"        FilenameRoot - Rootname of the full-field wind file to use (.wnd, .sum)
False          TowerFile  - Have tower file (.twr) [flag]
===== Parameters for HAWC-format binary files [Only used with WindType = 5] =====
"wasp\Output\basic_5u.bin"  FileName_u  - name of the file containing the u-component fluctuating wind
"wasp\Output\basic_5v.bin"  FileName_v  - name of the file containing the v-component fluctuating wind
"wasp\Output\basic_5w.bin"  FileName_w  - name of the file containing the w-component fluctuating wind
          64  nx        - number of grids in the x direction (in the 3 files above)
          32  ny        - number of grids in the y direction (in the 3 files above)
          32  nz        - number of grids in the z direction (in the 3 files above)
          16  dx        - distance (in meters) between points in the x direction

```

```

3   dy           - distance (in meters) between points in the y direction
3   dz           - distance (in meters) between points in the z direction
90  RefHt        - reference height; the height (in meters) of the vertical center of the grid
-----
Scaling parameters for turbulence
-----
1   ScaleMethod  - Turbulence scaling method [0 = none, 1 = direct scaling, 2 = calculate scaling
factor based on a desired standard deviation]
1   SFx          - Turbulence scaling factor for the x direction (-) [ScaleMethod=1]
1   SFy          - Turbulence scaling factor for the y direction (-) [ScaleMethod=1]
1   SFz          - Turbulence scaling factor for the z direction (-) [ScaleMethod=1]
12  SigmaFx      - Turbulence standard deviation to calculate scaling from in x direction (m/s)
[ScaleMethod=2]
8   SigmaFy      - Turbulence standard deviation to calculate scaling from in y direction (m/s)
[ScaleMethod=2]
2   SigmaFz      - Turbulence standard deviation to calculate scaling from in z direction (m/s)
[ScaleMethod=2]
-----
Mean wind profile parameters (added to HAWC-format files)
-----
5   URef         - Mean u-component wind speed at the reference height [m/s]
2   WindProfile  - Wind profile type (0=constant;1=logarithmic,2=power law)
0   PLExp        - Power law exponent [-] (used only when WindProfile=2)
0.03 Z0          - Surface roughness length [m] (used only when WindProfile=1)
===== OUTPUT =====
False      SumPrint  - Print summary data to <RootName>.IfW.sum (flag)
           OutList   - The next line(s) contains a list of output parameters. See OutListParameters.xlsx for
a listing of available output channels, (-)
"Wind1VelX"      X-direction wind velocity at point WindList(1)
"Wind1VelY"      Y-direction wind velocity at point WindList(1)
"Wind1VelZ"      Z-direction wind velocity at point WindList(1)
END of input file (the word "END" must appear in the first 3 columns of this last OutList line)
-----

```

```

----- AeroDyn v14.04.* INPUT FILE -----
NREL 5.0 MW offshore baseline aerodynamic input properties.
"BEDDOES"      StallMod      - Dynamic stall included [BEDDOES or STEADY] (unquoted string)
"USE_CM"       UseCm          - Use aerodynamic pitching moment model? [USE_CM or NO_CM] (unquoted string)
"DYNIN"        InfModel       - Inflow model [DYNIN or EQUIL] (unquoted string)
"SWIRL"        IndModel       - Induction-factor model [NONE or WAKE or SWIRL] (unquoted string)
      0.005     AToler        - Induction-factor tolerance (convergence criteria) (-)
"PRANDtl"     TLModel        - Tip-loss model (EQUIL only) [PRANDtl, GTECH, or NONE] (unquoted string)
"PRANDtl"     HLModel        - Hub-loss model (EQUIL only) [PRANDtl or NONE] (unquoted string)
"NEWTOWER"    TwrShad        - INSTEAD OF:  0.0      TwrShad      - Tower-shadow velocity deficit (-)
True          TwrPotent      - Calculate tower potential flow (flag)  INSTEAD OF  9999.9      ShadHWid      - Tower-
shadow half width (m)
False         TwrShadow      - Calculate tower shadow (flag)          INSTEAD OF  9999.9      T_Shad_Refpt- Tower-
shadow reference point (m)
"NRELOffshrBslne5MW_Tripod_AeroDyn_Tower.dat"  TwrFile          - Tower drag file name (quoted string)
True          CalcTwrAero      - Calculate aerodynamic drag of the tower at the ElastoDyn nodes.  TwrPotent must be
true.
      1.225     AirDens        - Air density (kg/m^3)
      1.464E-05 KinVisc        - Kinematic air viscosity [CURRENTLY IGNORED] (m^2/sec)
"Default"     DTAero          - Time interval for aerodynamic calculations (sec)
      8        NumFoil        - Number of airfoil files (-)
"AeroData/Cylinder1.dat"  FoilNm          - Names of the airfoil files [NumFoil lines] (quoted strings)
"AeroData/Cylinder2.dat"
"AeroData/DU40_A17.dat"
"AeroData/DU35_A17.dat"
"AeroData/DU30_A17.dat"
"AeroData/DU25_A17.dat"
"AeroData/DU21_A17.dat"
"AeroData/NACA64_A17.dat"
      17       BldNodes      - Number of blade nodes used for analysis (-)
RNodes      AeroTwst      DRNodes      Chord      Nfoil      PrnElm
2.8667000E+00  1.3308000E+01  2.7333000E+00  3.5420000E+00  1      NOPRINT
5.6000000E+00  1.3308000E+01  2.7333000E+00  3.8540000E+00  1      NOPRINT
8.3333000E+00  1.3308000E+01  2.7333000E+00  4.1670000E+00  2      NOPRINT

```

1.1750000E+01	1.3308000E+01	4.1000000E+00	4.5570000E+00	3	NOPRINT
1.5850000E+01	1.1480000E+01	4.1000000E+00	4.6520000E+00	4	NOPRINT
1.9950000E+01	1.0162000E+01	4.1000000E+00	4.4580000E+00	4	NOPRINT
2.4050000E+01	9.0110000E+00	4.1000000E+00	4.2490000E+00	5	NOPRINT
2.8150000E+01	7.7950000E+00	4.1000000E+00	4.0070000E+00	6	NOPRINT
3.2250000E+01	6.5440000E+00	4.1000000E+00	3.7480000E+00	6	NOPRINT
3.6350000E+01	5.3610000E+00	4.1000000E+00	3.5020000E+00	7	NOPRINT
4.0450000E+01	4.1880000E+00	4.1000000E+00	3.2560000E+00	7	NOPRINT
4.4550000E+01	3.1250000E+00	4.1000000E+00	3.0100000E+00	8	NOPRINT
4.8650000E+01	2.3190000E+00	4.1000000E+00	2.7640000E+00	8	NOPRINT
5.2750000E+01	1.5260000E+00	4.1000000E+00	2.5180000E+00	8	NOPRINT
5.6166700E+01	8.6300000E-01	2.7333000E+00	2.3130000E+00	8	NOPRINT
5.8900000E+01	3.7000000E-01	2.7333000E+00	2.0860000E+00	8	NOPRINT
6.1633300E+01	1.0600000E-01	2.7333000E+00	1.4190000E+00	8	NOPRINT



```

----- SERVODYN v1.03.* INPUT FILE -----
Master's Thesis: Assessment of Simulation Codes for Offshore Wind Turbine Foundations - DNV load case 6.1c
----- SIMULATION CONTROL -----
False      Echo      - Echo input data to <RootName>.ech (flag)
"DEFAULT"  DT      - Communication interval for controllers (s) (or "default")
----- PITCH CONTROL -----
      5   PCMode      - Pitch control mode {0: none, 3: user-defined from routine PitchCntrl, 4: user-defined
from Simulink/Labview, 5: user-defined from Bladed-style DLL} (switch)
      0   TPCOn      - Time to enable active pitch control (s) [unused when PCMode=0]
      0   TPitManS(1) - Time to start override pitch maneuver for blade 1 and end standard pitch control (s)
      0   TPitManS(2) - Time to start override pitch maneuver for blade 2 and end standard pitch control (s)
      0   TPitManS(3) - Time to start override pitch maneuver for blade 3 and end standard pitch control (s)
[unused for 2 blades]
      8   PitManRat(1) - Pitch rate at which override pitch maneuver heads toward final pitch angle for blade 1
(deg/s)
      8   PitManRat(2) - Pitch rate at which override pitch maneuver heads toward final pitch angle for blade 2
(deg/s)
      8   PitManRat(3) - Pitch rate at which override pitch maneuver heads toward final pitch angle for blade 3
(deg/s) [unused for 2 blades]
      90  BlPitchF(1) - Blade 1 final pitch for pitch maneuvers (degrees)
      90  BlPitchF(2) - Blade 2 final pitch for pitch maneuvers (degrees)
      90  BlPitchF(3) - Blade 3 final pitch for pitch maneuvers (degrees) [unused for 2 blades]
----- GENERATOR AND TORQUE CONTROL -----
      5   VSContrl   - Variable-speed control mode {0: none, 1: simple VS, 3: user-defined from routine
UserVSCont, 4: user-defined from Simulink/Labview, 5: user-defined from Bladed-style DLL} (switch)
      2   GenModel   - Generator model {1: simple, 2: Thevenin, 3: user-defined from routine UserGen} (switch)
[used only when VSContrl=0]
      94.4  GenEff    - Generator efficiency [ignored by the Thevenin and user-defined generator models] (%)
True      GenTiStr   - Method to start the generator {T: timed using TimGenOn, F: generator speed using
SpdGenOn} (flag)
True      GenTiStp   - Method to stop the generator {T: timed using TimGenOf, F: when generator power = 0}
(flag)
      9999.9  SpdGenOn - Generator speed to turn on the generator for a startup (HSS speed) (rpm) [used only
when GenTiStr=False]

```

```

0 TimGenOn - Time to turn on the generator for a startup (s) [used only when GenTiStr=True]
9999.9 TimGenOf - Time to turn off the generator (s) [used only when GenTiStp=True]
----- SIMPLE VARIABLE-SPEED TORQUE CONTROL -----
9999.9 VS_RtGnSp - Rated generator speed for simple variable-speed generator control (HSS side) (rpm)
[used only when VSContrl=1]
9999.9 VS_RtTq - Rated generator torque/constant generator torque in Region 3 for simple variable-speed
generator control (HSS side) (N-m) [used only when VSContrl=1]
9999.9 VS_Rgn2K - Generator torque constant in Region 2 for simple variable-speed generator control (HSS
side) (N-m/rpm^2) [used only when VSContrl=1]
9999.9 VS_SlPc - Rated generator slip percentage in Region 2 1/2 for simple variable-speed generator
control (%) [used only when VSContrl=1]
----- SIMPLE INDUCTION GENERATOR -----
9999.9 SIG_SlPc - Rated generator slip percentage (%) [used only when VSContrl=0 and GenModel=1]
9999.9 SIG_SySp - Synchronous (zero-torque) generator speed (rpm) [used only when VSContrl=0 and
GenModel=1]
9999.9 SIG_RtTq - Rated torque (N-m) [used only when VSContrl=0 and GenModel=1]
9999.9 SIG_PORT - Pull-out ratio (Tpullout/Trated) (-) [used only when VSContrl=0 and GenModel=1]
----- THEVENIN-EQUIVALENT INDUCTION GENERATOR -----
9999.9 TEC_Freq - Line frequency [50 or 60] (Hz) [used only when VSContrl=0 and GenModel=2]
9998 TEC_NPol - Number of poles [even integer > 0] (-) [used only when VSContrl=0 and GenModel=2]
9999.9 TEC_SRes - Stator resistance (ohms) [used only when VSContrl=0 and GenModel=2]
9999.9 TEC_RRes - Rotor resistance (ohms) [used only when VSContrl=0 and GenModel=2]
9999.9 TEC_VLL - Line-to-line RMS voltage (volts) [used only when VSContrl=0 and GenModel=2]
9999.9 TEC_SLR - Stator leakage reactance (ohms) [used only when VSContrl=0 and GenModel=2]
9999.9 TEC_RLR - Rotor leakage reactance (ohms) [used only when VSContrl=0 and GenModel=2]
9999.9 TEC_MR - Magnetizing reactance (ohms) [used only when VSContrl=0 and GenModel=2]
----- HIGH-SPEED SHAFT BRAKE -----
1 HSSBrMode - HSS brake model {0: none, 1: simple, 3: user-defined from routine UserHSSBr, 4: user-
defined from Simulink/Labview, 5: user-defined from Bladed-style DLL} (switch)
0 THSSBrDp - Time to initiate deployment of the HSS brake (s)
0.2 HSSBrDT - Time for HSS-brake to reach full deployment once initiated (sec) [used only when
HSSBrMode=1]
281160.2 HSSBrTqF - Fully deployed HSS-brake torque (N-m)
----- NACELLE-YAW CONTROL -----

```

```

0 YCMode - Yaw control mode {0: none, 3: user-defined from routine UserYawCont, 4: user-defined
from Simulink/Labview, 5: user-defined from Bladed-style DLL} (switch)
9999.9 TYCON - Time to enable active yaw control (s) [unused when YCMode=0]
0 YawNeut - Neutral yaw position--yaw spring force is zero at this yaw (degrees)
9.02832E+09 YawSpr - Nacelle-yaw spring constant (N-m/rad)
1.916E+07 YawDamp - Nacelle-yaw damping constant (N-m/(rad/s))
9999.9 TYawManS - Time to start override yaw maneuver and end standard yaw control (s)
0.3 YawManRat - Yaw maneuver rate (in absolute value) (deg/s)
0 NacYawF - Final yaw angle for override yaw maneuvers (degrees)
----- TUNED MASS DAMPER -----
False CompNTMD - Compute nacelle tuned mass damper {true/false} (flag)
"unused" NTMDfile - Name of the file for nacelle tuned mass damper (quoted string) [unused when CompNTMD is
false]
----- BLADED INTERFACE -----
"ServoData\DISCON_win32.dll" DLL_FileName - Name/location of the dynamic library {.dll [Windows] or .so [Linux]}
in the Bladed-DLL format (-) [used only with Bladed Interface]
"DISCON.IN" DLL_InFile - Name of input file sent to the DLL [used only with Bladed Interface] (-)
"default" DLL_DT - Communication interval for dynamic library [used only with Bladed Interface] (s) (or
"default")
false DLL_Ramp - Whether a linear ramp should be used between DLL_DT time steps [introduces time shift
when true] (flag)
9999.9 BPCutoff - Cutoff frequency for low-pass filter on blade pitch from DLL (Hz)
0 NacYaw_North - Reference yaw angle of the nacelle when the upwind end points due North (deg) [used
only with Bladed Interface]
0 Ptch_Cntrl - Record 28: Use individual pitch control {0: collective pitch; 1: individual pitch
control} (switch) [used only with Bladed Interface]
0 Ptch_SetPnt - Record 5: Below-rated pitch angle set-point (deg) [used only with Bladed Interface]
0 Ptch_Min - Record 6: Minimum pitch angle (deg) [used only with Bladed Interface]
0 Ptch_Max - Record 7: Maximum pitch angle (deg) [used only with Bladed Interface]
0 PtchRate_Min - Record 8: Minimum pitch rate (most negative value allowed) (deg/s) [used only with
Bladed Interface]
0 PtchRate_Max - Record 9: Maximum pitch rate (deg/s) [used only with Bladed Interface]
0 Gain_OM - Record 16: Optimal mode gain (Nm/(rad/s)^2) [used only with Bladed Interface]
0 GenSpd_MinOM - Record 17: Minimum generator speed (rpm) [used only with Bladed Interface]

```

```

0   GenSpd_MaxOM - Record 18: Optimal mode maximum speed (rpm) [used only with Bladed Interface]
0   GenSpd_Dem   - Record 19: Demanded generator speed above rated (rpm) [used only with Bladed Interface]
0   GenTrq_Dem   - Record 22: Demanded generator torque above rated (Nm) [used only with Bladed Interface]
0   GenPwr_Dem   - Record 13: Demanded power (W) [used only with Bladed Interface]
----- BLADED INTERFACE TORQUE-SPEED LOOK-UP TABLE -----
0   DLL_NumTrq   - Record 26: No. of points in torque-speed look-up table {0 = none and use the optimal
mode parameters; nonzero = ignore the optimal mode PARAMETERS by setting Record 16 to 0.0} (-) [used only with
Bladed Interface]
  GenSpd_TLU     GenTrq_TLU
  (rpm)          (Nm)
----- OUTPUT -----
True           SumPrint      - Print summary data to <RootName>.sum (flag) (currently unused)
                2   OutFile      - Switch to determine where output will be placed: {1: in module output file only; 2: in
glue code output file only; 3: both} (currently unused)
True           TabDelim      - Use tab delimiters in text tabular output file? (flag) (currently unused)
"ES10.3E2"     OutFmt          - Format used for text tabular output (except time). Resulting field should be 10
characters. (quoted string) (currently unused)
30            TStart        - Time to begin tabular output (s) (currently unused)
                OutList      - The next line(s) contains a list of output parameters. See OutListParameters.xlsx for
a listing of available output channels, (-)
"GenPwr"      - Electrical generator power and torque
"GenTq"       - Electrical generator power and torque
END of input file (the word "END" must appear in the first 3 columns of this last OutList line)
-----

```

```

----- HydroDyn v2.03.* Input File -----
Master's Thesis: Assessment of Simulation Codes for Offshore Wind Turbine Foundations - DNV load case 6.1c
FALSE          Echo          - Echo the input file data (flag)
----- ENVIRONMENTAL CONDITIONS -----
      1025    WtrDens          - Water density (kg/m^3)
      45     WtrDpth          - Water depth (meters)
      0      MSL2SWL          - Offset between still-water level and mean sea level (meters) [positive upward;
unused when WaveMod = 6; must be zero if PotMod=1 or 2]
----- WAVES -----
      1      WaveMod          - Incident wave kinematics model {0: none=still water, 1: regular (periodic), 1P#:
regular with user-specified phase, 2: JONSWAP/Pierson-Moskowitz spectrum (irregular), 3: White noise spectrum
(irregular), 4: user-defined spectrum from routine UserWaveSpctrm (irregular), 5: Externally generated wave-
elevation time series, 6: Externally generated full wave-kinematics time series [option 6 is invalid for PotMod/=0]}
(switch)
      0      WaveStMod        - Model for stretching incident wave kinematics to instantaneous free surface {0:
none=no stretching, 1: vertical stretching, 2: extrapolation stretching, 3: Wheeler stretching} (switch) [unused
when WaveMod=0 or when PotMod/=0]
      3630    WaveTMax         - Analysis time for incident wave calculations (sec) [unused when WaveMod=0;
determines WaveDOmega=2Pi/WaveTMax in the IFFT]
      0.25    WaveDT           - Time step for incident wave calculations (sec) [unused when WaveMod=0;
0.1<=WaveDT<=1.0 recommended; determines WaveOmegaMax=Pi/WaveDT in the IFFT]
      6.50    WaveHs           - Significant wave height of incident waves (meters) [used only when WaveMod=1, 2,
or 3]
      7.80    WaveTp           - Peak-spectral period of incident waves (sec) [used only when WaveMod=1 or 2]
"DEFAULT"    WavePkShp        - Peak-shape parameter of incident wave spectrum (-) or DEFAULT (string) [used only
when WaveMod=2; use 1.0 for Pierson-Moskowitz]
      0      WvLowCOff        - Low cut-off frequency or lower frequency limit of the wave spectrum beyond which
the wave spectrum is zeroed (rad/s) [unused when WaveMod=0, 1, or 6]
      500    WvHiCOff         - High cut-off frequency or upper frequency limit of the wave spectrum beyond which
the wave spectrum is zeroed (rad/s) [unused when WaveMod=0, 1, or 6]
      0      WaveDir          - Incident wave propagation heading direction (degrees)
[unused when WaveMod=0 or 6]
      0      WaveDirMod        - Directional spreading function {0: none, 1: COS2S} (-)
[only used when WaveMod=2,3, or 4]

```

```

1 WaveDirSpread - Wave direction spreading coefficient ( > 0 ) (-)
[only used when WaveMod=2,3, or 4 and WaveDirMod=1]
1 WaveNDir - Number of wave directions (-)
[only used when WaveMod=2,3, or 4 and WaveDirMod=1; odd number only]
0 WaveDirRange - Range of wave directions (full range: WaveDir +/- 1/2*WaveDirRange) (degrees)
[only used when WaveMod=2,3,or 4 and WaveDirMod=1]
123456789 WaveSeed(1) - First random seed of incident waves [-2147483648 to 2147483647] (-)
[unused when WaveMod=0, 5, or 6]
1011121314 WaveSeed(2) - Second random seed of incident waves [-2147483648 to 2147483647] (-)
[unused when WaveMod=0, 5, or 6]
False WaveNDamp - Flag for normally distributed amplitudes (flag)
[only used when WaveMod=2, 3, or 4]
"" WvKinFile - Root name of externally generated wave data file(s) (quoted string)
[used only when WaveMod=5 or 6]
1 NWaveElev - Number of points where the incident wave elevations can be computed (-)
[maximum of 9 output locations]
0 WaveElevxi - List of xi-coordinates for points where the incident wave elevations can be output
(meters) [NWaveElev points, separated by commas or white space; unused if NWaveElev = 0]
0 WaveElevyi - List of yi-coordinates for points where the incident wave elevations can be output
(meters) [NWaveElev points, separated by commas or white space; unused if NWaveElev = 0]
----- 2ND-ORDER WAVES ----- [unused with WaveMod=0 or 6]
False WvDiffQTF - Full difference-frequency 2nd-order wave kinematics (flag)
False WvSumQTF - Full summation-frequency 2nd-order wave kinematics (flag)
0 WvLowCOFFD - Low frequency cutoff used in the difference-frequencies (rad/s) [Only used with a
difference-frequency method]
3.5 WvHiCOFFD - High frequency cutoff used in the difference-frequencies (rad/s) [Only used with a
difference-frequency method]
0.1 WvLowCOFFS - Low frequency cutoff used in the summation-frequencies (rad/s) [Only used with a
summation-frequency method]
3.5 WvHiCOFFS - High frequency cutoff used in the summation-frequencies (rad/s) [Only used with a
summation-frequency method]
----- CURRENT ----- [unused with WaveMod=6]
1 CurrMod - Current profile model {0: none=no current, 1: standard, 2: user-defined from
routine UserCurrent} (switch)

```

```

0      CurrSSV0      - Sub-surface current velocity at still water level (m/s) [used only when
CurrMod=1]
0      CurrSSDir     - Sub-surface current heading direction (degrees) or DEFAULT (string) [used only
when CurrMod=1]
20     CurrNSRef     - Near-surface current reference depth (meters) [used only when
CurrMod=1]
0      CurrNSV0     - Near-surface current velocity at still water level (m/s) [used only when
CurrMod=1]
0      CurrNSDir     - Near-surface current heading direction (degrees) [used only when
CurrMod=1]
0.89   CurrDIV      - Depth-independent current velocity (m/s) [used only when
CurrMod=1]
0      CurrDIDir    - Depth-independent current heading direction (degrees) [used only when
CurrMod=1]
----- FLOATING PLATFORM ----- [unused with WaveMod=6]
0      PotMod        - Potential-flow model {0: none=no potential flow, 1: frequency-to-time-domain
transforms based on WAMIT output, 2: fluid-impulse theory (FIT)} (switch)
"unused" PotFile     - Root name of potential-flow model data; WAMIT output files containing the linear,
nondimensionalized, hydrostatic restoring matrix (.hst), frequency-dependent hydrodynamic added mass matrix and
damping matrix (.1), and frequency- and direction-dependent wave excitation force vector per unit wave amplitude
(.3) (quoted string) [MAKE SURE THE FREQUENCIES INHERENT IN THESE WAMIT FILES SPAN THE PHYSICALLY-SIGNIFICANT RANGE
OF FREQUENCIES FOR THE GIVEN PLATFORM; THEY MUST CONTAIN THE ZERO- AND INFINITE-FREQUENCY LIMITS!]
1      WAMITULEN     - Characteristic body length scale used to redimensionalize WAMIT output (meters)
[only used when PotMod=1]
0      PtfmVol0      - Displaced volume of water when the platform is in its undisplaced position (m^3)
[only used when PotMod=1; USE THE SAME VALUE COMPUTED BY WAMIT AS OUTPUT IN THE .OUT FILE!]
0      PtfmCOBxt     - The xt offset of the center of buoyancy (COB) from the platform reference point
(meters) [only used when PotMod=1]
0      PtfmCOByt     - The yt offset of the center of buoyancy (COB) from the platform reference point
(meters) [only used when PotMod=1]
1      RdtnMod       - Radiation memory-effect model {0: no memory-effect calculation, 1: convolution, 2:
state-space} (switch) [only used when PotMod=1; STATE-SPACE REQUIRES *.ss INPUT FILE]
60     RdtnTMax      - Analysis time for wave radiation kernel calculations (sec) [only used when
PotMod=1; determines RdtnDOmega=Pi/RdtnTMax in the cosine transform; MAKE SURE THIS IS LONG ENOUGH FOR THE RADIATION
IMPULSE RESPONSE FUNCTIONS TO DECAY TO NEAR-ZERO FOR THE GIVEN PLATFORM!]

```

```

0.025  RdtnDT          - Time step for wave radiation kernel calculations (sec) [only used when PotMod=1;
DT<=RdtnDT<=0.1 recommended; determines RdtnOmegaMax=Pi/RdtnDT in the cosine transform]
----- 2ND-ORDER FLOATING PLATFORM FORCES ----- [unused with WaveMod=0 or 6, or
PotMod=0 or 2]
0      MnDrift        - Mean-drift 2nd-order forces computed {0:
None; [7, 8, 9, 10, 11, or 12]: WAMIT file to use} [Only one of MnDrift, NewmanApp, or DiffQTF can be non-zero]
0      NewmanApp      - Mean- and slow-drift 2nd-order forces computed with Newman's approximation {0:
None; [7, 8, 9, 10, 11, or 12]: WAMIT file to use} [Only one of MnDrift, NewmanApp, or DiffQTF can be non-zero. Used
only when WaveDirMod=0]
0      DiffQTF        - Full difference-frequency 2nd-order forces computed with full QTF {0:
None; [10, 11, or 12]: WAMIT file to use} [Only one of MnDrift, NewmanApp, or DiffQTF can be non-zero]
0      SumQTF         - Full summation -frequency 2nd-order forces computed with full QTF {0:
None; [10, 11, or 12]: WAMIT file to use}
----- FLOATING PLATFORM FORCE FLAGS ----- [unused with WaveMod=6]
True   PtfmSgF        - Platform horizontal surge translation force (flag) or DEFAULT
True   PtfmSwF        - Platform horizontal sway translation force (flag) or DEFAULT
True   PtfmHvF        - Platform vertical heave translation force (flag) or DEFAULT
True   PtfmRF         - Platform roll tilt rotation force (flag) or DEFAULT
True   PtfmPF         - Platform pitch tilt rotation force (flag) or DEFAULT
True   PtfmYF         - Platform yaw rotation force (flag) or DEFAULT
----- PLATFORM ADDITIONAL STIFFNESS AND DAMPING -----
0      0      0      0      0      0      0      AddF0      - Additional preload
(N, N-m)
0      0      0      0      0      0      0      AddCLin      - Additional linear
stiffness (N/m, N/rad, N-m/m, N-m/rad)
0      0      0      0      0      0      0
0      0      0      0      0      0      0
0      0      0      0      0      0      0
0      0      0      0      0      0      0
0      0      0      0      0      0      0
0      0      0      0      0      0      0      AddBLin      - Additional linear
damping (N/(m/s), N/(rad/s), N-m/(m/s), N-m/(rad/s))
0      0      0      0      0      0      0
0      0      882607      0      0      0      0

```



```

0 0 0 0 0 0
0 0 0 0 0 0
0 0 0 0 0 0
0 0 0 0 0 0
0 0 0 0 0 0
quadratic drag (N/ (m/s)^2, N/ (rad/s)^2, N-m(m/s)^2, N-m/ (rad/s)^2)
0 0 0 0 0 0
0 0 0 0 0 0
0 0 0 0 0 0
0 0 0 0 0 0
0 0 0 0 0 0

```

----- AXIAL COEFFICIENTS -----

```

1 NAXCoef - Number of axial coefficients (-)
AxCoefID AxCd AxCa AxCp
(-) (-) (-) (-)
1 1.00 1.00 1.00

```

----- MEMBER JOINTS -----

```

67 NJoints - Number of joints (-) [must be exactly 0 or at least 2]
JointID Jointxi Jointyi Jointzi JointAxID JointOvrlp [JointOvrlp= 0: do nothing at joint. 1:
eliminate overlaps by calculating super member]
(-) (m) (m) (m) (-) (switch)
1 0 25.763700000000000 -35 1 0
2 22.312000000000000 -12.881800000000000 -35 1 0
3 -22.312000000000000 -12.881800000000000 -35 1 0
4 0 0 -35 1 0
5 0 25.763700000000000 -25 1 0
6 22.312000000000000 -12.881800000000000 -25 1 0
7 -22.312000000000000 -12.881800000000000 -25 1 0
8 0 25.763700000000000 -45.01 1 0
9 22.312000000000000 -12.881800000000000 -45.01 1 0
10 -22.312000000000000 -12.881800000000000 -45.01 1 0
11 0 0 0 1 0
12 0 0 10 1 0
13 0 0 -37 1 0

```

14	0	19.32277500000000	-35	1	0		
15	0	12.88185000000000	-35	1	0		
16	0	6.44092500000000	-35	1	0		
17	16.73400000000000	-9.66135000000000	-35	1	0		
18	11.15600000000000	-6.44090000000000	-35	1	0		
19	5.57800000000000	-3.22045000000000	-35	1	0		
20	-16.73400000000000	-9.66135000000000	-35	1	0		
21	-11.15600000000000	-6.44090000000000	-35	1	0		
22	-5.57800000000000	-3.22045000000000	-35	1	0		
23	0	25.76370000000000	-32.50000000000000	1	0		
24	0	25.76370000000000	-30	1	0		
25	0	25.76370000000000	-27.50000000000000	1	0		
26	22.31200000000000	-12.88180000000000	-32.50000000000000	1	0		
27	22.31200000000000	-12.88180000000000	-30	1	0		
28	22.31200000000000	-12.88180000000000	-27.50000000000000	1	0		
29	-22.31200000000000	-12.88180000000000	-32.50000000000000	1	0		
30	-22.31200000000000	-12.88180000000000	-30	1	0		
31	-22.31200000000000	-12.88180000000000	-27.50000000000000	1	0		
32	0	25.76370000000000	-42.50000000000000	1	0		
33	0	25.76370000000000	-40	1	0		
34	0	25.76370000000000	-37.50000000000000	1	0		
35	22.31200000000000	-12.88180000000000	-42.50000000000000	1	0		
36	22.31200000000000	-12.88180000000000	-40	1	0		
37	22.31200000000000	-12.88180000000000	-37.50000000000000	1	0		
38	-22.31200000000000	-12.88180000000000	-42.50000000000000	1	0		
39	-22.31200000000000	-12.88180000000000	-40	1	0		
40	-22.31200000000000	-12.88180000000000	-37.50000000000000	1	0		
41	5.57800000000000	16.10232500000000	-35	1	0		
42	11.15600000000000	6.44095000000000	-35	1	0		
43	16.73400000000000	-3.22042500000000	-35	1	0		
44	11.15600000000000	-12.88180000000000	-35	1	0		
45	0	-12.88180000000000	-35	1	0		
46	-11.15600000000000	-12.88180000000000	-35	1	0		

```

47  -16.734000000000000 -3.220425000000000 -35  1  0
48  -11.156000000000000 6.440950000000000 -35  1  0
49  -5.578000000000000 16.102325000000000 -35  1  0
50  0  0 -36.500000000000000 1  0
51  0  0 -36  1  0
52  0  0 -35.500000000000000 1  0
53  0  0 -26.250000000000000 1  0
54  0  0 -17.500000000000000 1  0
55  0  0 -8.750000000000000 1  0
56  0  19.322775000000000 -26.250000000000000 1  0
57  0  12.881850000000000 -17.500000000000000 1  0
58  0  6.440925000000000 -8.750000000000000 1  0
59  16.734000000000000 -9.661350000000000 -26.250000000000000 1  0
60  11.156000000000000 -6.440900000000000 -17.500000000000000 1  0
61  5.578000000000000 -3.220450000000000 -8.750000000000000 1  0
62  -16.734000000000000 -9.661350000000000 -26.250000000000000 1  0
63  -11.156000000000000 -6.440900000000000 -17.500000000000000 1  0
64  -5.578000000000000 -3.220450000000000 -8.750000000000000 1  0
65  0  0  2.500000000000000 1  0
66  0  0  5  1  0
67  0  0  7.500000000000000 1  0

```

----- MEMBER CROSS-SECTION PROPERTIES -----

72 NPropSets - Number of member property sets (-)

PropSetID	PropD	PropThck
(-)	(m)	(m)
1	0.800000000000000	0.028000000000000
2	0.800000000000000	0.028000000000000
3	0.800000000000000	0.028000000000000
4	0.800000000000000	0.028000000000000
5	0.800000000000000	0.028000000000000
6	0.800000000000000	0.028000000000000
7	0.800000000000000	0.028000000000000
8	0.800000000000000	0.028000000000000

9 0.8000000000000000 0.0280000000000000  
10 0.8000000000000000 0.0280000000000000  
11 0.8000000000000000 0.0280000000000000  
12 0.8000000000000000 0.0280000000000000  
13 4 0.0400000000000000  
14 4 0.0400000000000000  
15 4 0.0400000000000000  
16 4 0.0400000000000000  
17 4 0.0400000000000000  
18 4 0.0400000000000000  
19 4 0.0400000000000000  
20 4 0.0400000000000000  
21 4 0.0400000000000000  
22 4 0.0400000000000000  
23 4 0.0400000000000000  
24 4 0.0400000000000000  
25 4 0.0400000000000000  
26 4 0.0400000000000000  
27 4 0.0400000000000000  
28 4 0.0400000000000000  
29 4 0.0400000000000000  
30 4 0.0400000000000000  
31 4 0.0400000000000000  
32 4 0.0400000000000000  
33 4 0.0400000000000000  
34 4 0.0400000000000000  
35 4 0.0400000000000000  
36 4 0.0400000000000000  
37 0.8000000000000000 0.0160000000000000  
38 0.8000000000000000 0.0160000000000000  
39 0.8000000000000000 0.0160000000000000  
40 0.8000000000000000 0.0160000000000000  
41 0.8000000000000000 0.0160000000000000

```

42  0.8000000000000000 0.0160000000000000
43  0.8000000000000000 0.0160000000000000
44  0.8000000000000000 0.0160000000000000
45  0.8000000000000000 0.0160000000000000
46  0.8000000000000000 0.0160000000000000
47  0.8000000000000000 0.0160000000000000
48  0.8000000000000000 0.0160000000000000
49  4      0.0280000000000000
50  4.027025000000000 0.0285500000000000
51  4.054050000000000 0.0291000000000000
52  4.081075000000000 0.0296500000000000
53  4.108100000000000 0.0302000000000000
54  4.581075000000000 0.0396500000000000
55  5.054050000000000 0.0491000000000000
56  5.527025000000000 0.0585500000000000
57  1.200000000000000 0.0320000000000000
58  1.200000000000000 0.0320000000000000
59  1.200000000000000 0.0320000000000000
60  1.200000000000000 0.0320000000000000
61  1.200000000000000 0.0320000000000000
62  1.200000000000000 0.0320000000000000
63  1.200000000000000 0.0320000000000000
64  1.200000000000000 0.0320000000000000
65  1.200000000000000 0.0320000000000000
66  1.200000000000000 0.0320000000000000
67  1.200000000000000 0.0320000000000000
68  1.200000000000000 0.0320000000000000
69  6      0.0400000000000000
70  6      0.0400000000000000
71  6      0.0400000000000000
72  6      0.0400000000000000
----- SIMPLE HYDRODYNAMIC COEFFICIENTS (model 1) -----

```

SimplCd	SimplCdMG	SimplCa	SimplCaMG	SimplCp	SimplCpMG	SimplAxCa	SimplAxCaMG	SimplAxCp
(-)	(-)	(-)	(-)	(-)	(-)	(-)	(-)	(-)
1.00	0.00	1.00	0.00	1.00	0.00	1.00	0.00	1.00

----- DEPTH-BASED HYDRODYNAMIC COEFFICIENTS (model 2) -----

0 NCoefDpth		- Number of depth-dependent coefficients (-)							
Dpth	DpthCd	DpthCdMG	DpthCa	DpthCaMG	DpthCp	DpthCpMG	DpthAxCa	DpthAxCaMG	DpthAxCp
(m)	(-)	(-)	(-)	(-)	(-)	(-)	(-)	(-)	(-)

----- MEMBER-BASED HYDRODYNAMIC COEFFICIENTS (model 3) -----

0 NCoefMembers		- Number of member-based coefficients (-)																		
MemberID	MemberCd1	MemberCd2	MemberCdMG1	MemberCdMG2	MemberCa1	MemberCa2	MemberCaMG1	MemberCaMG2	MemberCp1	MemberCp2	MemberCpMG1	MemberCpMG2	MemberAxCa1	MemberAxCa2	MemberAxCaMG1	MemberAxCaMG2	MemberAxCp1	MemberAxCp2	MemberAxCpMG1	MemberAxCpMG2
(-)	(-)	(-)	(-)	(-)	(-)	(-)	(-)	(-)	(-)	(-)	(-)	(-)	(-)	(-)	(-)	(-)	(-)	(-)	(-)	(-)

----- MEMBERS -----

72 NMembers		- Number of members (-)								
MemberID	MJointID1	MJointID2	MPropSetID1	MPropSetID2	MDivSize	MCoefMod	PropPot	[MCoefMod=1: use simple coeff table. 2: use depth-based coeff table. 3: use member-based coeff table] [ PropPot/=0 if member is modeled with potential-flow theory]		
(-)	(-)	(-)	(-)	(-)	(m)	(switch)	(flag)			
1	1	14	1	1	1	1	FALSE			
2	14	15	2	2	1	1	FALSE			
3	15	16	3	3	1	1	FALSE			
4	16	4	4	4	1	1	FALSE			
5	2	17	5	5	1	1	FALSE			
6	17	18	6	6	1	1	FALSE			
7	18	19	7	7	1	1	FALSE			
8	19	4	8	8	1	1	FALSE			

9	3	20	9	9	1	1	FALSE
10	20	21	10	10	1	1	FALSE
11	21	22	11	11	1	1	FALSE
12	22	4	12	12	1	1	FALSE
13	1	23	13	13	1	1	FALSE
14	23	24	14	14	1	1	FALSE
15	24	25	15	15	1	1	FALSE
16	25	5	16	16	1	1	FALSE
17	2	26	17	17	1	1	FALSE
18	26	27	18	18	1	1	FALSE
19	27	28	19	19	1	1	FALSE
20	28	6	20	20	1	1	FALSE
21	3	29	21	21	1	1	FALSE
22	29	30	22	22	1	1	FALSE
23	30	31	23	23	1	1	FALSE
24	31	7	24	24	1	1	FALSE
25	8	32	25	25	1	1	FALSE
26	32	33	26	26	1	1	FALSE
27	33	34	27	27	1	1	FALSE
28	34	1	28	28	1	1	FALSE
29	9	35	29	29	1	1	FALSE
30	35	36	30	30	1	1	FALSE
31	36	37	31	31	1	1	FALSE
32	37	2	32	32	1	1	FALSE
33	10	38	33	33	1	1	FALSE
34	38	39	34	34	1	1	FALSE
35	39	40	35	35	1	1	FALSE
36	40	3	36	36	1	1	FALSE
37	1	41	37	37	1	1	FALSE
38	41	42	38	38	1	1	FALSE
39	42	43	39	39	1	1	FALSE
40	43	2	40	40	1	1	FALSE
41	2	44	41	41	1	1	FALSE

42	44	45	42	42	1	1	FALSE
43	45	46	43	43	1	1	FALSE
44	46	3	44	44	1	1	FALSE
45	3	47	45	45	1	1	FALSE
46	47	48	46	46	1	1	FALSE
47	48	49	47	47	1	1	FALSE
48	49	1	48	48	1	1	FALSE
49	13	50	49	49	1	1	FALSE
50	50	51	50	50	1	1	FALSE
51	51	52	51	51	1	1	FALSE
52	52	4	52	52	1	1	FALSE
53	4	53	53	53	1	1	FALSE
54	53	54	54	54	1	1	FALSE
55	54	55	55	55	1	1	FALSE
56	55	11	56	56	1	1	FALSE
57	1	56	57	57	1	1	FALSE
58	56	57	58	58	1	1	FALSE
59	57	58	59	59	1	1	FALSE
60	58	11	60	60	1	1	FALSE
61	2	59	61	61	1	1	FALSE
62	59	60	62	62	1	1	FALSE
63	60	61	63	63	1	1	FALSE
64	61	11	64	64	1	1	FALSE
65	3	62	65	65	1	1	FALSE
66	62	63	66	66	1	1	FALSE
67	63	64	67	67	1	1	FALSE
68	64	11	68	68	1	1	FALSE
69	11	65	69	69	1	1	FALSE
70	65	66	70	70	1	1	FALSE
71	66	67	71	71	1	1	FALSE
72	67	12	72	72	1	1	FALSE

----- FILLED MEMBERS -----



```

0      NFillGroups      - Number of filled member groups (-) [If FillDens = DEFAULT. then FillDens =
WtrDens; FillFSLoc is related to MSL2SWL]
FillNumM  FillMList      FillFSLoc      FillDens
(-)      (-)              (m)              (kg/m^3)
  68     1     2     3     4     5     6     7     8     9     10    11    12    13    14    15    16    17    18    19
      20    21    22    23    24    25    26    27    28    29    30    31    32    33    34    35    36    37    38
      39    40    41    42    43    44    45    46    47    48    49    50    51    52    53    54    55    56    57
      58    59    60    61    62    63    64    65    66    67    68    0.00          1025
----- MARINE GROWTH -----
0      NMGDepths      - Number of marine-growth depths specified (-)
MGDpth    MGThck      MGDens
(m)      (m)          (kg/m^3)
----- MEMBER OUTPUT LIST -----
0      NMOutputs      - Number of member outputs (-) [must be < 10]
MemberID  NOutLoc      NodeLocs [NOutLoc < 10; node locations are normalized distance from the start of the member,
and must be >=0 and <= 1] [unused if NMOutputs=0]
(-)      (-)          (-)
----- JOINT OUTPUT LIST -----
0      NJOutputs      - Number of joint outputs [Must be < 10]
0      JOutLst        - List of JointIDs which are to be output (-)[unused if NJOutputs=0]
----- OUTPUT -----
True      HDSum        - Output a summary file [flag]
False     OutAll      - Output all user-specified member and joint loads (only at each member end, not
interior locations) [flag]
2      OutSwch      - Output requested channels to: [1=Hydrodyn.out, 2=GlueCode.out, 3=both files]
"ES11.4e2" OutFmt      - Output format for numerical results (quoted string) [not checked for validity!]
"A11"    OutSfmt      - Output format for header strings (quoted string) [not checked for validity!]
----- OUTPUT CHANNELS -----
"Wave1Elev"      - Wave elevation at ( 0, 0)
END of output channels and end of file. (the word "END" must appear in the first 3 columns of this line)

```

----- SubDyn v1.01.x MultiMember Support Structure Input File -----

Master's Thesis: Assessment of Simulation Codes for Offshore Wind Turbine Foundations - DNV load case 6.1c

----- SIMULATION CONTROL -----

False Echo - Echo input data to "<rootname>.SD.ech" (flag)  
"DEFAULT" SDdeltaT - Local Integration Step. If "default", the glue-code integration step will be used.  
3 IntMethod - Integration Method [1/2/3/4 = RK4/AB4/ABM4/AM2].  
True SttcSolve - Solve dynamics about static equilibrium point

----- FEA and CRAIG-BAMPTON PARAMETERS-----

3 FEMMod - FEM switch: element model in the FEM. [1= Euler-Bernoulli(E-B); 2=Tapered E-B (unavailable); 3= 2-node Timoshenko; 4= 2-node tapered Timoshenko (unavailable)]  
1 NDiv - Number of sub-elements per member  
True CBMod - [T/F] If True perform C-B reduction, else full FEM dofs will be retained. If True, select Nmodes to retain in C-B reduced system.  
12 Nmodes - Number of internal modes to retain (ignored if CBMod=False). If Nmodes=0 --> Guyan  
1 JDampings - Damping Ratios for each retained mode (% of critical) If Nmodes>0, list Nmodes structural damping ratios for each retained mode (% of critical), or a single damping ratio to be applied to all retained modes. (last entered value will be used for all remaining modes).

---- STRUCTURE JOINTS: joints connect structure members (~Hydrodyn Input File)---

67 NJoints - Number of joints (-)

JointID	JointXss	JointYss	JointZss	[Coordinates of Member joints in SS-Coordinate System]
(-)	(m)	(m)	(m)	
1	0	25.76370000000000	-35	
2	22.31200000000000	-12.88180000000000	-35	
3	-22.31200000000000	-12.88180000000000	-35	
4	0	0	-35	
5	0	25.76370000000000	-25	
6	22.31200000000000	-12.88180000000000	-25	
7	-22.31200000000000	-12.88180000000000	-25	
8	0	25.76370000000000	-45	
9	22.31200000000000	-12.88180000000000	-45	
10	-22.31200000000000	-12.88180000000000	-45	
11	0	0	0	
12	0	0	10	

13	0	0	-37	
14	0	19.32277500000000	-35	
15	0	12.88185000000000	-35	
16	0	6.44092500000000	-35	
17	16.73400000000000	-9.66135000000000	-35	
18	11.15600000000000	-6.44090000000000	-35	
19	5.57800000000000	-3.22045000000000	-35	
20	-16.73400000000000	-9.66135000000000	-35	
21	-11.15600000000000	-6.44090000000000	-35	
22	-5.57800000000000	-3.22045000000000	-35	
23	0	25.76370000000000	-32.50000000000000	
24	0	25.76370000000000	-30	
25	0	25.76370000000000	-27.50000000000000	
26	22.31200000000000	-12.88180000000000	-32.50000000000000	
27	22.31200000000000	-12.88180000000000	-30	
28	22.31200000000000	-12.88180000000000	-27.50000000000000	
29	-22.31200000000000	-12.88180000000000	-32.50000000000000	
30	-22.31200000000000	-12.88180000000000	-30	
31	-22.31200000000000	-12.88180000000000	-27.50000000000000	
32	0	25.76370000000000	-42.50000000000000	
33	0	25.76370000000000	-40	
34	0	25.76370000000000	-37.50000000000000	
35	22.31200000000000	-12.88180000000000	-42.50000000000000	
36	22.31200000000000	-12.88180000000000	-40	
37	22.31200000000000	-12.88180000000000	-37.50000000000000	
38	-22.31200000000000	-12.88180000000000	-42.50000000000000	
39	-22.31200000000000	-12.88180000000000	-40	
40	-22.31200000000000	-12.88180000000000	-37.50000000000000	
41	5.57800000000000	16.10232500000000	-35	
42	11.15600000000000	6.44095000000000	-35	
43	16.73400000000000	-3.22042500000000	-35	
44	11.15600000000000	-12.88180000000000	-35	
45	0	-12.88180000000000	-35	

```

46  -11.156000000000000 -12.881800000000000 -35
47  -16.734000000000000 -3.220425000000000 -35
48  -11.156000000000000 6.440950000000000 -35
49  -5.578000000000000 16.102325000000000 -35
50  0 0 -36.500000000000000
51  0 0 -36
52  0 0 -35.500000000000000
53  0 0 -26.250000000000000
54  0 0 -17.500000000000000
55  0 0 -8.750000000000000
56  0 19.322775000000000 -26.250000000000000
57  0 12.881850000000000 -17.500000000000000
58  0 6.440925000000000 -8.750000000000000
59  16.734000000000000 -9.661350000000000 -26.250000000000000
60  11.156000000000000 -6.440900000000000 -17.500000000000000
61  5.578000000000000 -3.220450000000000 -8.750000000000000
62  -16.734000000000000 -9.661350000000000 -26.250000000000000
63  -11.156000000000000 -6.440900000000000 -17.500000000000000
64  -5.578000000000000 -3.220450000000000 -8.750000000000000
65  0 0 2.500000000000000
66  0 0 5
67  0 0 7.500000000000000

```

----- BASE REACTION JOINTS: 1/0 for Locked/Free DOF @ each Reaction Node -----

3 NReact - Number of Joints with reaction forces; be sure to remove all rigid motion DOFs of the structure (else det([K])=[0])

RJointID	RctTDXss	RctTDYss	RctTDZss	RctRDYss	RctRDZss	[Global Coordinate System]
(-)	(flag)	(flag)	(flag)	(flag)	(flag)	(flag)
8	1	1	1	1	1	1
9	1	1	1	1	1	1
10	1	1	1	1	1	1

----- INTERFACE JOINTS: 1/0 for Locked (to the TP)/Free DOF @each Interface Joint (only Locked-to-TP implemented thus far (=rigid TP)) -----

1 NInterf - Number of interface joints locked to the Transition Piece (TP): be sure to remove all rigid motion dofs

IJointID	ItfTDXss	ItfTDYss	ItfTDZss	ItfRDYss	ItfRDZss	[Global Coordinate System]
(-)	(flag)	(flag)	(flag)	(flag)	(flag)	
12	1	1	1	1	1	

----- MEMBERS -----

MemberID	MJointID1	MJointID2	MPropSetID1	MPropSetID2	COSMID
(-)	(-)	(-)	(-)	(-)	(-)
1	1	14	1	1	
2	14	15	2	2	
3	15	16	3	3	
4	16	4	4	4	
5	2	17	5	5	
6	17	18	6	6	
7	18	19	7	7	
8	19	4	8	8	
9	3	20	9	9	
10	20	21	10	10	
11	21	22	11	11	
12	22	4	12	12	
13	1	23	13	13	
14	23	24	14	14	
15	24	25	15	15	
16	25	5	16	16	
17	2	26	17	17	
18	26	27	18	18	
19	27	28	19	19	
20	28	6	20	20	
21	3	29	21	21	
22	29	30	22	22	
23	30	31	23	23	
24	31	7	24	24	
25	8	32	25	25	
26	32	33	26	26	

27	33	34	27	27
28	34	1	28	28
29	9	35	29	29
30	35	36	30	30
31	36	37	31	31
32	37	2	32	32
33	10	38	33	33
34	38	39	34	34
35	39	40	35	35
36	40	3	36	36
37	1	41	37	37
38	41	42	38	38
39	42	43	39	39
40	43	2	40	40
41	2	44	41	41
42	44	45	42	42
43	45	46	43	43
44	46	3	44	44
45	3	47	45	45
46	47	48	46	46
47	48	49	47	47
48	49	1	48	48
49	13	50	49	49
50	50	51	50	50
51	51	52	51	51
52	52	4	52	52
53	4	53	53	53
54	53	54	54	54
55	54	55	55	55
56	55	11	56	56
57	1	56	57	57
58	56	57	58	58
59	57	58	59	59

60	58	11	60	60
61	2	59	61	61
62	59	60	62	62
63	60	61	63	63
64	61	11	64	64
65	3	62	65	65
66	62	63	66	66
67	63	64	67	67
68	64	11	68	68
69	11	65	69	69
70	65	66	70	70
71	66	67	71	71
72	67	12	72	72

----- MEMBER X-SECTION PROPERTY data 1/2 [isotropic material for now: use this table for circular-tubular elements] -----

72 NPropSets - Number of structurally unique x-sections (i.e. how many groups of X-sectional properties are utilized throughout all of the members)

PropSetID	YoungE	ShearG	MatDens	XsecD	XsecT
(-)	(N/m <sup>2</sup> )	(N/m <sup>2</sup> )	(kg/m <sup>3</sup> )	(m)	(m)
1	210000000000.000	81000000000.0000	7850	0.8000000000000000	0.0280000000000000
2	210000000000.000	81000000000.0000	7850	0.8000000000000000	0.0280000000000000
3	210000000000.000	81000000000.0000	7850	0.8000000000000000	0.0280000000000000
4	210000000000.000	81000000000.0000	7850	0.8000000000000000	0.0280000000000000
5	210000000000.000	81000000000.0000	7850	0.8000000000000000	0.0280000000000000
6	210000000000.000	81000000000.0000	7850	0.8000000000000000	0.0280000000000000
7	210000000000.000	81000000000.0000	7850	0.8000000000000000	0.0280000000000000
8	210000000000.000	81000000000.0000	7850	0.8000000000000000	0.0280000000000000
9	210000000000.000	81000000000.0000	7850	0.8000000000000000	0.0280000000000000
10	210000000000.000	81000000000.0000	7850	0.8000000000000000	0.0280000000000000
11	210000000000.000	81000000000.0000	7850	0.8000000000000000	0.0280000000000000
12	210000000000.000	81000000000.0000	7850	0.8000000000000000	0.0280000000000000
13	210000000000.000	81000000000.0000	7850	4	0.0400000000000000
14	210000000000.000	81000000000.0000	7850	4	0.0400000000000000

15	210000000000.000	81000000000.0000	7850	4	0.04000000000000000	
16	210000000000.000	81000000000.0000	7850	4	0.04000000000000000	
17	210000000000.000	81000000000.0000	7850	4	0.04000000000000000	
18	210000000000.000	81000000000.0000	7850	4	0.04000000000000000	
19	210000000000.000	81000000000.0000	7850	4	0.04000000000000000	
20	210000000000.000	81000000000.0000	7850	4	0.04000000000000000	
21	210000000000.000	81000000000.0000	7850	4	0.04000000000000000	
22	210000000000.000	81000000000.0000	7850	4	0.04000000000000000	
23	210000000000.000	81000000000.0000	7850	4	0.04000000000000000	
24	210000000000.000	81000000000.0000	7850	4	0.04000000000000000	
25	210000000000.000	81000000000.0000	7850	4	0.04000000000000000	
26	210000000000.000	81000000000.0000	7850	4	0.04000000000000000	
27	210000000000.000	81000000000.0000	7850	4	0.04000000000000000	
28	210000000000.000	81000000000.0000	7850	4	0.04000000000000000	
29	210000000000.000	81000000000.0000	7850	4	0.04000000000000000	
30	210000000000.000	81000000000.0000	7850	4	0.04000000000000000	
31	210000000000.000	81000000000.0000	7850	4	0.04000000000000000	
32	210000000000.000	81000000000.0000	7850	4	0.04000000000000000	
33	210000000000.000	81000000000.0000	7850	4	0.04000000000000000	
34	210000000000.000	81000000000.0000	7850	4	0.04000000000000000	
35	210000000000.000	81000000000.0000	7850	4	0.04000000000000000	
36	210000000000.000	81000000000.0000	7850	4	0.04000000000000000	
37	210000000000.000	81000000000.0000	7850	0.8000000000000000	0.01600000000000000	
38	210000000000.000	81000000000.0000	7850	0.8000000000000000	0.01600000000000000	
39	210000000000.000	81000000000.0000	7850	0.8000000000000000	0.01600000000000000	
40	210000000000.000	81000000000.0000	7850	0.8000000000000000	0.01600000000000000	
41	210000000000.000	81000000000.0000	7850	0.8000000000000000	0.01600000000000000	
42	210000000000.000	81000000000.0000	7850	0.8000000000000000	0.01600000000000000	
43	210000000000.000	81000000000.0000	7850	0.8000000000000000	0.01600000000000000	
44	210000000000.000	81000000000.0000	7850	0.8000000000000000	0.01600000000000000	
45	210000000000.000	81000000000.0000	7850	0.8000000000000000	0.01600000000000000	
46	210000000000.000	81000000000.0000	7850	0.8000000000000000	0.01600000000000000	
47	210000000000.000	81000000000.0000	7850	0.8000000000000000	0.01600000000000000	



```

48 210000000000.000 81000000000.0000 7850 0.8000000000000000 0.01600000000000000
49 210000000000.000 81000000000.0000 7850 4 0.02800000000000000
50 210000000000.000 81000000000.0000 7850 4.027025000000000 0.02855000000000000
51 210000000000.000 81000000000.0000 7850 4.054050000000000 0.02910000000000000
52 210000000000.000 81000000000.0000 7850 4.081075000000000 0.02965000000000000
53 210000000000.000 81000000000.0000 7850 4.108100000000000 0.03020000000000000
54 210000000000.000 81000000000.0000 7850 4.581075000000000 0.03965000000000000
55 210000000000.000 81000000000.0000 7850 5.054050000000000 0.04910000000000000
56 210000000000.000 81000000000.0000 7850 5.527025000000000 0.05855000000000000
57 210000000000.000 81000000000.0000 7850 1.200000000000000 0.03200000000000000
58 210000000000.000 81000000000.0000 7850 1.200000000000000 0.03200000000000000
59 210000000000.000 81000000000.0000 7850 1.200000000000000 0.03200000000000000
60 210000000000.000 81000000000.0000 7850 1.200000000000000 0.03200000000000000
61 210000000000.000 81000000000.0000 7850 1.200000000000000 0.03200000000000000
62 210000000000.000 81000000000.0000 7850 1.200000000000000 0.03200000000000000
63 210000000000.000 81000000000.0000 7850 1.200000000000000 0.03200000000000000
64 210000000000.000 81000000000.0000 7850 1.200000000000000 0.03200000000000000
65 210000000000.000 81000000000.0000 7850 1.200000000000000 0.03200000000000000
66 210000000000.000 81000000000.0000 7850 1.200000000000000 0.03200000000000000
67 210000000000.000 81000000000.0000 7850 1.200000000000000 0.03200000000000000
68 210000000000.000 81000000000.0000 7850 1.200000000000000 0.03200000000000000
69 210000000000.000 81000000000.0000 7850 6 0.04000000000000000
70 210000000000.000 81000000000.0000 7850 6 0.04000000000000000
71 210000000000.000 81000000000.0000 7850 6 0.04000000000000000
72 210000000000.000 81000000000.0000 7850 6 0.04000000000000000

```

----- MEMBER X-SECTION PROPERTY data 2/2 [isotropic material for now: use this table if any section other than circular, however provide COSM(i,j) below] -----

0 NXPropSets - Number of structurally unique non-circular x-sections (if 0 the following table is ignored)

PropSetID	YoungE	ShearG	MatDens	XsecA	XsecAsx	XsecAsy	XsecJxx
XsecJyy	XsecJ0						
(-)	(N/m2)	(N/m2)	(kg/m3)	(m2)	(m2)	(m2)	(m4)
(m4)	(m4)						

----- MEMBER COSINE MATRICES COSM(i,j) -----

```

0      NCOSMs      - Number of unique cosine matrices (i.e., of unique member alignments including
principal axis rotations); ignored if NXPropSets=0 or 9999 in any element below
COSMID  COSM11    COSM12    COSM13    COSM21    COSM22    COSM23    COSM31    COSM32    COSM33
(-)      (-)      (-)      (-)      (-)      (-)      (-)      (-)      (-)      (-)
----- JOINT ADDITIONAL CONCENTRATED MASSES -----
0      NCmass      - Number of joints with concentrated masses; Global Coordinate System
CMJointID  JMass      JMX      JMY      JMZZ
(-)      (kg)      (kg*m^2)      (kg*m^2)      (kg*m^2)
----- OUTPUT: SUMMARY & OUTFILE -----
True      SSSum      - Output a Summary File (flag).It contains: matrices K,M and C-B reduced M_BB, M-BM,
K_BB, K_MM(OMG^2), PHI_R, PHI_L. It can also contain COSMs if requested.
False      OutCOSM      - Output cosine matrices with the selected output member forces (flag)
False      OutAll      - [T/F] Output all members' end forces
2      OutSwch      - [1/2/3] Output requested channels to: 1=<rootname>.SD.out; 2=<rootname>.out
(generated by FAST); 3=both files.
True      TabDelim      - Generate a tab-delimited output in the <rootname>.SD.out file
1      OutDec      - Decimation of output in the <rootname>.SD.out file
"ES11.4e2"  OutFmt      - Output format for numerical results in the <rootname>.SD.out file
"A11"      OutSFmt      - Output format for header strings in the <rootname>.SD.out file
----- MEMBER OUTPUT LIST -----
1      NMOutputs      - Number of members whose forces/displacements/velocities/accelerations will be output
(-) [Must be <= 9].
MemberID  NOutCnt      NodeCnt [NOutCnt=how many nodes to get output for [< 10]; NodeCnt are local ordinal numbers
from the start of the member, and must be >=1 and <= NDiv+1] If NMOutputs=0 leave blank as well.
(-)      (-)      (-)
72      1      2      !M1
----- SSOutList: The next line(s) contains a list of output parameters that will be output in
<rootname>.SD.out or <rootname>.out. -----
"M1N1TDXss, M1N1TDYss, M1N1TDZss"
"-ReactFXss. -ReactFYss. -ReactMXss. -ReactMYss. -ReactMZss. -ReactFZss" - Base reactions: fore-aft shear. side-to-
side shear. side-to-side moment. fore-aft moment. yaw moment. vertical force
END of output channels and end of file. (the word "END" must appear in the first 3 columns of this line)

```